Carbon fluxes in selected sites of Bay of Bengal and Southern Ocean and their significance

A Thesis submitted to Goa University for the Award of the Degree of

DOCTOR OF PHILOSOPHY

in

Marine Sciences

By

Suhas S. Shetye

Research Guide

Dr. M. Sudhakar

Goa University

Taleigao - Goa

(2015)

Statement of the Candidate

As required under the University Ordinance O.9.9 (ii), I hereby state that the present thesis titled "**Carbon fluxes in selected sites of Bay of Bengal and Southern Ocean and their significance**" is my original contribution and the same has not been submitted on any previous occasion. To the best of my knowledge, the present study is the first comprehensive work of its kind from the area mentioned.

The literature related to the problem investigated has been cited. Due acknowledgements have been made wherever facilities and suggestions have been availed.

May 2013 **Suhas S. Shetye**

Certificate

As required under the University Ordinance OB.9.9. (vi), I certify that the thesis titled "**Carbon fluxes in selected sites of Bay of Bengal and Southern Ocean and their significance**", submitted by Mr. **Suhas S. Shetye** for the award of the degree of Doctor of Philosophy in Marine Sciences, is based on original studies carried-out by him under my supervision. The thesis or any part of thesis has not been previously submitted for any other degree or diploma in any university or institution.

Dr. Maruthadu Sudhakar

Acknowledgements

I wish to express my sincere thanks to all those who helped me during my Ph.D research. My supervisor, Dr. Maruthadu Sudhakar, Advisor, Ministry of Earth Sciences, who brought out the best in me. I thank him for his support, immense patience and supervision during the work of my thesis.

I express my sincere gratitude to Prof. G. N. Nayak, Dean Life Sciences and Head of Marine Sciences for being my co-guide and guiding me through various administrative processes and suggestions.

I acknowledge NCAOR for providing me Junior Research fellowships and Research Scientist “B’ position. I thank my project investigator Dr. Rahul Mohan for the support and guidance. I thank the Director of NCAOR for giving me an opportunity to work and carry out my research work at NCAOR.

I thank Dr. Dileep Kumar, FRC Member, for duly assessing progress of my work and giving valuable suggestions. I also thank my lecturers at Goa University Prof. Harilal Menon, Dr. Upadhyay, Dr. Matta, Dr. Rivonker, Dr. Aftab and all support staff in Marine Science Department.

I thank Dr. Sugandha Sardessai, Dr. Prasanna Kumar and Dr. V.S.N Murthy for giving me the opportunity to start my Research Career in NIO in 2006. Special thanks to Dr. Sugandha, for teaching me basic analysis in Marine Chemistry and also for being my idol. Thanks to Dr. Satish Shetye, Director NIO, for giving me chance to work in NIO.

I am thankful to Dr. R. Ramesh (PRL) and Dr. V.V.S. Sarma (NIO-Vizag) for the guidance whenever I required it.

Thanks to NCAOR, NIO, Goa university library, which is the back bone for us researchers!!

Thanks to all my friends in NCAOR, NIO, Goa University, St. Xaviers College and St. Anthonys High School. Special thanks to Mr. Shramik Patil, Mr. Shridhar Jawak, Dr. Babula Jena, Dr. Mahesh and Dr. Anish.

Thanks to my family to keep me happy back home. Special thanks to my Grand-parents for motivating me.

I am very much thankful to God for giving me enough strength to carry out my research

Suhas S. Shetye

Preface

Earth's climate due to mankind's emission of fossil fuels is changing rapidly, atmospheric CO_2 concentrations have already reached 400 ppm and presents a major challenge with regards to understanding the oceanic carbon cycle, and ocean biogeochemistry. Next to the lithosphere, the ocean is the largest global carbon reservoir, containing approximately 50 times the amount of carbon in dissolved form, as in the atmosphere (Takahashi et al., 1993). Presently, atmospheric carbon dioxide (CO_2) concentrations have exceeded levels not seen for at least 650 000 years (Siegenthaler et al., 2005), principally caused by the burning n of fossil fuel. Oceanic CO_2 uptake has significantly dampened the atmospheric CO_2 increase, the ocean having taken up nearly half of the CO_2 emitted since the onset of the industrial revolution (Sabine et al., 2004). The uptake of anthropogenic CO_2 has caused a lowering of the average surface ocean pH of 0.1 units. This process is known as ocean acidification and it is also called as the other half of the CO_2 problem. This may have adverse effects on marine life (Raven et al., 2005). In parallel, oceanic dissolved oxygen (O_2) concentrations are declining and the oxygen minimum zones are expanding; mostly due to CO_2 induced global warming, and reduced ventilation. This may exert additional stress on marine life living in vulnerable areas (Stramma et al., 2008). The combined effect of decreasing pH and O_2 will impact marine systems through modifications of the respiration index (Hofmann and Schnellenhuber 2009).

Air-sea CO_2 fluxes, and the distribution of carbon within the world oceans, are largely controlled by three conceptual carbon pumps; (i) the solubility pump, (ii) the organic carbon pump (or soft tissue pump), and (iii) the carbonate counter pump (Volk and Hoffert 1985, Heinze et al. 1991).

Few oceans act as a sink, while the others act as a source to the atmospheric CO_2 depending on the dominant physical, chemical and biological processes. Understanding the effects of such processes on oceanic CO_2 forms the theme of the present study. I have studied two oceanic regions, Southern Ocean and Bay of Bengal.

Chapter 1 provides an introduction to the carbon cycling, carbon chemistry and climate change studies. **Chapter 2** describes the study area and geographic settings. **Chapter 3** describes the Sample locations, Analytical methods and Errors in analysis. The results are presented in **Chapter 4.** Chapter 4 is further divided into 4 sub chapters, **4.1** provides detailed description of the Hydrography. **4.2** provides detailed description on Nutrient Variations. **4.3** include variations in surface pCO_2 in Indian Sector of Southern Ocean and Bay of Bengal. **4.4** provide information on Carbon and Carbon dioxide fluxes in Southern Ocean and Bay of Bengal. The discussion of the results is presented in **Chapter 5.** Again chapter 5 is subdivided into 2 subchapters (5.1 and 5.2). **5.1** provide description on factors controlling CO_2 in Southern Ocean and Bay of Bengal. **5.2** Comparison with previous studies. **5.3** explain the effects of pCO_2 on marine organisms. **5.4** explains significance of this study. **Chapter 6** is dedicated for Conclusions of the present study.

Contents

FIGURE CAPTIONS:

List of Tables:

CHAPTER 1

Introduction

1. Introduction

Carbon dioxide, one of the major greenhouse gas is directly related with the global climate and the rise in global temperatures. Anthropogenic emissions of CO_2 due to fossil fuel burning have led to a higher atmospheric CO_2 since the industrial revolution and values have already reached 400 ppm. Such high atmospheric CO_2 concentration has not been recorded in the geological past during the past 420,000 years (Houghton et al., 2001). The oceans so far have acted as a sink for half of the anthropogenic CO_2 (Broecker and Peng 1989). However, recently the CO_2 sink capacity of the oceans has decreased drastically. Generally, the atmosphere exchanges CO_2 in with two major reservoirs: the terrestrial biosphere and the ocean. As compared to the oceanic CO_2, the atmospheric CO_2 concentrations are well studied because the atmosphere CO_2 is distributed uniformly in the troposphere due to the rapid mixing. Also, a world-wide network of CO_2 observations exists including the one main center at Mauna Loa in Hawaii, which continuously monitors the atmospheric CO_2 content (Conway et al., 1994). In recent years, the atmospheric CO_2 curve given by keeling, which is also known as the keeling curve has gained importance and has rung alarms about the growth rate of atmospheric CO_2. On, the other hand, the oceanic variability is much higher and thus making it difficult for carbon budgeting in the oceans. Various carbon species exists in the terrestrial biosphere and since land use owing to growing population demand is changing, thus making it difficult to calculate carbon sources and sinks (Wallace, 2001). Although oceanic CO_2 variability is high, but since most of the carbon in oceans exist as inorganic carbon, thus the accuracy of measurements are high compared to terrestrial biosphere.

A lot of research has been conducted to find out about the general mechanisms

that regulate the complex carbon cycle in the ocean. The Southern Ocean plays an important role in the global ocean with regard to the uptake of anthropogenic CO_2.

Within my thesis - I came across major questions and topics that are required to understand carbon cycling and global implications of climate change:

- How does the oceanic carbon cycle work? How does the CO_2 distribution vary from tropics to higher latitudes?
- Which parameters regulate the CO_2 in the Southern Ocean, whether the biological or the physical processes?
- How important is the addition of new CO_2 data from regions like Indian sector of the Southern Ocean?
- What are the impacts of rising CO_2 on the oceanic biota?

1.1. Carbon dioxide chemistry of the sea

1.1.1. The Carbonate System

The oceanic carbon cycle is well known with regards to pathways of CO_2, however, actual fluxes and quantities are still subject of debate. CO_2 is exchanged between ocean and atmosphere, where the flux largely depends on the concentration gradient. Since the oceanic CO_2 variability is much higher as compared to the atmosphere, it controls the fluxes. In regions where the oceanic partial pressure of CO_2 is higher than in the atmosphere the flux of CO_2 will be from the ocean into the atmosphere i.e. the ocean acts as a source of CO_2 for the atmosphere. Hence, the reverse process, when atmospheric CO_2 is high as compared to the oceanic CO_2, the ocean act as a sink for atmospheric CO_2. The flux of CO_2 is controlled by various processes, e.g.: wind speed, sea state, surface

processes, bubble entrainment and biological productivity (McGillis et al., 2001). The CO_2 flux is mostly derived from estimated transfer velocities, solubility of CO_2, and the difference between the pCO_2 in the atmosphere and ocean (ΔpCO_2) (Wanninkhof 1992).

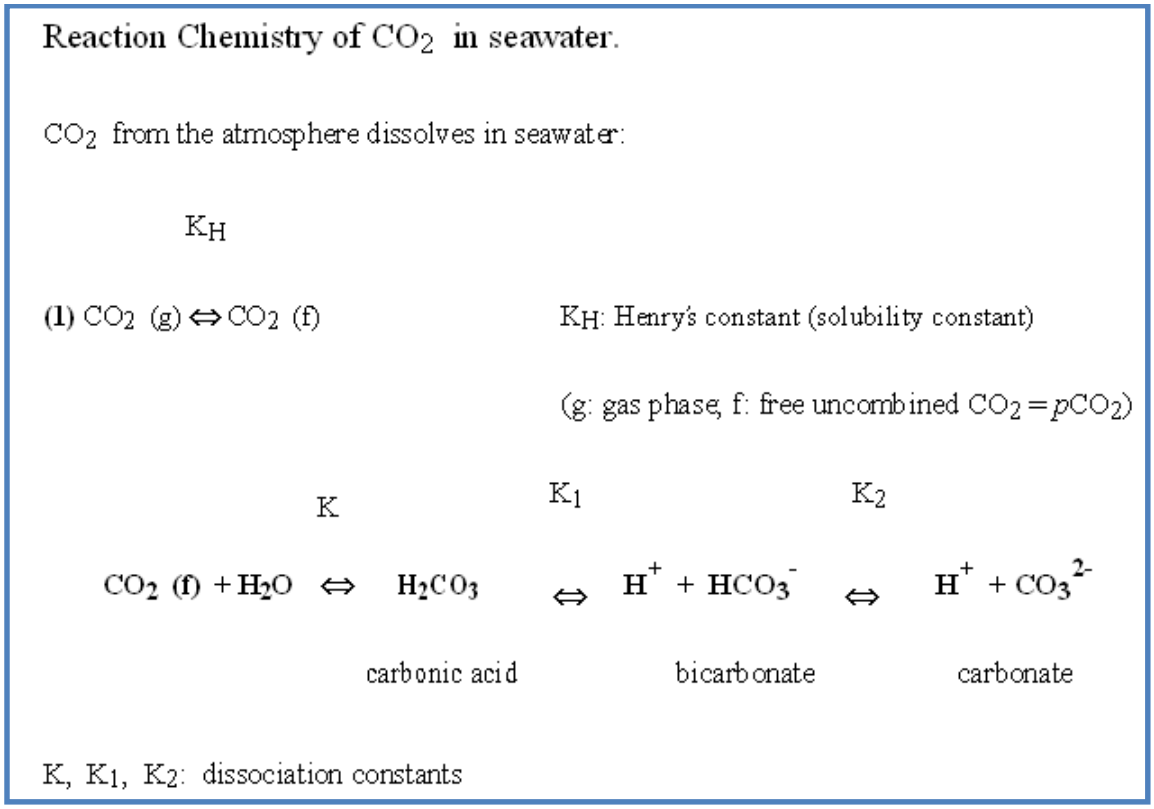

Fig. 1: Reaction chemistry of CO_2 in seawater

Fig. 1 shows the chemical reactions that occur once CO_2 dissolves in sea water. The hydration of CO_2 to carbonic acid is a slow reaction: In one second, only about 3 % of the molecules of free CO_2 in the solution combine with a water molecule (K_H**=** 0.03 s^{-1}; Pilson, 1998). Carbon dioxide dissolves to form bicarbonates, carbonates and carbonic acid and is controlled by dissociation constants which depend on pressure, temperature and salinity (Mehrbach et al., 1973). The complete CO_2 chemistry in ocean which involves the reactions, CO_2 species and dissociation constants is called as the carbonate system. So far, it is not possible

to analytically detect the concentrations of carbonic acid, bicarbonate or carbonate. However, the CO_2 system can be calculated from the combination of any two of the four parameters: *p*H, pCO_2 (partial pressure of CO_2), DIC (dissolved inorganic carbon), and TA (total alkalinity). All these parameters can be measured by chemical analysis with different accuracies.

pH, which is the negative logarithm to the base 10 of the hydrogen ion concentration, is the master variable of the carbonate system as it determines the whether CO2 will be in carbonic acid, bi carbonate or carbonate. Seawater has slightly basic *p*H (~ 8.1). pCO_2 is calculated from the total pressure (p) and the mole fraction of CO_2 (xCO_2)

$$pCO_2 = p \cdot xCO_2 \quad (1)$$

Total dissolved inorganic carbon (DIC) contains the sum of the concentration of the CO_2 species:

$$DIC = [H_2CO_3] + [HCO_3^-] + [CO_3^{2-}] \quad (2)$$

The coulometric technique for the determination of DIC involves the acidification of a sample of seawater with phosphoric acid which leads to an outgassing of CO_2. The CO_2 gas sample is titrated following faradays law and the CO_2 concentration is measured coulometrically.

Total Alkalinity (TA), the fourth parameter of the carbonate system, describes the buffer capacity of the seawater and encompasses bases that are formed from weak acids. It is determined by titrating a sample with strong acid (HCl) to the point where all such bases, mainly carbonate species, are protonated (Pilson, 1998). Generally, TA is described as following:

$$TA = 2[CO_3^{2-}] + [HCO_3^-] + [B(OH)_4^-] + [OH^-] - [H^+] \quad (3)$$

Total alkalinity is a conservative quantity (not affected by any biological reaction)

and linearly correlated with salinity. The carbonate species and to a lesser extent borate contribute mostly to the total alkalinity.

1.1.2. *p*CO_2 variability with time

The atmospheric CO_2 concentrations have increased steadily due to human activities; the ocean absorbs the anthropogenic CO_2 and regulates our atmospheric CO_2. Thus making it important to gather enough *p*CO_2 data to resolve the seasonal variability of the oceanic *p*CO_2. Recently, Takahashi et al., 2009 came up with CO_2 data base with about 940,000 datapoints of the global oceans and interpolated to a 4°x5° grid. They not only published *p*CO_2 data but also calculated the CO_2 flux. When it comes to Indian sector of Southern Ocean, Nicolas Metzl (2009) has done some work on decadal changes in oceanic pCO_2. A major problem in this context is the strong time-dependency of the seawater *p*CO_2. It is a fact that the ocean takes up CO_2, but the same region could act as a source or sink at different point of time. Our knowledge does not extend to where and when CO_2 is taken up. Different regions behave in a different way at different points of time.

1.1.3. Air-Sea Flux of CO_2

The air-sea flux of CO_2 is calculated by the following formula:

$$F(CO_2) = K \; S \; (pCO_{2\,sw} - pCO_{2\,atm}) \qquad (1)$$

where *K* is the gas transfer velocity, S is the solubility of CO_2 in seawater, *p*CO_{2sw} and *p*CO_{2atm} are the partial pressures of CO_2 in seawater and atmosphere, respectively. The transfer velocity is commonly related to wind speed (Wanninkhof, 1992).

1.1.4. Exchange with the Organic Carbon Pool

The inorganic carbon concentrations in the oceans are changed by biological

reactions at the surface, water column and also in sediment.

In this work I am concerned mostly with the surface waters and deeper waters upto 1000m. The surface water which denotes the upper part of the ocean is affected by wind, sunlight and weather conditions. The depth at which 1 % of the daylight is still visible is referred to as the euphotic zone. Another zone of importance is the mixed layer depth and it can affect the biological production. This is the depth where vertical mixing leads to a more-or-less homogenous distribution of conservative properties such as temperature, salinity and nutrients. The depth of the mixed layer varies seasonally and spatially with deeper depths during the winter months when convection increases. At the surface the effects of CO_2 air-sea exchange and biological reactions such as photosynthesis, respiration and calcification are significant. Photosynthesis consumes inorganic carbon and produces particulate organic matter and the reverse reaction corresponds to respiration. The uptake of CO_2 during photosynthesis decreases the pCO_2 and increases the gradient of CO_2 between surface ocean and atmosphere ($\mathbf{\Delta}pCO_2$). The overall reaction can be displayed as following:

$$106\ CO_2 + 16\ NO_3^- + HPO_4^{2-} + 18\ H^+ + 122\ H_2O \leftrightarrow (CH_2O)106(NH_3)16H_3PO_4 + 138\ O_2 \quad (1)$$

This equation represents the Redfield ratio which encompasses the ratio of C:N:P = 106:16:1 (Redfield et al., 1963). Different approaches have been used to improve these elemental ratios (Anderson and Sarmiento, 1994; Anderson, 1995). The Redfield ratio is often used to estimate the new production. New production is defined as that part of the primary production that is based on nutrients newly introduced to the euphotic zone, either via advection or from vertical supply from sub surface waters or from Aeolian input (Dugdale and Goering, 1967). Whereas regenerated production is based on recycled nutrients (eg. Ammonia, urea etc.).

A part of the particulate organic matter sinks, and is consumed in the deeper parts of the ocean by the zooplankton and other organisms. It is estimated that only about 10% of the organic matter is exported below the euphotic zone. The export of organic matter is part of the biological pump and plays an important role for the sequestration of carbon to the deep ocean. About 80% of the water column gradients in dissolved inorganic carbon are due to the biological pump (Sarmiento et al., 1995).

Carbon can also be exported to the deep waters via calcification, i.e. the formation of calcium carbonate (calcium carbonate pump). The process of precipitation and dissolution of calcium carbonate ($CaCO_3$) also modulates the carbon chemistry in the ocean. Marine organisms like foraminifera, pteropods and coccolithophores form calcareous shells in ocean using calcium and carbonate following this equation:

$$Ca^{2+} + 2HCO_3 \leftrightarrow CaCO_3 + CO_2 + H_2O \qquad (2)$$

The formation of $CaCO_3$ increases the concentration of CO_2 as it releases CO_2, but at the same time consumes 2 moles of bicarbonate (HCO_3^-). This counter intuitive behaviour reduces the total alkalinity (TA) and dissolved inorganic carbon (DIC) by 2 and 1 units, respectively and increases the pCO_2 at the same time (Zeebe and Wolf-Gladrow 2001). $CaCO_3$ in the ocean is present in two forms: aragonite and calcite. Aragonite which is orthorhombic is less stable and hence more soluble than calcite, therefore it is less abundant than calcite (Pilson, 1998). The major calcite producers in the ocean are coccolithophorids and foraminifera, while the most abundant pelagic aragonite organisms are pteropods (Zeebe and Wolf-Gladrow 2001).

1.2. Ocean acidification

Anthropogenic increase in atmospheric CO_2, increases CO_2 dissolving in the Surface Ocean, and lowers pH due to carbonic acid formation (Wolf-Gladrow et al., 1999), this process is termed as 'ocean acidification'. Surface oceanic pH has already decreased by 0.1 units in last one century and will further decrease by 0.3 to 0.4 units by 2100 (Feely et al., 2004). Ocean acidification is also known as the other half of the CO_2 problem.

Decrease in pH influences the calcification rates of various calcareous organisms (Riebesell, 2000). Non-calcifying phytoplankton, such as diatoms which produce siliceous shells, reduce the CO_2 concentration in the upper ocean by their photosynthetic activity. Calcifying organisms like coccolithophores are autotrophic and produce oxygen, however, next to their photosynthetical activity also produce CO_2 (as seen from equation 2) through calcification thus offsetting some of the CO_2 drawdown.

CHAPTER 2

Geographic Location and Oceanography of the Study Area

2.1. Southern Ocean

The Indian Ocean (IO) sector of the Southern Ocean (SO) is located between 30°–60°S, 20°–150°E. Southern Ocean is often associated with rough weather and cyclonic conditions especially between the 40-60^{0}S. Spanning 45-55°S, the Antarctic Circumpolar Current (ACC) flows zonally (Orsi et al., 1995), linking various southern ocean basins like the Pacific, Atlantic and the Indian Ocean and supplies high saline warm waters. The Indian sector of Southern Ocean has two major islands, the Crozet and the Kerguellen Island. The waters in Indian sector of Southern ocean are cold and have high dissolved oxygen about 350µM and thereby supplying oxygen to the bottom layers of equatorial and northern Indian Ocean. The Indian sector of Southern ocean have a unique quasi –zonal frontal system. The frontal zones are highly productive as compared to the remaining SO (Weeks and Shillington, 1996). The southern ocean also has high macro nutrient concentrations, where in the concentrations of nutrients found at 1000-2000m water depth in northern Indian Ocean are found in surface waters of southern ocean.

The Southern Indian Ocean exhibit remarkable regional differences determined by peculiarities of bottom topography (Fig. 2). Anilkumar et al., 2006 reported southern shift in fronts by 2 degrees from 48^{0}E to 57^{0}E. They identified five major fronts as Agulhas Front (AF) the North and South Subtropical fronts (NSTF and SSTF, respectively) the Subantarctic and Polar fronts (SAF and PF, respectively). Fronts are known to merge in the vicinity of islands such as Crozet and Kerguellen islands (Belkin and Gordon, 1996).

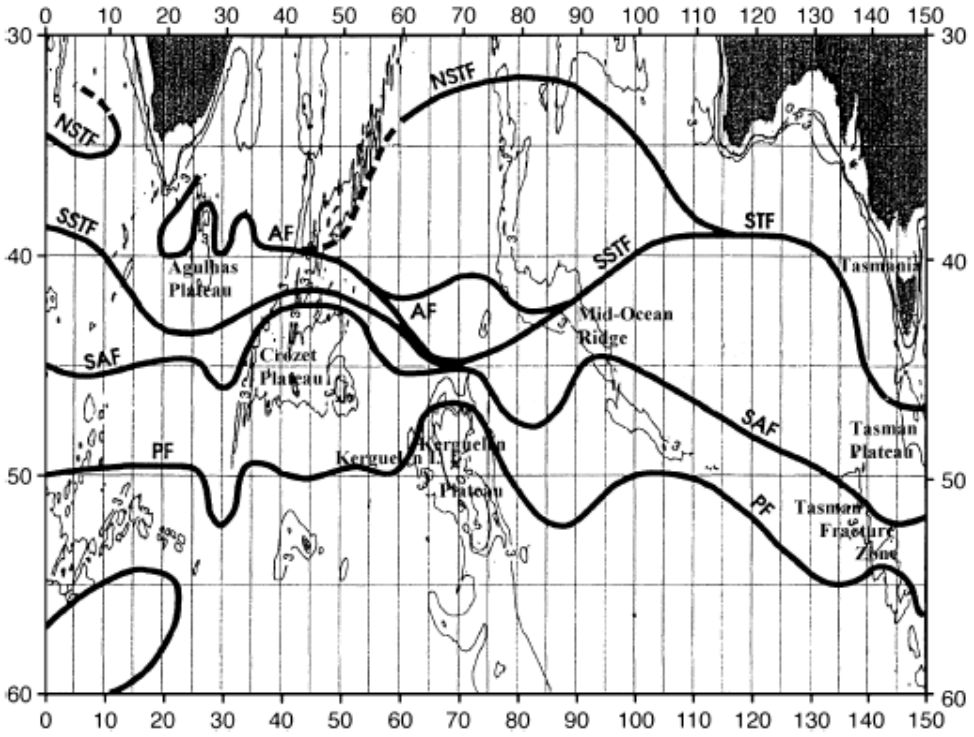

Fig. 2: Study area with frontal paths according to Belkin and Gordon (1996).

The Southern ocean is a high nutrient low chlorophyll region, however it is a major sink for atmospheric CO_2 (Heinze et al., 1991). Marginal ice zones that form sea ice cover show large gradients in pCO_2 and change rapidly from CO_2 undersaturated conditions in summer to CO_2 saturation in winter. Antarctic cold water areas, in combination with their potential physical sink function, are of major interest in the studies of greenhouse gases, especially CO_2 (Poisson and Chen 1987, Anderson and Jones 1991).

At present, the Southern Ocean accounts for ~40% of the oceanic sink of anthropogenic CO_2 (Sabine et al., 2004). The carbon uptake capacity of the ocean seems to have reduced recently (Sabine et al., 2004; Canadell et al., 2007). There are also concerns for climate interactions that could reduce the efficiency of the carbon sink, a process that is already occurring in the Southern Ocean (Le Quere et al., 2007; Lovenduski et al., 2007), the sampling of which has been both

temporally and spatially sparse owing to its remoteness, difficulty and cost of making such measurements (McNeil et al., 2007). Metzl (2009) showed that the growth rate of oceanic pCO_2 is higher in the subtropical and sub-Antarctic zones of the Southern Indian Ocean compared to other oceans. Areas west of the Crozet Plateau are the key regions where the fronts confluence and split (Belkin et al., 1996 and Park et al., 1998). But still studies in the Indian sector of Southern Ocean are rare compared to the Atlantic and the Pacific sectors.

2.2. Bay of Bengal

The Bay of Bengal is located on the south east part of the Indian continent. The Bay of Bengal experiences semi-annual reversing winds. During northeast monsoon the winds are weak and from north-easterly direction. Whereas during southwest monsoon the winds are relatively strong and from south west direction. Most of the rivers flowing from the Indian subcontinent like the Ganges and Brahmaputra drain into the Bay of Bengal adding tremendous amount of fresh water to the Bay. This freshening reduces the salinity and forms a strong stratified layer. Strong stratification prevents vertical mixing leading to shallow mixed layers (Vinayachandran et al., 2002) and thus preventing vertical supply of nutrients limiting primary production. Along with fresh water the rivers also brings large sediment load (1387×10^6 tons of suspended solids annually) (Subramanian, 1993) in the northern Bay of Bengal making the surface waters turbid which curtails the light penetration.

This process makes the Bay of Bengal less productive as seen from the average annual primary productivity in the Bay (fig. 3). The reason behind this is that the strong stratification prevents supply of nutrients to the surface layers (Prasanna

Kumar et al., 2002).

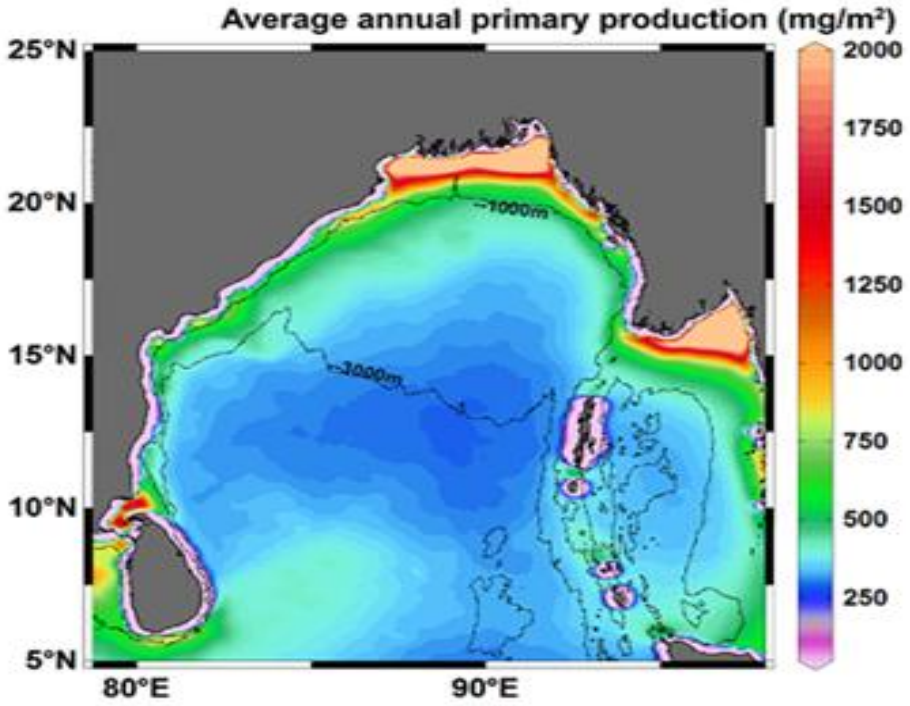

Fig. 3: Map showing average annual primary productivity (mg/m^2/yr) in Bay of Bengal.

Recent studies indicated the presence of several cyclonic and anticyclonic eddies which alters the hydrography and biogeochemistry of the Bay of Bengal (Prasanna Kumar et al., 2004; Nuncio, 2007). These eddies (cyclonic) enhances the biological productivity as compared to non-eddy region (Prasanna Kumar et al., 2007). Apart from eddies, the Bay of Bengal is also a site for tropical cyclones. The cyclones are associated with large-scale air-sea exchange, deepening of mixed layer and increased biological productivity through pumping of nutrients (Prasanna Kumar et al., 2004, Sardessai et al., 2010).

Objectives

1. To investigate carbon and carbon fluxes in the oceanic environment with particular reference to the selected sites in Bay of Bengal and Southern Ocean.
2. To decipher the variations in nutrient dynamics and it's bearing on carbon dioxide.
3. To understand the impact of ocean acidification on marine organisms

Chapter 3

Material and Method

3.1. Sampling Details

3.1.1. Southern Ocean (open ocean)

3.1.1.1 March 2009

Surface seawater and air sampling was carried out onboard *R/V Akademik Boris Petrov* along the two transects, T_W (30° to 65°S along 48°E) and T_E (30°S to 66°S along 57.30°E) during February-March 2009 in the Indian sector of Southern Ocean. Samples were collected at standard depths upto 1000m along the two transects using a Rosette sampler with 5 litre Niskin bottles mounted on the CTD assembly. Surface water samples were collected along coastal Antarctica between 48°E to 57.30°E.

3.1.1.2 February 2010

Surface seawater was carried out onboard *ORV Sagar Nidhi* along the two transects, T_W (30° to 65°S along 48°E) and T_E (30°S to 66°S along 57.30°E) during January-February 2010 in the Indian sector of Southern Ocean (Fig. 4). Samples were collected at standard depths upto 120m along T_E using a Rosette sampler with 5 litre Niskin bottles mounted on the CTD assembly.

3.1.1.3 January 2012

Surface seawater was sampled onboard *Ivan Papavin* between (20° to 72° E) and (38°S to 66°S) during January 2012 in the Indian sector of Southern Ocean (Fig. 4).

3.1.2 Southern Ocean (Coastal Antarctic region)

Three underway surveys of the Enderby Basin were conducted onboard the R/V Akademik Boris Petrov, ORV Sagar Nidhi and Ivan Papanin during late Austral

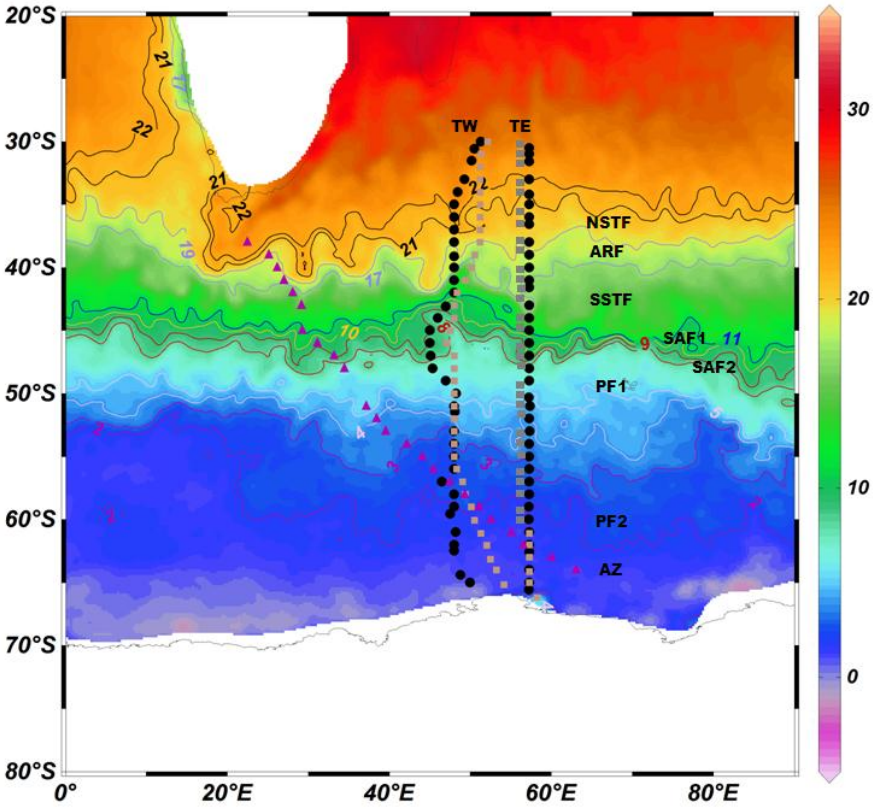

Fig. 4: The research area between 30-66°S along 48°E and 57.30°E in the Indian Sector of Southern Ocean (2009 & 2010). Climatological AMSR-E Sea Surface Temperature for 2010. Fronts were marked following Anilkumar et al., 2006. Black circles, grey boxes and pink triangles denote sampling points during March 2009, February 2010 and January 2012, respectively.

and Austral summer of 2009, 2010 and 2012 respectively. The surveys were conducted during February 2010, when freezing was yet to commence, and during January 2012 (early summer) and March 2009 (early winter), when surface was covered with sea ice layer (Fig. 5).

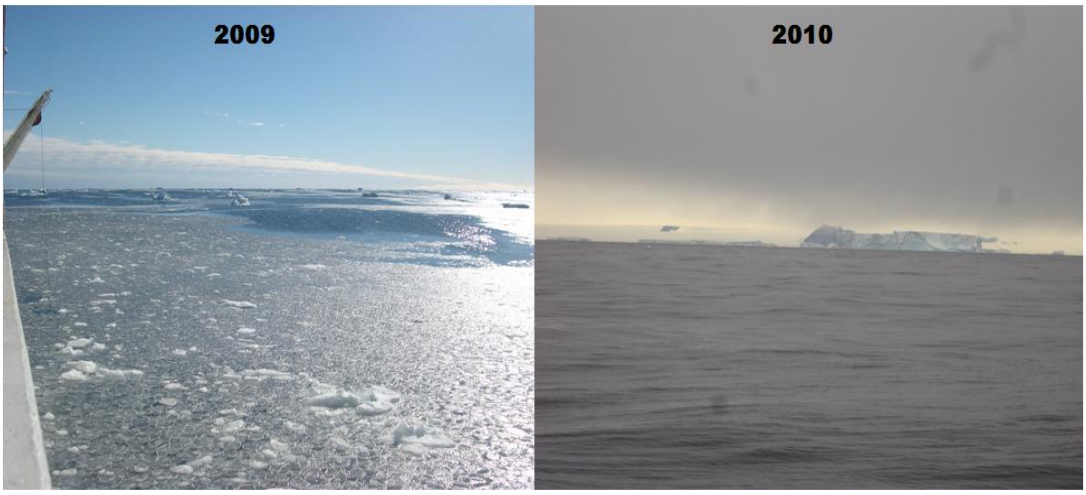

Fig. 5. Photographs taken onboard Boris Petrov and Sagar Nidhi during the March 2009 and February 2010, depicting the sea ice condition

During 2009 a horizontal transect was conducted, whereas during 2010, apart from the horizontal transect, 2 vertical transects were carried out (T_W & T_E). During 2012, a wider area from 18°E to 72°E was covered (Fig. 6).

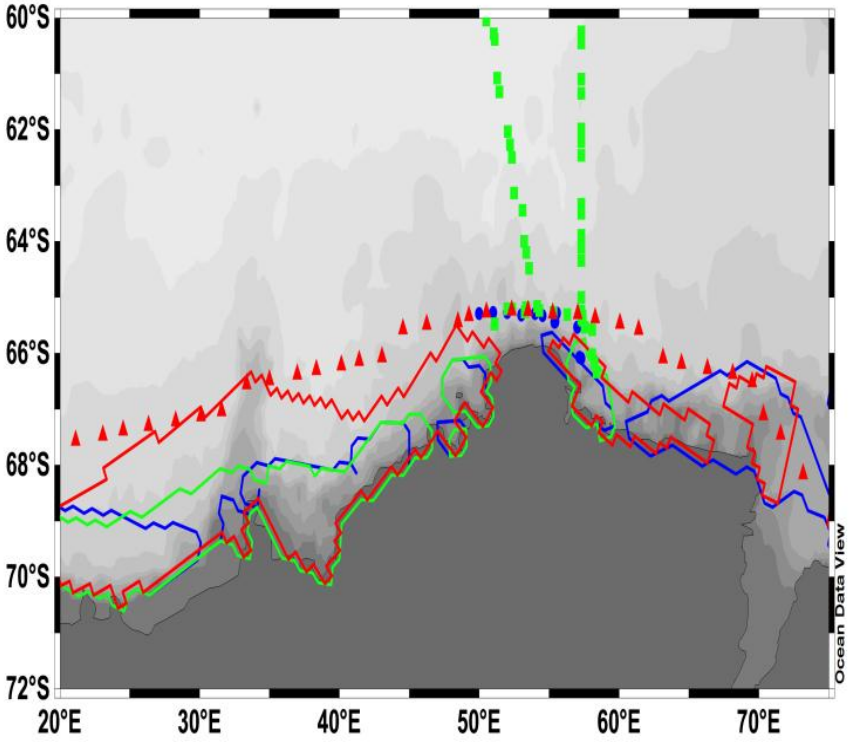

Fig.6. Study area map, with station locations. Blue dots are the stations occupied during 2009 expedition, green dots are the stations occupied during 2010 expedition and red during 2012. The sea ice extent is marked with the corresponding color for each year.

3.1.3 Sea ice samples

During Antarctic expedition of 2012, sea ice was drilled upto 1.7 m, and the seawater samples under the ice cover were collected at 8 different locations (Fig. 7).

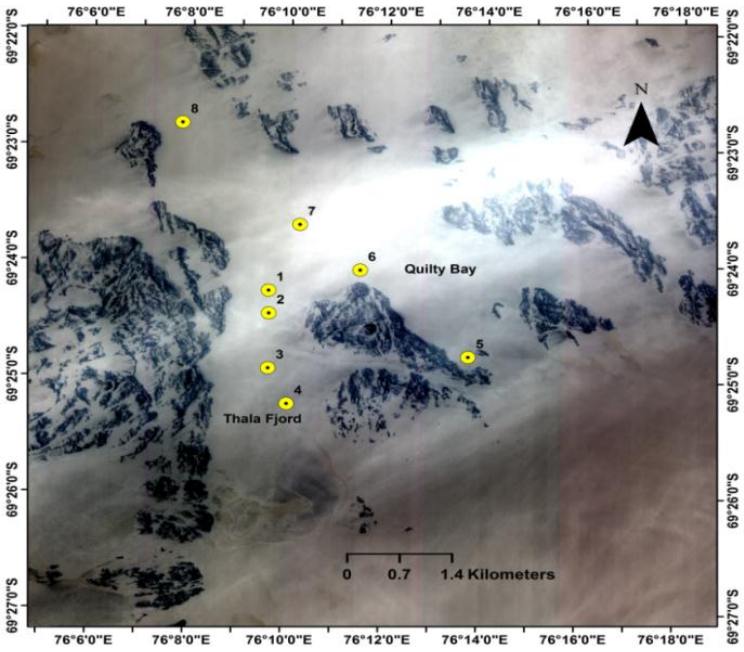

Fig.7. The locations of drilled points in East Antarctica, in Indian Sector of Southern Ocean.

3.1.4 Coastal Bay of Bengal

Vertical profiles were collected from six different coastal regions along the east coast of India onboard ORV *Sagar Sampada* during april-may 2009 (Fig. 8). At each region, samples at 5 stations were collected based upon the water depths

(50, 100, 200, 500 and 1000). Vertical profiles were taken at 1000 m depth station of each region using a Rosette sampler with 5 litre Niskin bottles mounted on the CTD assembly.

Water samples were collected from coastal western Bay of Bengal, including samples from upwelled water near the coastal Thamnapatnam (in Tamil Nadu, India). Five stations were selected based on water depths (50, 100, 200, 500, 1000m) at Karaikal, Cuddalore, Chyeur, Chennai, Thamnapatnam, Singarayakonda. Vertical profiles were taken at each station with 1000m water depth.

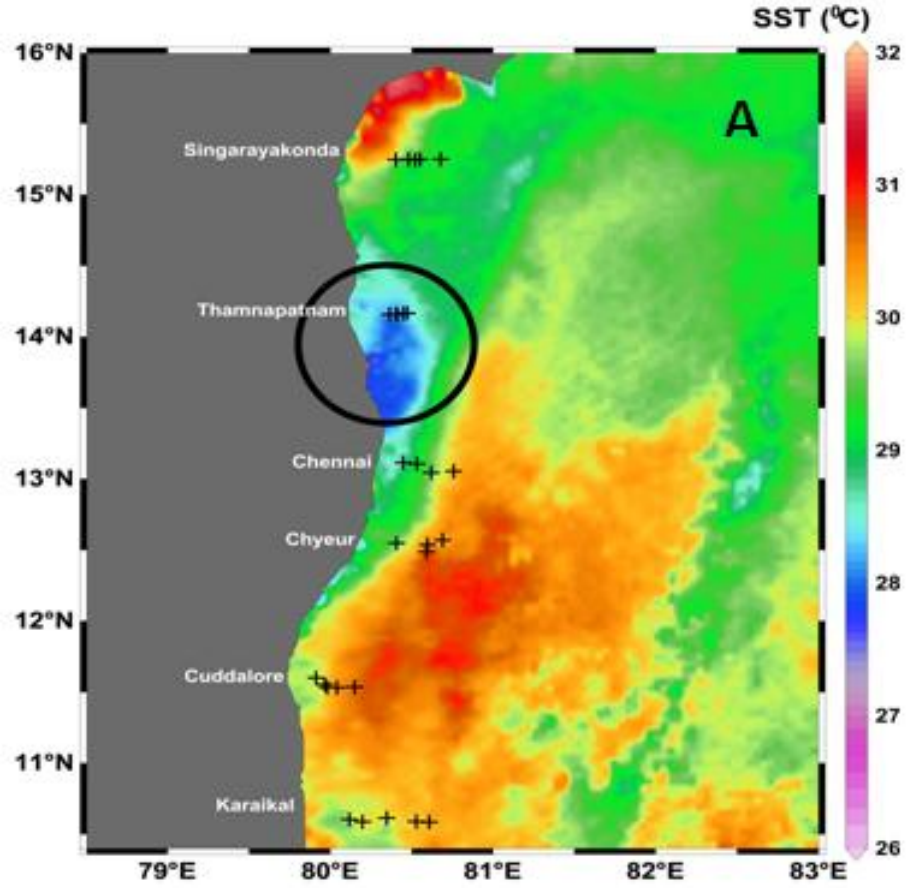

Fig.8. Study area map with sample locations along east coast of India. Sampling locations (+) overlaid over the NOAA-AVHRR weekly composite sea surface temperature (SST) map during 9th-16th May 2009. Circle showing

the cooling feature (~27ºC to ~27.5ºC) associated with the upwelled water near Thamnapatnam.

3.1.5 Open BOB waters

Sampling was carried out between 86-89°E in Bay of Bengal onboard ORV *Sagar Kanya* during December 2007. Time series measurements were done within and outside a cyclonic eddy (Fig 9).

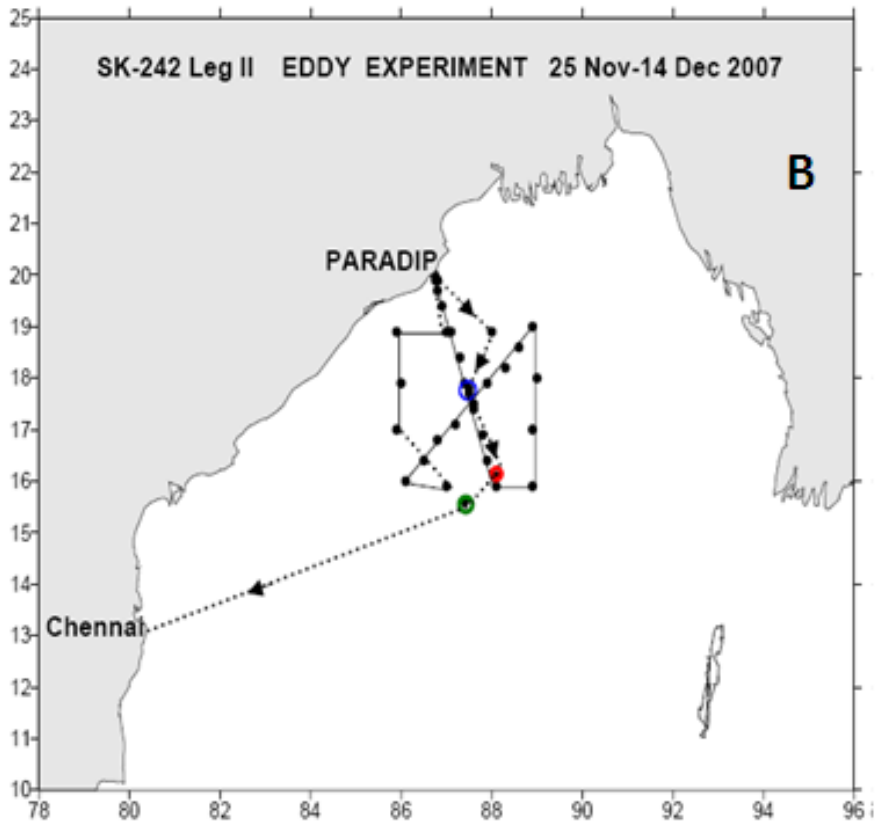

Fig. 9. Cruise track and station locations during SK 242. Blue and red circles indicate time series stations within and outside the cyclonic eddy.

3.2 Analytical Methods

3.2.1 Physical Oceanographic Data

Sea surface temperature (SST) was also recorded using an onboard bucket thermometer (accuracy: ± 0.1°C). Salinity was measured with the help of an Autosal. The error between Salinity measured by CTD and Autosal was ±0.1%.

3.2.2 pCO_2 calculation

3.2.2.1 Partial pressure of CO_2 in seawater (pCO_2^{sw})

For measuring the total carbon dioxide (TCO_2) content of seawater samples, a subsample was acidified with 8.5% phosphoric acid to 1 M H_3P0_4. Gaseous CO_2 was captured in an ethanol-amine solution with an indicator. The solution was photometrically back titrated by a coulometer (model 5014 of U.I.C. Inc., USA). The reliability of the coulometric titration was regularly checked with certified referenced materials (CRMs, Batch # 92) provided by A. Dickson (SIO, University of California). Standards were run with every batch of 50 samples. The TCO_2 of the standard CRM was 1996 µM. The accuracy estimated from the CRMs values was 2 μM. The precision estimated from replicate analysis of samples (mean difference) was on average 2μM. The pH was measured by a spectrophotometer following Byrne and Breland (1989). The pH_T of the samples was then corrected to the *in situ* temperature following equation of Gieskes, (1969). Analytical precision was ~0.002 for pH_f, whereas accuracy was ±0.005. The seawater pCO_2 was calculated with TCO_2 and pH_T using the program of Lewis and Wallace (1998) with the dissociation constants of Mehrbach et al., (1973) as refit by Dickson and Millero, (1987). The precision estimated for pCO_2 analysis from replicate analysis of samples was ±5 μatm. The accuracy estimated for computed pCO_2 is of ±5µatm, whereas standard error is ±4 µatm.

A total of 1414 samples were analysed during this study. Out of which 264 surface samples and 446 deeper depth samples were studied from Southern Ocean. 8 under-ice surface samples were studied. From Bay of Bengal 104 surface samples and 592 samples from deeper depths were studied. The data sets are significant as seen from the single factor Anova, as shown in table 1 to 5.

Table 1: Anova Single Factor for pCO_2 variations during March 2009 along 48E and 57.30E.

SUMMARY						
Groups	*Count*	*Sum*	*Average*	*Variance*	pCO2	
Column 1	35	11822.53	337.7867	2100.632	48E 2009	
Column 2	36	11353.2	315.3667	1008.08	57.30 E 2009	

ANOVA

Source of Variation	*SS*	*df*	*MS*	*F*	*P-value*	*F crit*
Between Groups	8920.393	1	8920.393	5.768344	0.019014852	3.979807
Within Groups	106704.3	69	1546.439			
Total	115624.7	70				

Table 2: Anova Single Factor for pCO_2 variations during February 2010 along 48E and 57.30E.

SUMMARY						
Groups	*Count*	*Sum*	*Average*	*Variance*		
Column 1	36	10795.59	299.8774	2973.936867	48E 2010	
Column 2	36	9253.737	257.0482	3108.844364	57.30 E 2010	
ANOVA						
Source of Variation	*SS*	*df*	*MS*	*F*	*P-value*	*F crit*

Between Groups	33018.05	1	33018.05	10.85623595	0.001547268	3.977779
Within Groups	212897.3	70	3041.391			
Total	245915.4	71				

Table 3: Anova Single Factor for pCO_2 variations during March 2009 and February 2010 along 48E.

SUMMARY						
Groups	*Count*	*Sum*	*Average*	*Variance*		
Column 1	36	12149.53	337.4871	2043.846	48 2009	
Column 2	36	10795.59	299.8774	2973.937	48 2010	
ANOVA						
Source of Variation	*SS*	*df*	*MS*	*F*	*P-value*	*F crit*
Between Groups	25460.76	1	25460.76	10.14821	0.002158	3.977779
Within Groups	175622.4	70	2508.892			
Total	201083.2	71				

Table 4: Anova Single Factor for *p*CO_2 variations during March 2009 and January 2012.

SUMMARY						
Groups	*Count*	*Sum*	*Average*	*Variance*		
Column 1	28	9572.359	341.87	2199.907	March	
Column 2	25	7182.805	287.3122	1144.354	January	
ANOVA						
Source of Variation	*SS*	*df*	*MS*	*F*	*P-value*	*F crit*
Between Groups	39312.95	1	39312.95	23.08214	0.000141	4.030392
Within Groups	86861.99	51	1703.176			
Total	126174.9	52				

Table 5: Anova Single Factor for *p*CO_2 variations during February 2010 and January 2012.

SUMMARY						
Groups	*Count*	*Sum*	*Average*	*Variance*		
Column 1	25	7182.805	287.3122	1144.354	January	
Column 2	28	8860.286	316.4388	2542.336	February	
ANOVA						
Source of Variation	*SS*	*df*	*MS*	*F*	*P-value*	*F crit*
Between Groups	11204.75	1	11204.75	5.945864	0.018274	4.030392
Within Groups	96107.57	51	1884.462			
Total	107312.3	52				

3.2.2.2 Partial pressure of CO_2 in air (pCO_2^{atm})

The Air samples were collected by means of 1 L Pyrex flasks. The flasks were evacuated using a rotary pump and then opened for ~2 minutes on the windward side of the ship, about 15 m above sea level. After the sample collection, the flasks were closed by means of high vacuum stopcocks and stored until the analysis. The quantitative separation of the CO_2 from air was carried out in the laboratory by pumping the flask air samples in a high vacuum line at a rate of about ~5 mL/min through a digital mass flow controller and a spiral Pyrex trap cooled at liquid nitrogen temperature (-196 ^oC). After the completion of the air pumping, the Pyrex trap was isolated by means of high vacuum stopcocks and heated to about −80°C by means of an ethyl alcohol-liquid nitrogen slash. The evolved CO_2 was measured by expanding it in a fixed volume with a calibrated pressure gauge. CO_2 standard gas of known concentration (375 ppm) was regularly measured. The error in the concentration measurement is 0.1%.

3.2.3 Flux calculation

The CO_2 exchange flux (mmol/m^2/d) across the air-sea interface was calculated using equation given in Wanninkhof, (1992).

$$F = k \times s \times \Delta pCO_2 \quad (3)$$

Where *k* is the gas transfer velocity, *s* is the solubility of CO_2 gas in seawater (*Weiss*, 1974), and ΔpCO_2 is the difference between surface seawater pCO_2 and atmospheric pCO_2 (pCO_2^{sw} - pCO_2^{atm}). The air-sea pCO_2 difference is computed using the atmospheric pCO_2 values from Global View CO_2. In-situ ship board wind data was used for flux calculation.

3.2.4 Chlorophyll *a*

For chlorophyll *a* measurement, 5 litre seawater samples were filtered on 0.7 µm pore size 47 mm polycarbonate filters at low vacuum. The pigments were extracted from the phytoplankton in 90% acetone with the aid of a mechanical tissue grinder and allowed to steep for a minimum of 2 h, but not to exceed 24 h, to ensure thorough extraction of the chlorophyll *a*. The filter slurry was centrifuged for 15 min to clarify the solution. An aliquot of the supernatant was transferred to a glass cuvette and fluorescence was measured on fluorometer (Model 10-AU, Turner Designs) before and after acidification to 0.003 N HCl with 0.1 N HCl. Sensitivity calibration factors, which have been previously determined on solutions of pure chlorophyll *a* of known concentration, are used to calculate the concentration of chlorophyll *a.* Precision, measured as relative standard deviation was always <2%.

3.2.5 Nutrient analysis

Nutrients (silicate, phosphate, nitrate and nitrite) were measured with a Skalar Autoanalyzer by standard colorimetric methods following Grasshoff (1983).

Standards were used to calibrate the auto-analyzer and frequent baseline checks were made. The standard deviation for duplicates was 0.07 µM for silicate, 0.06 µM for nitrate, 0.01 µM for nitrite and phosphate. Standard error for the measurement was ±0.4 µM, ±0.02µM and ±1.5 µM for nitrate, phosphate and silicate respectively.

3.2.6 TOC analysis

Total Organic Carbon (TOC) which is a sum of Dissolved organic carbon (DOC) and Particulate organic carbon (POC) was measured using the TOC-V-CSH analyzer by high temperature catalytic oxidation method. Standard deviations of triplicate measurements were found to be about 0.2 %.

3.2.7 Foraminiferal analysis

Since carbonates control the shell thickness of calcareous organisms, inorder to investigate any dissolution of foraminiferal shells, samples were collected in 2009 expedition. The samples were collected by filtering water through 63µm mesh. Immediately after collection, samples were preserved in 5% buffered formalin. The planktic foraminifera were identified according to the taxonomy of Kennett and Srinivasan (1983). For microscopic imaging specimens were analyzed using a Scanning Electron Microscope (JEOL 6360 LV SEM).

3.2.8 Iceberg analysis

Iceberg samples were collected using nylon nets. Ice samples were transferred to acid-washed zip-lock plastic bags and stored at -20°C. Later in lab, the samples were melted and filtered through 0.45 µm filter paper. The filter paper was analyzed using a Scanning Electron Microscope (JEOL 6360 LV SEM) equipped with an Oxford Instruments Energy Dispersive Spectrometry (EDS) and INCA software.

3.2.9 Drilled Samples

Sea ice was manually drilled, the thickness was 1.7 m, and the water samples under the sea ice cover were collected (Fig. 9).

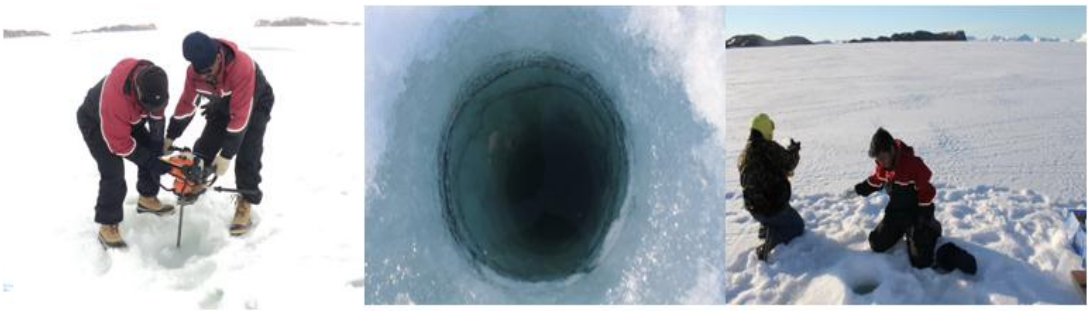

Fig.10. Collection of samples by drilling sea ice in East Antarctica, in Indian Sector of Southern Ocean

3.2.10 Satellite Derived Environmental Parameters

SeaWiFS (Sea-viewing Wide Field-of-view Sensor) based Level-3 global standard mapped images (SMI) of climatological Chl-*a* values (9-km spatial resolution) were acquired from Goddard Space Flight Centre (GSFC), for the study period. Chl-*a* datasets based up on SeaWiFS operational bio-optical algorithm (i.e ocean color, OC4) developed by O'Reilly et al., (2000) and later updated (OC4v6) by National Aeronautics and Space Administration (NASA) Ocean Biology Processing Group (OBPG). The above algorithm yields a strong linear correlation coefficient (r = 0.892) with *in situ* Chl-*a* on global scale that includes samples from all water types (O'Reilly et al., 2000). Level-3 Pathfinder SSTs data set (4-km spatial resolution) from the Advanced Very High Resolution Radiometer (AVHRR), were obtained from NASA's Jet Propulsion Laboratory (JPL). Multiple satellite altimeters (Jason-1, TOPEX/Poseidon, ERS 1/2, and GFO) based merged product on sea surface height anomalies (SSHA) at a spatial resolution of 1°×1° were obtained from the

NASA Physical Oceanography Distributed Active Archive Center (PODAAC). QuikScat measured wind vector (scalar wind speed with corresponding u and v component) data files available at spatial resolution of 25 km were downloaded from www.ssmi.com. The wind stress (τ) was then calculated using variable drag coefficients (C_D) given by Yelland and Taylor (1996). Integrated primary productivity was modelled by Relative vertical distribution model following Behrenfeld and Falkowski 1997.

3.2.11 Phytoplankton Analysis

Phytoplankton samples were filtered through 5 µm multiple plankton net (Hydrobios, Kiel, Germany). Samples were preserved in 5% buffered formaldehyde solution and analyzed over Nikon microscope following Uthermöhl (1958).

3.2.12 Dissolved Oxygen

Dissolved oxygen was measured following winkler's method. Standard error for the measurement was ±3.6 µM.

Table 6: Anova Single Factor for Dissolved oxygen analysis during March 2009 and January 2012.

SUMMARY						
Groups	*Count*	*Sum*	*Average*	*Variance*		
Column 1	26	7864.179	302.4684	2440.083	March	
Column 2	23	8370.356	363.9285	1990.16	January	
ANOVA						
Source of Variation	*SS*	*df*	*MS*	*F*	*P-value*	*F crit*
Between Groups	46098.98	1	46098.98	20.677	0.0000382	4.0471
Within Groups	104785.6	47	2229.481			
Total	150884.6	48				

Table 7: Anova Single Factor for Dissolved oxygen analysis during March 2009 and February 2010.

SUMMARY						
Groups	*Count*	*Sum*	*Average*	*Variance*		
Column 1	37	10454.46	282.553	1831.642	March	
Column 2	36	12148.67	337.4632	4092.11	February	
ANOVA						
Source of Variation	*SS*	*df*	*MS*	*F*	*P-value*	*F crit*
Between Groups	55015.81854	1	55015.82	18.67502	0.0000495	3.975810047
Within Groups	209162.9585	71	2945.957			
Total	264178.777	72				

3.3 Lab Experiment

Live Sea urchin specimens were sampled from coastal Antarctic waters with the help of a Russian scuba diver. Lab experiment were conducted by subjecting it to CO_2-acidified seawater, to mimic the scenarios defined by IPCC models predicted for the Southern Ocean by the end of 2100. The species were identified. Specimens were reared in 3 different pH conditions (pH 6, 7.8 and 8.1). After, 48 hours, the shells of sea urchin were placed on an aluminum stub and micrographs were taken using Scanning Electron Microscope (JEOL 6360 LV SEM).

Chapter 4

Results

4.1. Hydrography

4.1.1. Southern Ocean

Frontal zones are defined by sharp changes in temperature and salinity, and are also areas of enhanced biological production (Eynaud et al., 1999). We adopted surface temperature gradient and salinity as property indicators for identification of frontal zones (Anilkumar et al., 2005 and Luis and Sudhakar, 2009). We identified four fronts, namely: Agulhas Retroflection Front (ARF), Sub Tropical Front (STF), Sub Antarctic Front (SAF) and the Polar Front (PF). The STF divides warmer tropical waters and colder sub-tropical waters and is seen in our data as a sharp temperature gradient from 41°S to 43°S at T_W and 43°S to 46°S at T_E. The SAF was found from 43°S to 48°S at T_W and from 46°S to 48°S at T_E and is marked by a sharp temperature decrease. The PF, considered to be an important ecological boundary, was found between 49°S to 55°S at T_W and from 50°S to 56°S at T_E. The Polar Frontal Zone (PFZ) is characterized by strong lateral mixing and relatively low biological production (Trull et al., 2001). A comparison between all the 3 years transects show that the surface temperature was nearly same from 30°S to 66°S (Fig. 11, Table 8). However the temperature is slightly higher during February and lowest during March, which could be due to late austral summer (March) sampling in 2009 (Fig. 11). Surface temperatures varied from 25°C to 0°C upto 60°S, whereas along Antarctic coast it varied from 1°C to -2.5°C. Surface salinity was however higher during March and lowest during February (Table 9). Salinity ranged from 32.2 to 35.7 upto 60°S and in Antarctic coast it ranged from 32.5 to 34.

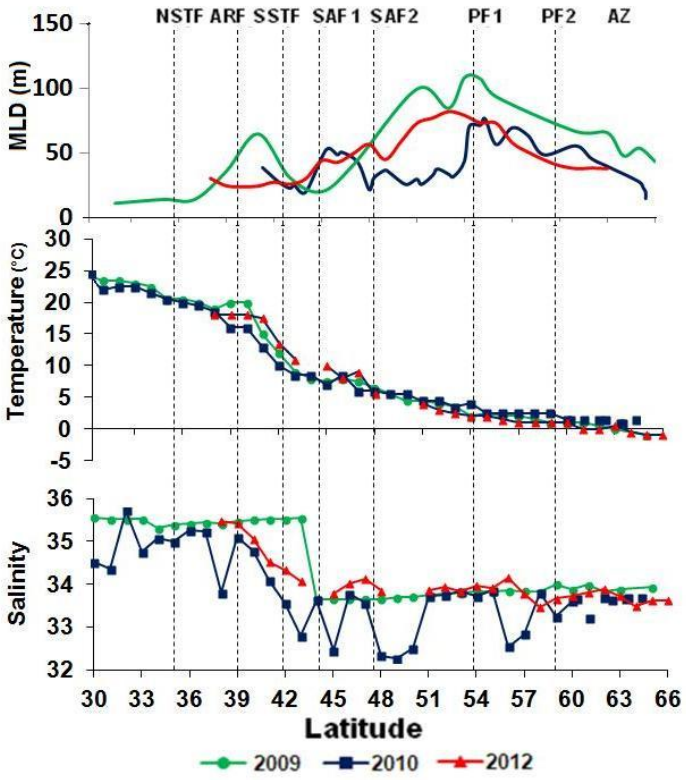

Fig.11. Latitudinal variations in Temperature, Salinity and MLD during March, February and January.

The Mixed-layer depth (MLD) was quite shallow at all stations sampled during January ranging over 50m in the PF. By the end of January mixed layer started shoaling. During February, shallow mixed layers were found upto 45m due to enhanced stratification as a result of melt waters (Fig 11). By March, mixed layers increased again to around 60 m, with a deeper mixed layers >100m at the PF.

Longitudinal comparison during March and February shows that surface temperature and salinity are lower along T_W as compared to T_E during both March and February periods (Fig. 12). However surface temperatures during March were higher along T_W upto 40°S.

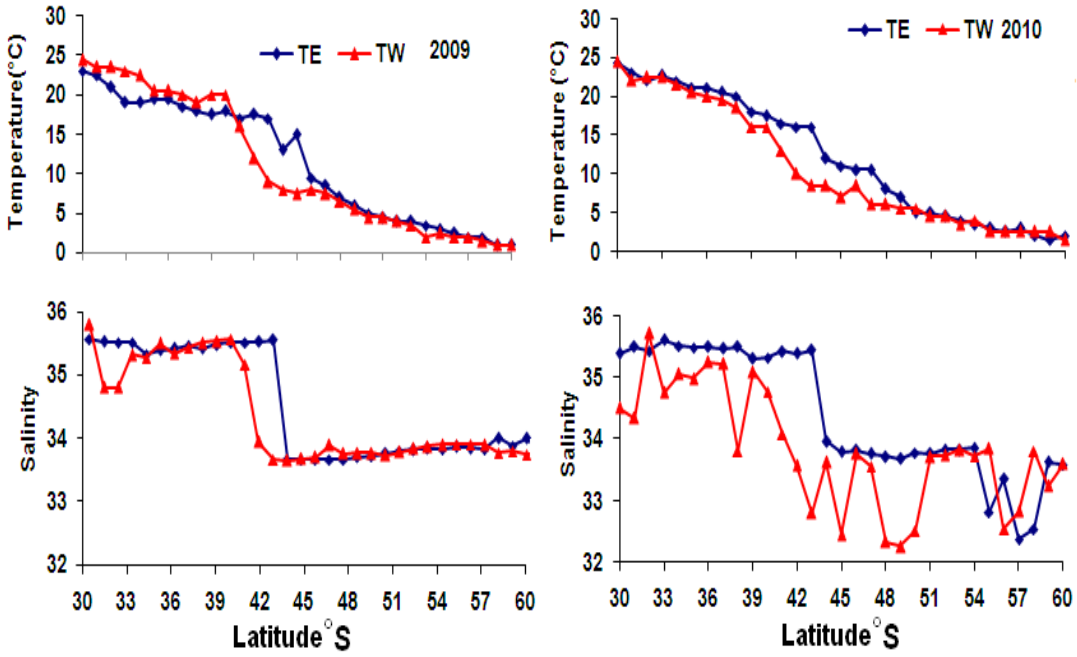

Fig.12. Longitudinal comparison in Temperature and Salinity along T_W and T_E during March 2009 and February 2010.

Vertical distribution shows that surface temperature and salinity are lower along T_W as compared to T_E during March, however temperatures are higher along T_W upto the subtropical front (Fig. 13). A distinct feature is seen at 46°S along T_W in the vicinity of the Crozet Island, which may be responsible for the lower temperatures due to bathymetry driven upwelling. The subtropical front shifts from 41°S along T_W to 43°S along T_E indicating much stronger physical processes along T_W. The frontal positions keep changing with time.

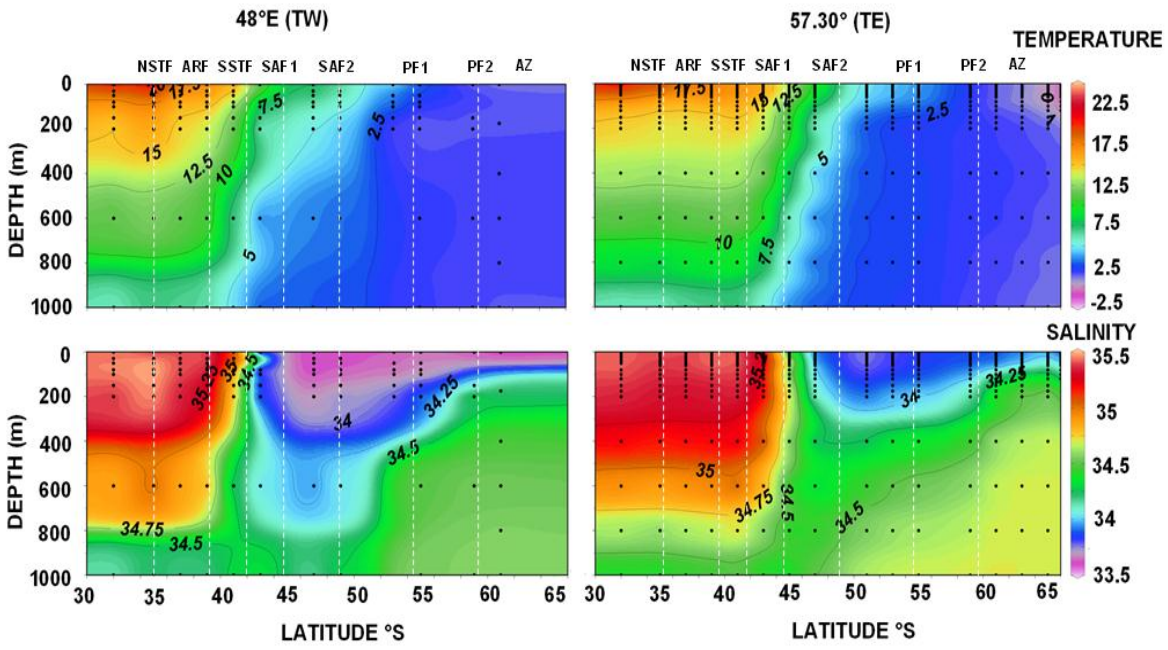

Fig.13. Vertical distribution of Temperature and Salinity during March along the two transects T_E (57.30 °E) and T_W (48°E).

The largest variations are seen at the subtropical front where rapid decrease in temperature and salinity are seen. A comparison of March and February shows lower temperature and salinity waters south of 60° during February, indicating influence of glacial melt water (Fig. 14). Figure 14 summarises the vertical profile data and the differences between the February and March stations. Comparison of March and February shows lower temperature and salinity south of 60°S during February, indicating influence of melt water. Surface salinity values drops upto 32.75. This is well supported by the sea ice extent map showing melting induced less sea ice extent during February (Figure 6). From the straight gradient in the vertical profiles it is clearly seen that the mixing is high during March leading to deeper MLD as seen in Figure 11.

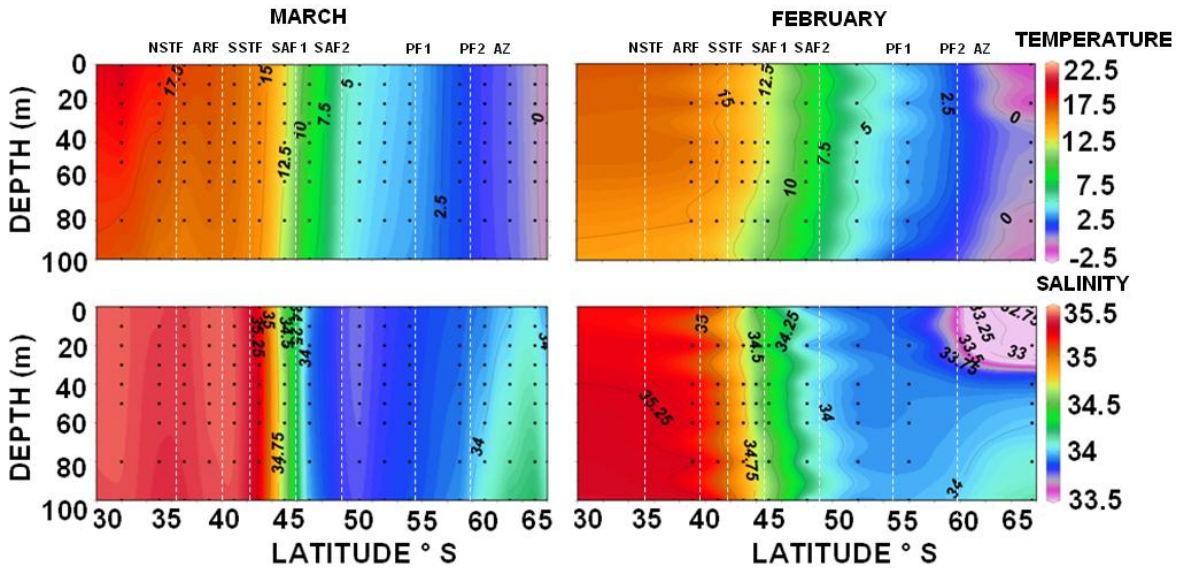

Fig.14. Vertical distribution of Temperature and Salinity during March and February along T_E.

Table 8: Latitudinal variations in Temperature during March 2009, February 2010 and January 2012.

LATITUDE (°S)	2009 (48° E)	2009 (57° 30'E)	2010 (48° E)	2010 (57° 30'E)	2012
30°S	24.5	23	24.5	24.37	
31°S	23.5	22.5	22	23.02	
32°S	23.5	21	22.5	22	
33°S	23	19	22.5	22.71	
34°S	22.5	19	21.5	21.92	
35°S	20.5	19.5	20.5	21	
36°S	20.5	19.5	20	21	
37°S	20	18.5	19.5	20.5	
38°S	19	18	18.5	20	18
39°S	20	17.5	16	18	18
40°S	20	18	16	17.5	18
41°S	15	17	13	16.5	17.5
42°S	12	17.5	10	16	13.5
43°S	9	17	8.5	16	11
44°S	8	13	8.5	12	
45°S	7.5	15	7	11	10
46°S	8	9.5	8.5	10.5	8
47°S	7.5	8.5	6	10.5	9
48°S	6.5	7	6	8	5.5
49°S	5.5	6	5.5	7	

50°S	4.5	5	5.5	5	
51°S	4.5	4.5	4.5	5	4
52°S	4	4	4.5	4.5	3
53°S	3.5	4	3.5	4	2.5
54°S	2	3.5	4	3.5	2
55°S	2.5	3	2.5	3	2
56°S	2	2.5	2.5	2.5	1.5
57°S	2	2	2.5	3	1
58°S	1.5	2	2.5	2	1
59°S	1	1	2.5	1.5	1
60°S	1	1	1.5	2	1
61°°S	1	1	1.5	1.5	0
62°S	0.5	0.5	1.5	1	0
63°S	0	0.5	1.5	1	0.5
64°S		0.5	1.5	0.5	-0.5
65°S	-1	0	1.5	0.5	-1

Table 9: Latitudinal variations in Salinity during March 2009, February 2010 and January 2012.

LATITUDE (°S)	2009 (48° E)	2009 (57° 30'E)	2010 (48° E)	2010 (57° 30'E)	2012
30°S	35.56464	35.8017	34.51	35.39	
31°S	35.52146	34.79403	34.35	35.5	
32°S	35.51494	34.79403	35.72	35.44	
33°S	35.5173	35.32111	34.76	35.61	
34°S	35.32329	35.27659	35.07	35.52	
35°S	35.38701	35.49789	34.99	35.49	
36°S	35.42067	35.33457	35.26	35.51	
37°S	35.4567	35.4365	35.23	35.48	
38°S	35.41829	35.50997	33.81	35.51	35.464
39°S	35.48205	35.53671	35.1	35.31	35.422
40°S	35.51314	35.56484	34.78	35.33	35.065
41°S	35.51514	35.16643	34.09	35.43	34.518
42°S	35.52997	33.94303	33.57	35.4	34.337
43°S	35.54939	33.65719	32.8	35.45	34.066
44°S	33.6564	33.63775	33.63	33.97	
45°S	33.6564	33.67329	32.45	33.79	33.785
46°S	33.6564	33.70215	33.77	33.82	34.017
47°S	33.6564	33.87856	33.56	33.76	34.13
48°S	33.6564	33.74654	32.33	33.72	33.843
49°S	33.69508	33.75871	32.26	33.69	
50°S	33.70883	33.75871	32.51	33.78	
51°S	33.74883	33.72061	33.72	33.77	33.851

52°S	33.78896	33.77757	33.74	33.83	33.942
53°S	33.81313	33.8314	33.83	33.83	33.838
54°S	33.82688	33.86933	33.73	33.86	33.958
55°S	33.81804	33.89605	33.85	32.82	33.9
56°S	33.85852	33.90038	32.54	33.35	34.15
57°S	33.84142	33.90352	32.83	32.38	33.782
58°S	33.82079	33.89291	33.81	32.54	33.45
59°S	34.00163	33.76539	33.24	33.63	33.659
60°S	33.8705	33.79014	33.6	33.59	33.732
61°°S	33.9912	33.74084	33.66	33.56	33.803
62°S	33.82079	33.73534	33.31	33.39	33.876
63°S	33.89079	33.92908	33.22	33.29	33.727
64°S		33.97823	33.01	33.53	33.477
65°S	33.92908	33.91255	33.69	33.59	33.62

4.1.2. Bay of Bengal

4.1.2.1. Coastal Bay of Bengal

BoB receives large volume of freshwater from river discharge which makes low sea surface salinity (SSS).

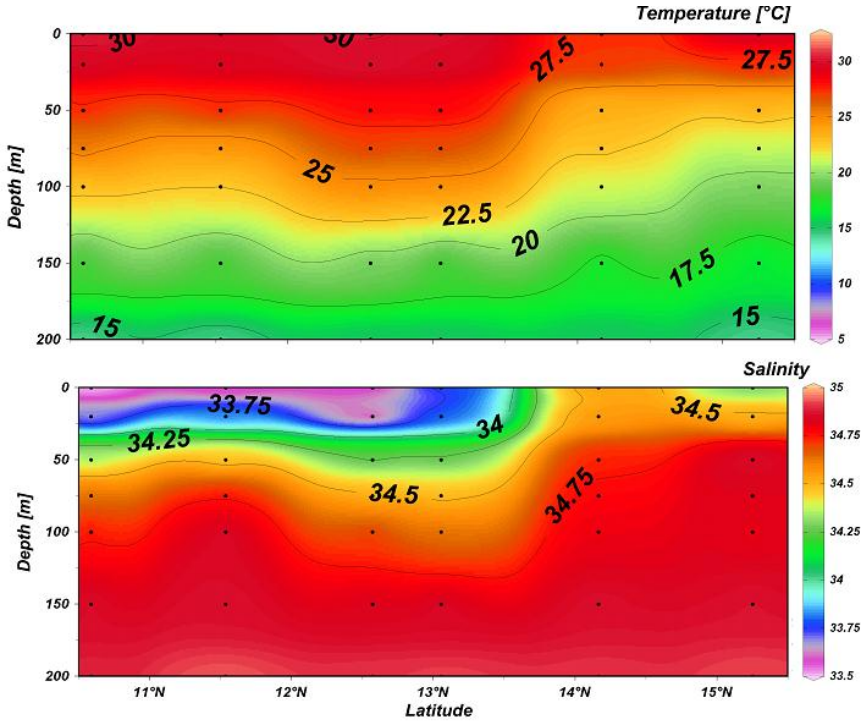

Fig.15. Cross section of the zonal (80.15°E to 80.75°E) physical parameters collected onboard ORV-Sagar Sampada during April -May 2009.

All stations had salinity < 34 psu and temperature >29 ºC except Thamnapatnam (Fig. 15). At Thamnapatnam surface salinity was 34.53 psu and the SST was 27.2 ºC. At Thamnapatnam there is shoaling of water from subsurface to surface.

4.1.2.2. Open Bay of Bengal waters

The vertical distribution of temperature and salinity show lower temperature and higher salinity waters at the surface with in the cyclonic eddy, whereas outside the eddy the temperature and salinity are comparatively higher and lower respectively.

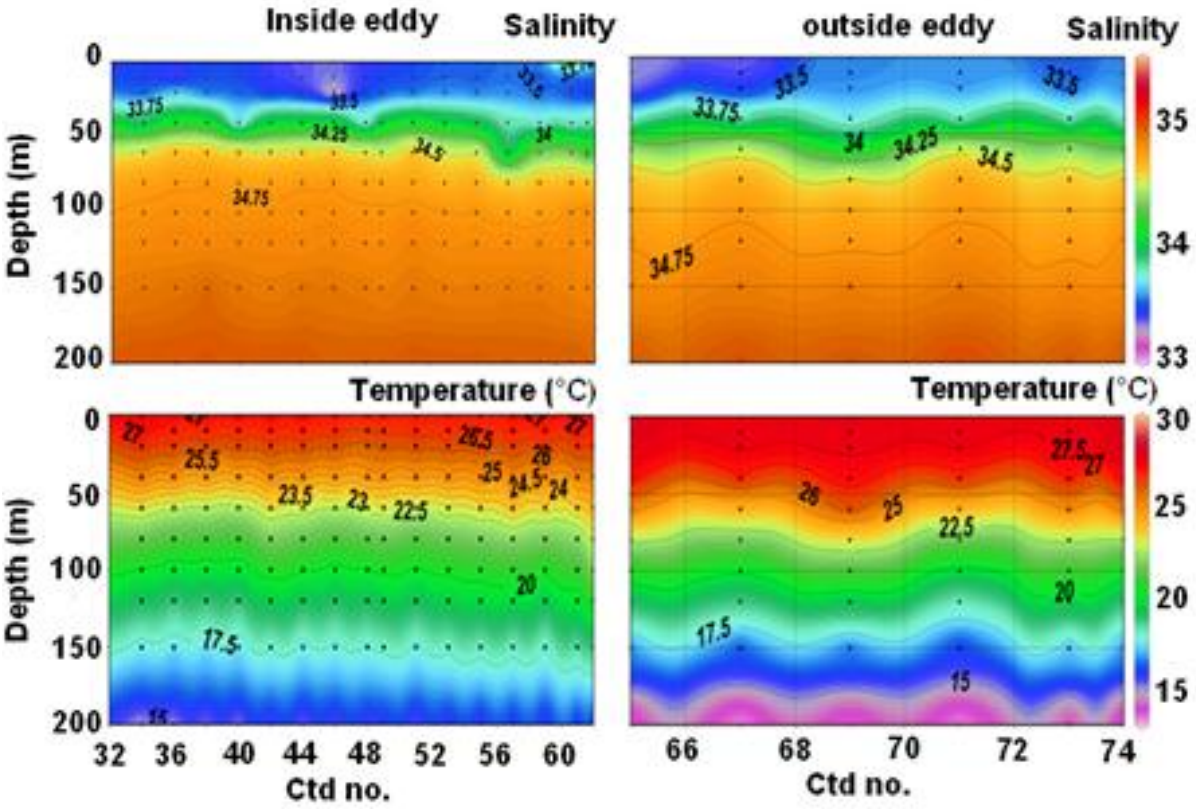

Fig.16. Vertical distribution of temperature and salinity within and outside a cyclonic eddy.

The average temperature within eddy at 50 m was 23°C, whereas outside eddy the average temperature at 50 m was 25°C. The average salinity at 50 m decreased by 0.25 psu from within eddy to outside eddy.

4.2. Nutrient variations

4.2.1. Southern ocean

The Southern Ocean in general is characterized by elevated macronutrient levels. Comparison of March, February and January showed the highest SiO_4 during January, whereas February had the highest PO_4 and NO_3 (Fig. 17, Table 10, 11, 12). During February the nutrient concentrations were higher than in March. During March the maximum surface NO_3, PO_4 and SiO_4 concentrations were found at 60°S reaching maximum concentration of 33.7, 3.38 and 38.7 µM respectively. However, during February maximum concentration of NO_3 and SiO_4

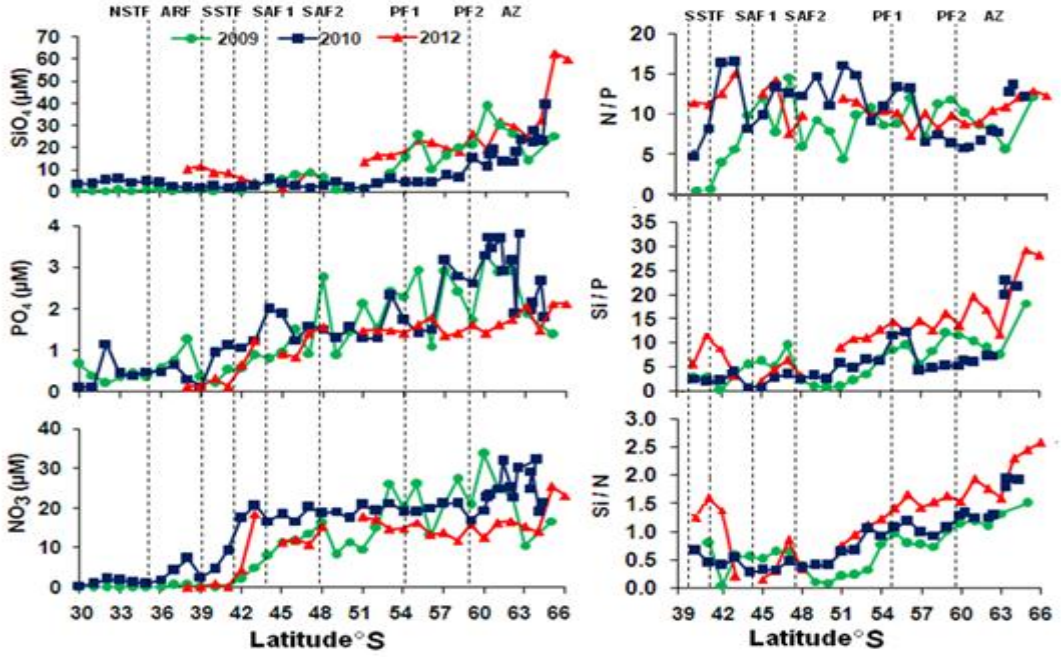

Fig. 17. Spatial distribution of macronutrients and Redfield Ratios in Southern ocean during March, February and January.

were reaching 30 and 39 µM respectively. During March, surface NO_3 concentrations were <1 µM up to the STF and reached to a maximum concentration of 33.67 µM 60°S. Peak nitrate concentrations near 25 µM were found south of PF. In the PF and south, SiO_4 levels of greater than 30 µM were found. SiO_4 concentrations were <2 µM up to the STF and reached to a maximum

concentration of 38.76 µM at 60°S. Similarly PO_4 concentrations were <1 µM up to the STF and reached to a maximum concentrations of 3.3 µM at 60°S. The average N/P ratio from 30°S to the STF was 6, indicating large deviations from the standard Redfield's N/P ratio of 16 and increases towards south upto 9.

Louanchi et al., 2001, studied the Antarctic Polar front in the Indian Ocean sector of the SO and observed minimum values of nitrate (23-24 µM) in late summer (March) and it increased to 28 µM in winter (August-September) following the increase of the Mixed Layer Depth, which entrains subsurface nutrient-rich waters. The Redfield ratios of nutrients indicate that N/P was < 16 for all the study periods. During January the N/P ratio was 10.2 whereas during March it reduced to 6.1; Si/N and Si/P also indicate Silicate limitation from January towards March (Fig.17). The Si/N ratio decreased from 1.32 during January to 0.97 during February and further upto 0.69 during March and was greater than the diatom uptake ratio of 1 (Richards, 1958) only during January.

Higher concentrations are seen also in the vertical profiles of February than in March (Fig 18). The MLD integrated NO_3, PO_4 and SiO_4 during March were 0.2 µM, 0.2 µM, 0.7 µM within STF, 5.2 µM, 0.5 µM, 3.66 µM within SAF, 19 µM, 1.5 µM, 11 µM within PF and 18 µM, 1.8 µM, 23 µM within ANZ respectively. Whereas during February MLD integrated NO_3, PO_4 and SiO_4 were 3.6 µM, 0.4 µM, 4 µM within STF, 13 µM, 1.2 µM and 3.9 µM within SAF, 24 µM, 1.7 µM, 14 µM within PF and 27 µM, 2 µM and 58 µM (Fig 18). NO_3 concentration was 20 µM at 50°S during February, whereas it was 20 µM at 57°S during March. SiO_4 concentrations reached upto 60 µM at 100 m during February, whereas during March it reached

maximum of 30 µM. Phosphate was also high during February reaching 1.5 µM at 47°S, whereas it was 1.5 µM during 56°S during March. From Figure 6 low nutrients during March are clearly visible from the extent of the pink color. Pink color depicting low nutrients extends during March upto SAF1 for NO_3 and PO_4, and upto PF1 for SiO_4, whereas during February the pink color extent upto SSTF for NO_3 and PO_4 and upto SAF2 for SiO_4. Similarly, the reddish orange color depicting high nutrients was seen in coastal Antarctic waters during February, but it was not seen during March.

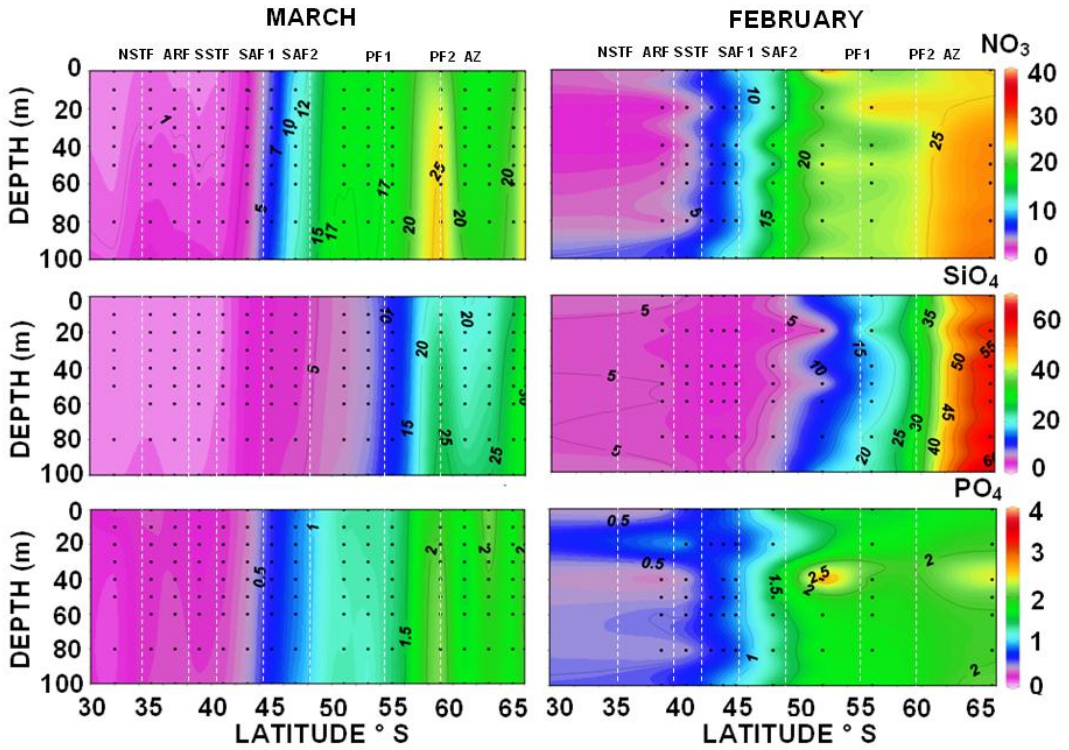

Fig. 18. Vertical distribution of macronutrients in Southern ocean during March and February in micromoles/l (µM).

A comparison of the vertical distribution of Nutrients during March along the 2 transects shows higher nutrient concentrations along TE (Fig 19). NO_3 concentrations were 5 µM around 800 m along TW, whereas it was higher than 5 µM below 400m depth along TE. Vertical mixing brings nutrients and CO_2 from

deeper layers to the surface. Surface NO_3 concentrations were <1 µM up to the STF along the two transects and reached to a maximum concentration of 33.67

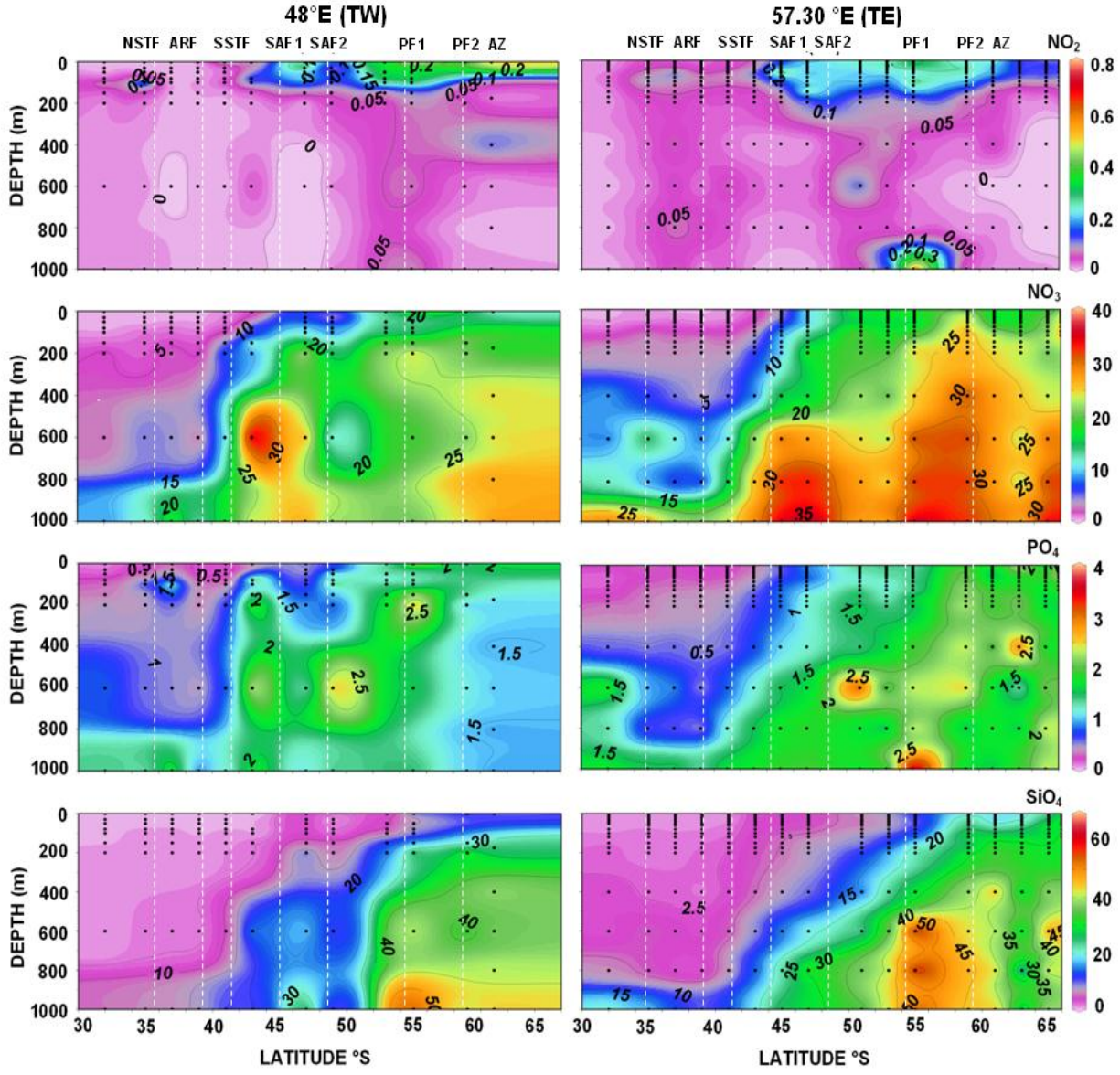

Fig.19. Vertical distribution of macronutrients during March 2009 along the 2 transects TE (57.30 °E) and TW (48°E) in micromoles/l (µM).

µM and 31.65 µM at T_W and T_E respectively at 60°S. SiO_4 concentrations were <2 µM up to the STF along the two transects and reached to a maximum concentration of 38.76 µM and 35.83 µM at T_W and T_E respectively at 60°S. Similarly PO_4 concentrations were <1 µM up to the STF along both the transects

and reached to a maximum concentrations of 3.3 µM and 3.38 µM at T_W and T_E at 60°S and 63°S respectively. During March the maximum surface NO_3, PO_4 and SiO_4 concentrations were found at 60°S and along T_W reaching maximum concentration of 33.7, 3.38 and 38.7 µM respectively (Fig. 20). However, during February maximum concentration of NO_3 and SiO_4 were along T_E reaching 30 and 39 µM respectively.

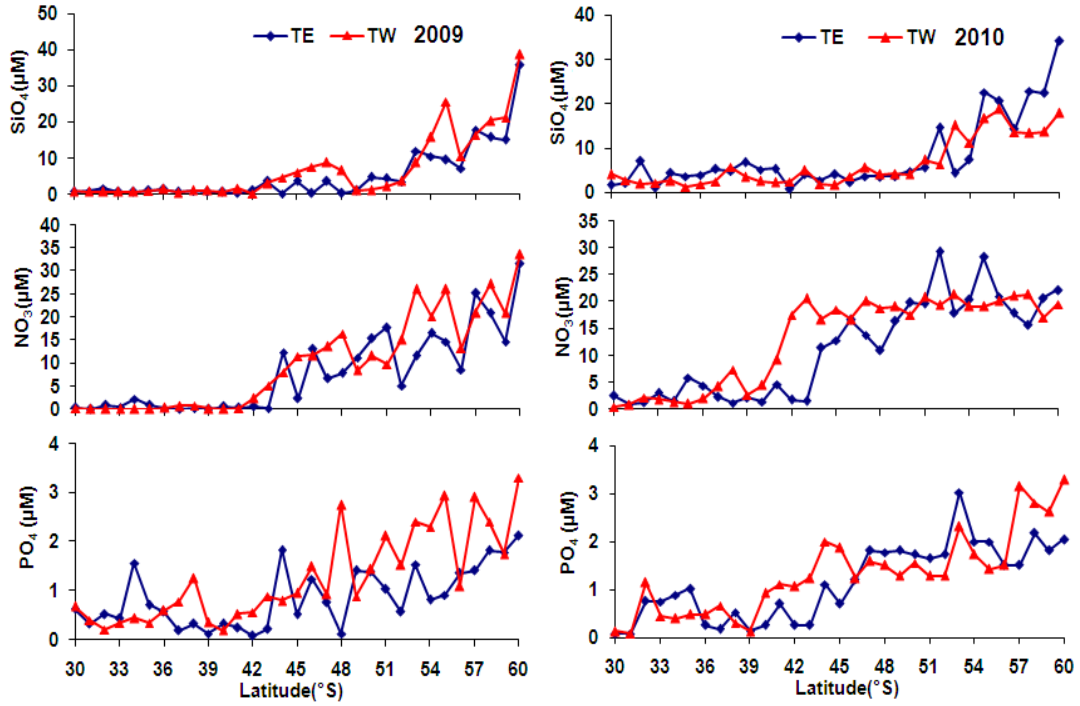

Fig.20. Spatial distribution of macronutrients in Southern ocean during March and February along the 2 transects.

The degree to which the flux of nutrients upwelled from depth is in balance with biological consumption is an important factor regulating the partitioning of CO_2 between the atmosphere and the deep sea (Siegenthaler and Wenk, 1984).

Table 10: Latitudinal variations in Nitrate during March 2009, February 2010 and January 2012.

LATITUDE (°S)	2009 (48° E)	2009 (57° 30'E)	2010 (48° E)	2010 (57° 30'E)	2012
30°S	0.17	0.28	0.54	2.54	-
31°S	0.03	0.03	5.91	1.03	-
32°S	0.04	0.83	0.63	2.19	-
33°S	0.01	0.41	1.24	1.40	-
34°S	0.02	2.19	0.43	1.82	-
35°S	0	0.82	1.18	3.64	-
36°S	0.22	0.15	0.47	2.54	-
37°S	0.65	0	0.86	0.96	-
38°S	0.69	0.17	2.14	1.32	0.044
39°S	0.07	0	1.85	3.01	0.132
40°S	0	0.62	1.35	1.48	0.858
41°S	0.18	0.26	1.00	5.91	0.154
42°S	2.27	0.52	2.01	4.42	4.466
43°S	5.11	0.14	4.27	2.36	18.502
44°S	8	12.35	7.39	1.22	-
45°S	11.46	2.25	2.63	2.16	11.44
46°S	11.66	13.04	4.55	1.42	12.034
47°S	13.63	6.72	9.28	4.67	10.802
48°S	16.35	7.87	17.48	1.73	15.29
49°S	8.35	11.18	20.62	1.51	-
50°S	11.52	15.28	16.68	11.39	-
51°S	9.67	17.77	18.49	12.79	17.82
52°S	15.08	5.11	16.71	16.66	17.204
53°S	26.18	11.61	20.18	13.80	14.696
54°S	20.14	16.43	18.75	10.91	14.85
55°S	26.02	14.62	19.14	16.35	16.434
56°S	13.18	8.54	17.47	19.82	13.376
57°S	20.94	25.19	20.87	19.54	13.794
58°S	27.21	20.81	19.30	29.32	11.814
59°S	20.89	14.66	21.33	17.81	15.972
60°S	33.67	31.55	19.07	20.36	12.496
61°°S	25	15.29	23.00	28.26	16.324
62°S	23.86	10.06	25.03168	20.99	16.654
63°S	10.6	10.29	31.77536	17.89	15.356
64°S	-	10.1	25.14144	15.64	14.058
65°S	16.76	13.08	22.82208	20.63	25.366
66°S	-	27.33	30.05952	22.12	23.122

Table 11: Latitudinal variations in Phosphate during March 2009, February 2010 and January 2012.

LATITUDE (°S)	2009 (48° E)	2009 (57° 30'E)	2010 (48° E)	2010 (57° 30'E)	2012
30°S	0.7	0.6	0.1	0.1	-
31°S	0.4	0.3	0.1	0.1	-
32°S	0.2	0.5	1.2	0.8	-
33°S	0.4	0.4	0.4	0.8	-
34°S	0.5	1.6	0.4	0.9	-
35°S	0.4	0.7	0.5	1.0	-
36°S	0.6	0.6	0.5	0.3	-
37°S	0.8	0.2	0.7	0.2	-
38°S	1.3	0.3	0.3	0.5	0.1
39°S	0.4	0.1	0.1	0.1	0.1
40°S	0.2	0.3	0.9	0.3	0.3
41°S	0.5	0.3	1.1	0.7	0.1
42°S	0.6	0.1	1.1	0.3	0.6
43°S	0.9	0.2	1.2	0.3	1.2
44°S	0.8	1.8	2.0	1.1	-
45°S	1.0	0.5	1.9	0.7	0.9
46°S	1.5	1.2	1.2	1.2	0.8
47°S	0.9	0.8	1.6	1.8	1.4
48°S	2.8	0.1	1.5	1.8	1.5
49°S	0.9	1.4	1.3	1.8	-
50°S	1.4	1.4	1.6	1.7	-
51°S	2.1	1.0	1.3	1.6	1.5
52°S	1.5	0.6	1.3	1.7	1.5
53°S	2.4	1.5	2.3	3.0	1.5
54°S	2.3	0.8	1.7	2.0	1.4
55°S	2.9	0.9	1.4	2.0	1.6
56°S	1.1	1.4	1.5	1.5	1.8
57°S	2.9	1.4	3.2	1.5	1.4
58°S	2.4	1.8	2.8	2.2	1.4
59°S	1.8	1.8	2.6	1.8	1.6
60°S	3.3	2.1	3.3	2.0	1.4
61°°S	2.9	2.1	3.1	3.7	1.6
62°S	2.9	2.8	2.9	3.5	1.7
63°S	1.9	3.4	2.3	3.7	2.1
64°S	-	3.2	2.8	2.9	1.5
65°S	1.4	2.4	2.1	3.2	2.1
66°S	-	2.7	2.3	2.3	2.1

Table 12: Latitudinal variations in Silicates during March 2009, February 2010 and January 2012.

LATITUDE (°S)	2009 (48° E)	2009 (57° 30'E)	2010 (48° E)	2010 (57° 30'E)	2012
30°S	0.75	0.67	4.14	1.63	-
31°S	0.6	0.9	2.70	2.13	-
32°S	0.58	1.55	1.94	7.02	-
33°S	0.66	0.74	2.13	1.07	-
34°S	0.58	0.61	2.63	4.33	-
35°S	0.81	0.94	1.19	3.64	-
36°S	1.39	1.36	1.82	3.95	-
37°S	0.39	0.61	2.45	5.27	-
38°S	0.93	0.88	5.71	4.77	10.3435
39°S	1.07	0.67	3.51	6.84	11.476
40°S	0.63	0.74	2.51	5.14	8.6825
41°S	1.51	0.33	2.20	5.33	8.5315
42°S	0.13	1.01	2.38	0.69	6.04
43°S	3	3.52	5.02	4.01	4.077
44°S	4.5	0.1	1.76	2.70	-
45°S	6	3.54	1.69	4.14	1.8875
46°S	7.5	0.21	3.64	2.32	3.775
47°S	8.86	3.65	5.64	3.58	9.2865
48°S	6.49	0.33	4.08	3.51	5.285
49°S	0.98	0.93	4.14	3.58	-
50°S	1.15	4.64	4.08	4.77	-
51°S	2.11	4.42	7.40	5.58	13.439
52°S	3.57	3.49	6.27	14.55	16.308
53°S	8.84	11.94	15.24	4.33	16.459
54°S	15.91	10.42	11.16	7.40	18.1955
55°S	25.64	9.61	16.75	22.58	23.3295
56°S	10.51	7.2	18.82	20.51	22.2725
57°S	16.32	17.8	13.55	14.30	19.8565
58°S	20.32	15.87	13.36	22.83	18.0445
59°S	21.16	15.04	13.74	22.45	26.123
60°S	38.76	35.83	17.94	34.25	19.2525
61°°S	30	18.38	23.39456	20.39456	31.6345
62°S	26.45	10.91	23.39456	21.39456	29.596
63°S	14.08	12.51	22.39104	23.39104	24.613
64°S		12.76	28.03584	25.03584	32.465
65°S	25.23	18.14	22.95552	21.95552	62.514
66°S	-	33.29	39.45088	35.45088	59.8715

4.2.2 Nutrient Availability in Enderby Basin

Among the nutrients, nitrate and phosphate are the principal variables that limit the phytoplankton growth. The nutrient concentrations are high during March 2009, February 2010 and January 2012, reaching a maximum value of 41.7µM, 3.8 µM and 58 µM for NO_3, PO_4 and SiO_4, respectively (Fig. 21). During March, at Enderby basin, the concentration of SiO_4 is less than that of nitrate at most of the stations.

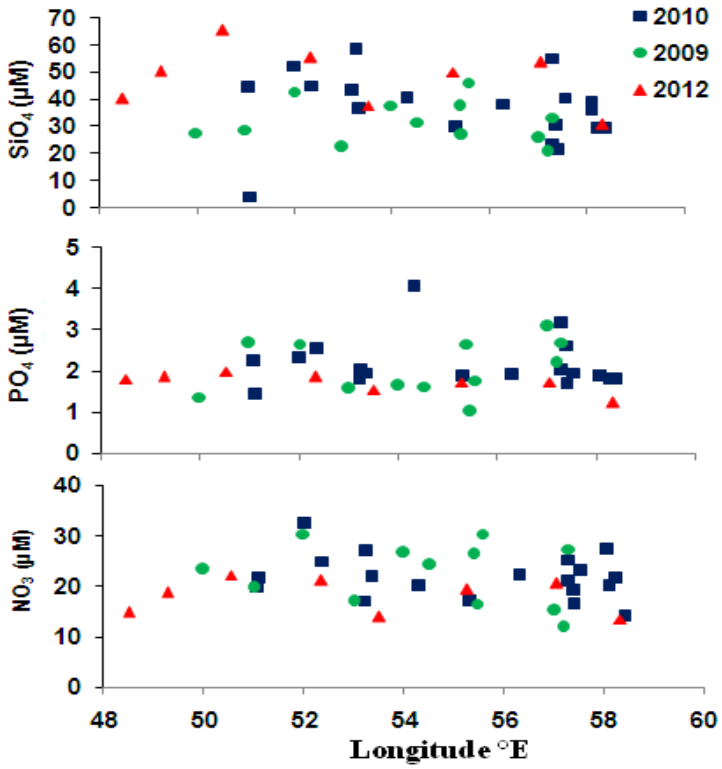

Fig.21.Spatial distribution of macronutrients along Antarctic coast in Indian Sector of Southern Ocean.

From summer (2010) to late austral summer (2009) PO_4 and SiO_4 decrease, however NO_3 show an increase of 2 µM, which may be a result of the increase in the MLD under the sea ice cover (Louanchi et al., 2001). Si/N ranges from 1.06 to 1.7 from open ocean waters to ACS waters (Fig. 22 a&b), and was greater than diatom uptake ratio (Richards, 1958). Comparing all the 3 years, the Si/N values

decrease from 2.7 to1.4 during January to March respectively, which is a result of the silicate utilization under the sea ice cover

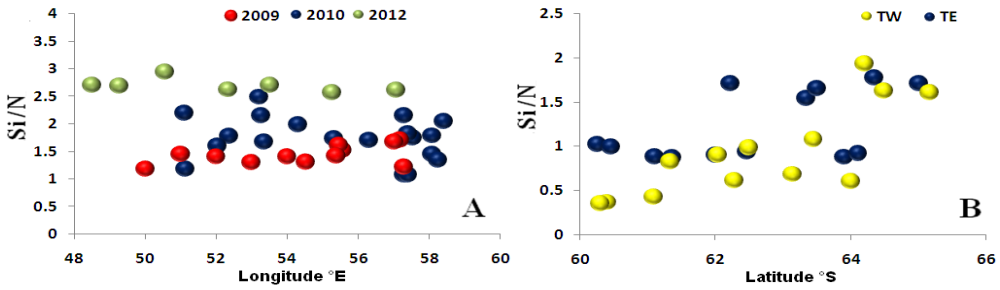

Fig.22. (A) depicts variations in Si/N in the Antarctic continental shelf area during March 2009, February 2010 and January 2012. (B) Shows the variations in the open ocean along the two transect T_E and T_W collected during February 2010.

during March 2009 (Fig. 22 a). In the open waters higher Si/N were observed along the T_E transect (Fig. 22 b). High Si/N uptake ratios were reported in Iron depleted areas in southern ocean (TreHguer and Jacques, 1992; Hutchins and Bruland, 1998; Takeda, 1998). Thus, the high Si/N found at Enderby Basin is possibly due to the iron limitation in the southern Indian Ocean (Blain et al., 2000) and Antarctic Ocean (Louanchi et al., 2001).

Although the coastal Antarctic waters are rich in nutrients, the waters under the thick ice cover (2m) are devoid with nutrients. The SiO_4 values reach as low as 2µM as compared to coastal Antarctic waters with SiO_4 values upto 60 µM (Fig. 23). Similarly, nitrate and phosphate are utilised under the thick ice cover. However, the concentrations under the ice cover tend to be high on moving towards marine high saline waters.

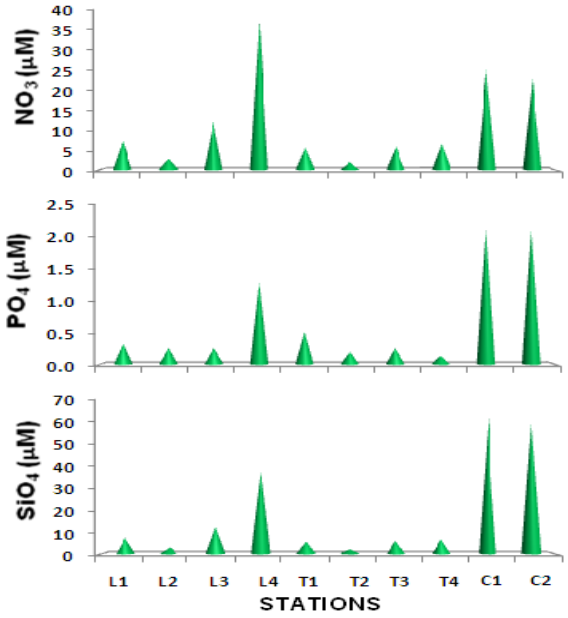

Fig. 23. A comparison of nutrients from under the ice cover (2m) and open coastal Antarctic waters in Indian sector of Southern Ocean collected during January 2012.

Evidences for low silicate concentrations are also seen from the types of spicules produced by a siliceous sponge from under the ice cover. Lab experiments by Maldonado (1999) concluded that different sponge spicule types may be secreted by a specific sclerocyte type, which is activated by a particular threshold of silicate concentration. In the Antarctic sponge two types of spicules were found, small styles spicules (Fig. 24 a), and a bunch of spines fused together (Fig. 24 b), which indicates very low silicate concentrations under the ice cover. Surface silicate concentration, in ice free water was 62 µM, but under the sea ice cover silica was <3 µM. The bottom water silicate concentrations were 75 µM and 12 µM, under ice free and ice covered areas, respectively. These results are also supported by Nelson & Smith (1986), who found that intense diatom blooms in summer can suppress silicate values to <l0 µM in the marginal ice zone of the Ross Sea.

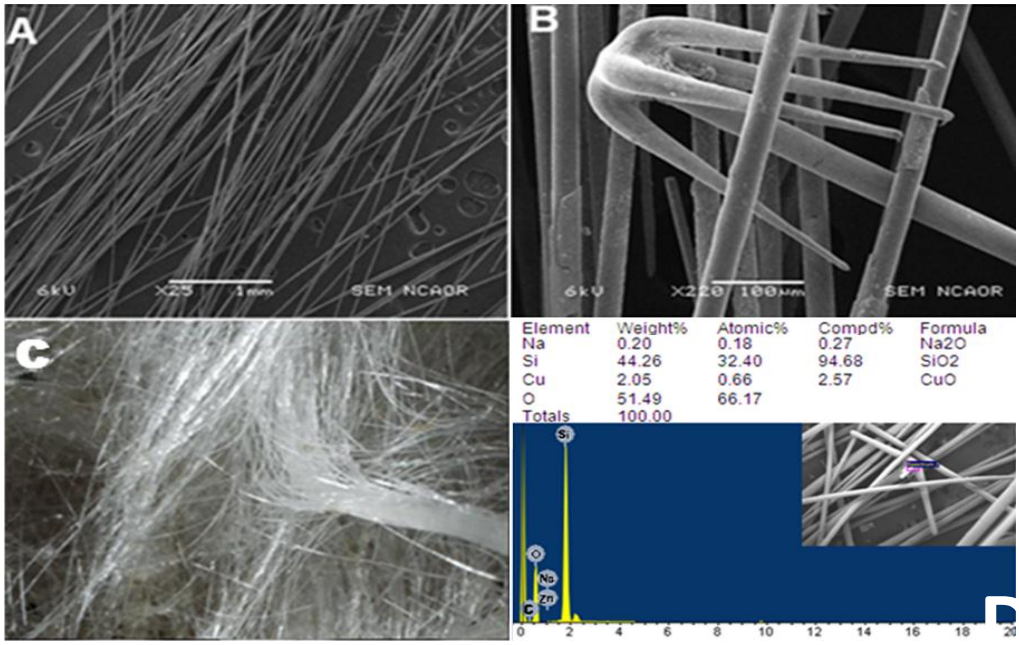

Fig.24. (A-B) Scanning electron micrographs of sponge spicules. (C) Light microscopic image of spicule bearing sponge-mat. (D) EDS analysis of sponge spicules.

Table 13: Variations in macronutrients during March 2009, February 2010 and January 2012 under the Land—fast sea ice.

STATION	PO_4 (µM)	SiO_4 (µM)	NO_3 (µM)
L1	0.3	7.2	7.2
L2	0.3	2.8	2.8
L3	0.3	12.3	12.3
L4	1.3	37.8	37.8
T1	0.5	5.6	5.6
T2	0.2	2.0	2.0
T3	0.3	5.8	5.8
T4	0.1	6.6	6.6

4.2.2.1 Micronutrient Fe Availability

Although, the Southern Ocean is a high nutrient region, but its primary productivity is low because of low iron concentrations. Icebergs have been implicated as a

source of Fe to the surrounding waters (Martin 1990). But the Antarctic coastal regions are generally macro and micronutrient replete and could support 25% of phytoplankton biomass (Lancelot et al., 2009). Recent study by Maria Vernet et al., 2011 indicated presence of healthy phytoplankton cells in vicinity of iceberg. Icebergs can deliver substantial smaller Fe-rich particles that are potentially bio-available (Raiswell 2011, Raiswell and Canfield 2012). The EDS results of the iceberg samples showed Fe particles within the iceberg that had Fe concentrations as high as 73% (Fig. 25).

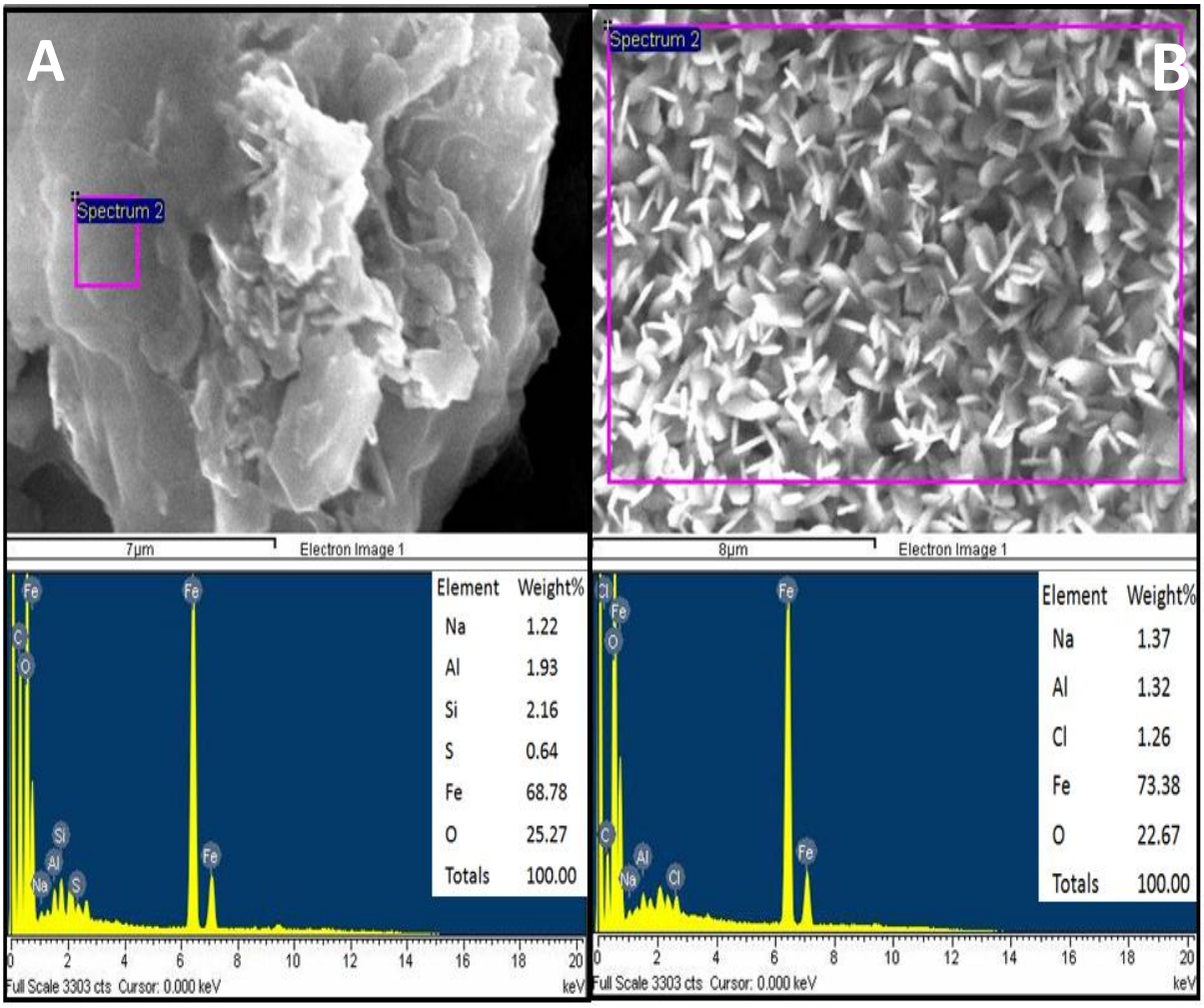

Fig.25. A and B are SEM and EDS images showing Fe particles and Fe percentage in iceberg samples SS_1 and SS_2 collected from Antarctic coastal region.

4.2.3 Bay of Bengal

4.2.3.1 Coastal

Surface NO_3 concentrations were <1 µM upto 75 m depth at all stations except Thamnapatnam, where it reached to concentrations of 13 µM at 20 m and went on increasing with depth (Fig. 26). SiO_4 concentrations were <5 µM up to 20 m at all stations except Thamnapatnam (Fig. 26). Phosphate concentrations also were <0.5 µM in surface waters, except Thamnapatnam.

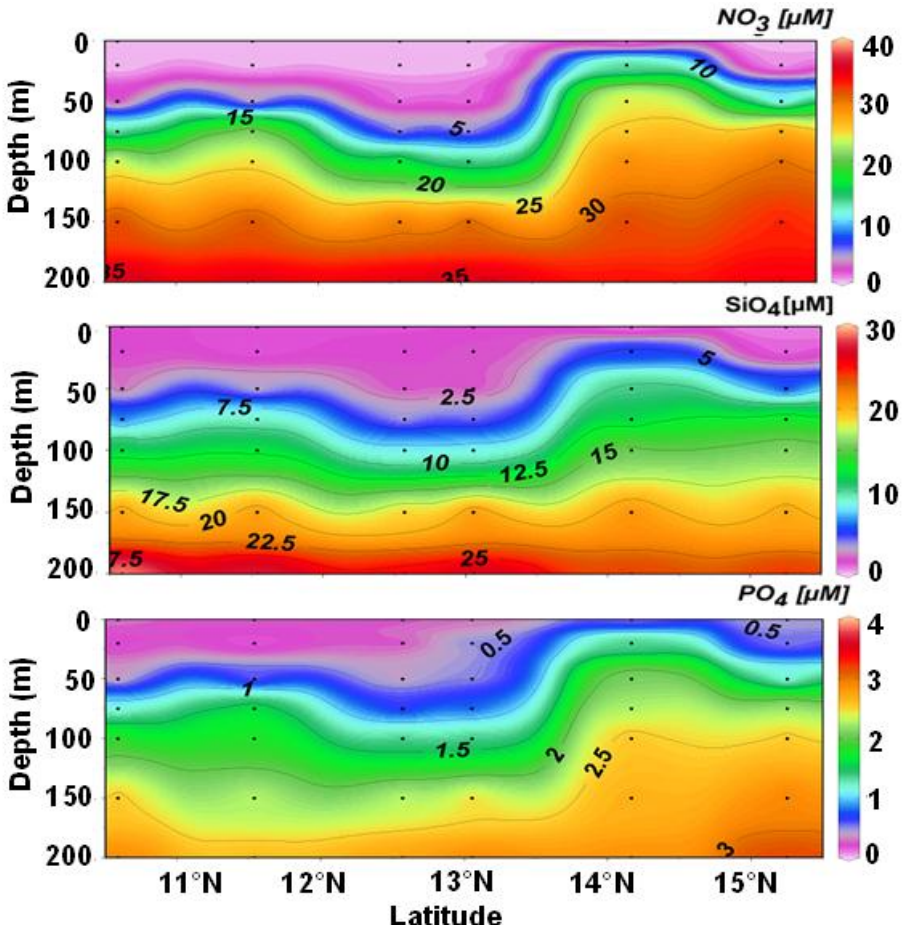

Fig.26. Cross section of the zonal (80.15°E to 80.75°E) nutrients collected onboard ORV-SagarSampada during April -May 2009. The upliftment of nutricline near 14° N (Off Thamnapatnam) is due to upwelling resulted from divergence of water masses.

At Thamnapatnam (14 °N) higher nutrient subsurface waters were brought to the surface, thus increasing the surfacial nutrient concentrations (Fig. 26).

4.2.3.2 Open waters

A detailed study in northern Bay of Bengal, within and outside a cyclonic eddy indicate higher PO_4 and SiO_4 within the eddy (Fig. 27).

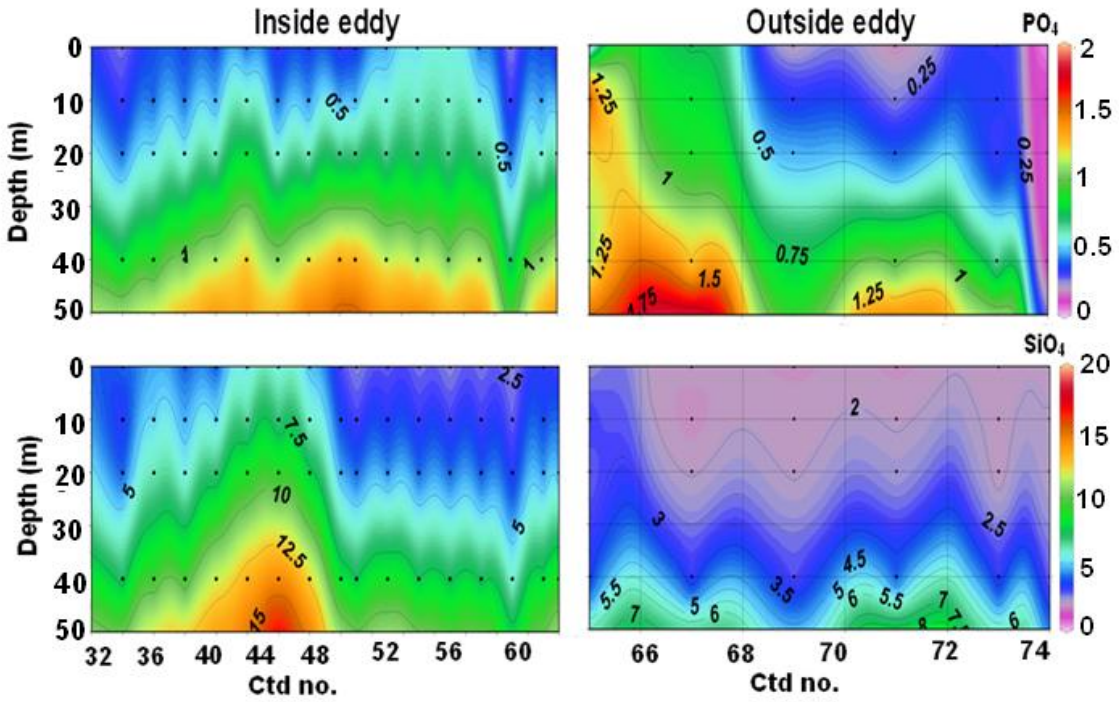

Fig.27. Vertical profiles of macronutrients collected after every 3 hrs, within and outside a cyclonic eddy.

4.3 Variability in pCO_2

4.3.1 Southern Ocean

When all the 3 years data were compared, March showed the highest pCO_2, whereas January showed the lowest pCO_2 (Fig. 28, Table 14). The average sea surface pCO_2 decreased from 337 µatm during March to 297 µatm during February and further to 286 µatm during January. The high pCO_2 values resulted in lowering the seawater pH due to the carbonic acid formation. Surface water pH

averaged 8.11 during March, 8.3 during February and 8.24 during January. However within the PF averaged pH was 8.08 during March, 8.2 during February and 8.27 during January. This variation in pCO_2 showed opposite trend of dissolved oxygen and was higher in January reaching upto 374 µM in coastal Antarctic waters. AOU showed opposite trends to oxygen indicating higher respiration of organic matter during January, whereas TOC variations matched with dissolved oxygen. The source of TOC, in the open ocean is in situ production from several biological processes (Copin-Monte´gut and Avril, 1993). Chl *a* was high during January as compared to March and averaged 0.5 mg/m^3 and 0.21 mg/m^3 respectively. Chl *a* concentrations declined in the PF and further south increased towards Antarctic coast.

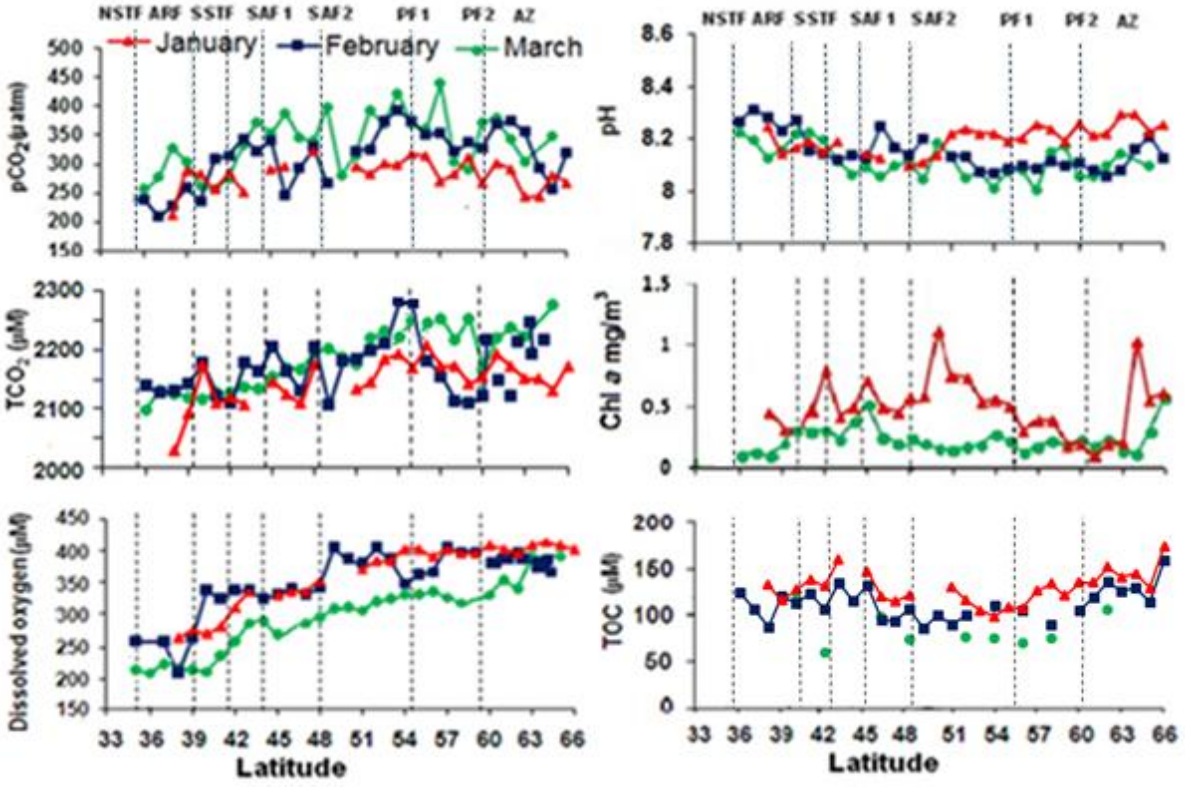

Fig.28. Spatial distribution of pCO_2 and related parameters in Indian sector of Southern Ocean during March, February and January.

Mean pCO_2 upto MLD during March was maximum in the PF, and was 287 µatm, 297 µatm, 302 µatm and 289 µatm within STF, SAF, PF and ANZ respectively. Whereas during February, mean pCO_2 upto MLD was 188 µatm, 273 µatm, 294 µatm and 280 µatm within STF, SAF, PF and ANZ respectively. A comparison of the March and February, along the same transect TE (57.30° E) indicates that the pCO_2 values were much lower during February as compared to March (Fig. 29). This is clearly seen from the pinkish blue color during February. pH showed just the opposite trend of pCO_2. The dissolved oxygen values reached upto 374 µM in Antarctic coast during January and February within the influence of sea ice. Thomas and Diekmann, (2010) have reported super-saturation in dissolved oxygen in sea ice micro habitats. Whereas maximum dissolved oxygen during March was 308 µM. These variations are clearly seen in Figure 29 which shows reddish colored high oxygen waters during February. All these parameters also clearly show vertical gradients during March as compared to February supporting well mixed and deeper MLD.

Vertical distribution of pCO_2 and associated parameters is plotted in figure 29. It shows higher pCO_2 values during March 2009. The dissolved oxygen values reached upto 374 µM during February 2010, whereas maximum dissolved oxygen during March 2009 was 308 µM (Table 15).

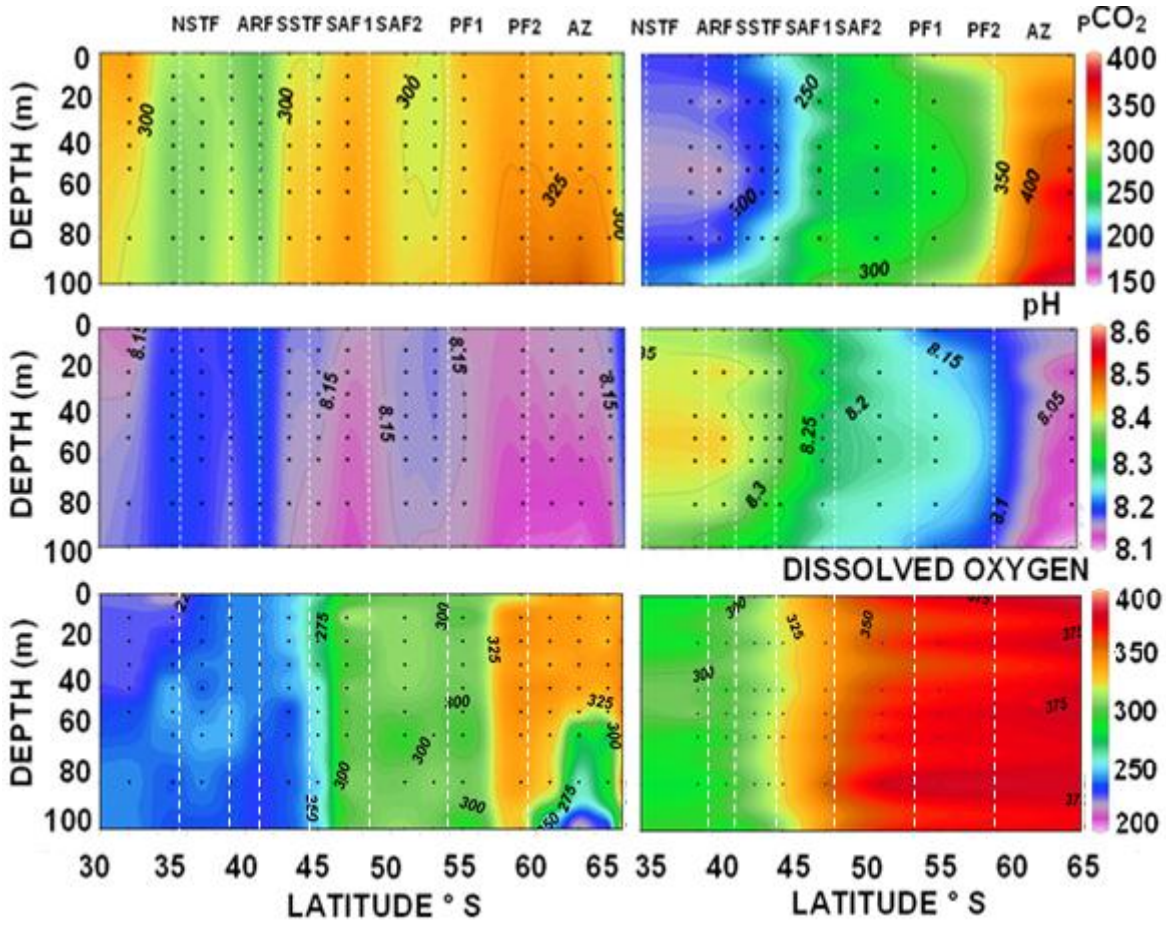

Fig. 29. Vertical distribution of *p*CO_2 (µatm), pH, and DO (µM) during March 2009 and February 2010 along 57.30°E (TE). Various fronts identified have been marked in dashed lines.

During March 2009, average *p*CO_2 was higher, that is 338 µatm on T_W, it decreased by 24 µatm and was 313 µatm on T_E. The average *p*CO_2 increased from the ARF to the PF. It was 259 µatm, 289 µatm, 355 µatm and 364 µatm at ARF, STF, SAF and PF, respectively, along T_W; 280 µatm, 313 µatm, 322 µatm and 332 µatm, respectively, along T_E.

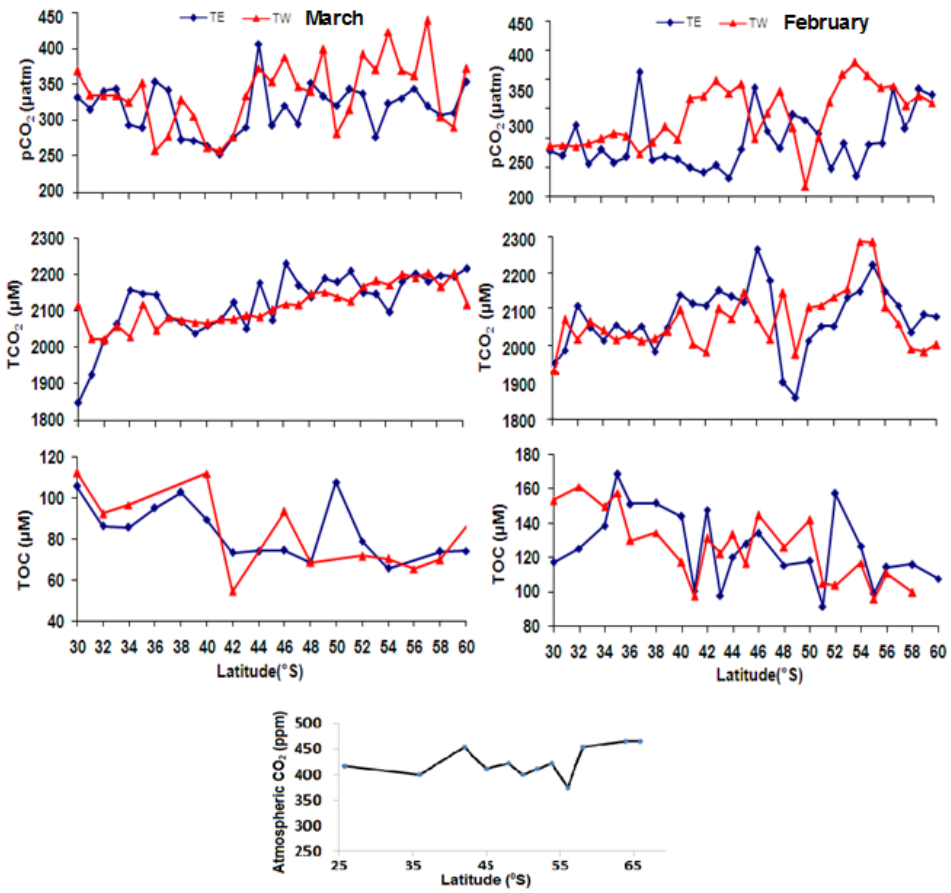

Fig.30. (A) Variations in sea surface *p*CO_2, TCO_2, TOC during March 2009 and February 2010 along both transects. Variations in atmospheric CO_2 during March 2009.

Due to the presence of high macronutrient concentrations, the Southern Ocean so far has been a sink for atmospheric CO_2. *p*CO_2 values along both the transects indicated that a majority of the surface water *p*CO_2 was below the atmospheric *p*CO_2 values (Fig. 30). Atmospheric *p*CO_2 varied from 400-460 µatm. In the western transect T_W, a few stations near the polar front around the Crozet Island showed values higher than the atmospheric CO_2 values, which may be related to the upwelling of the CO_2 and phosphate enriched deep water (Keeling, 1968; Semiletov, 1995).

A comparison of the March 2009 and February 2010 along the same transect T_E (57.30° E) indicates that the pCO_2 values were much lower during 2009 as compared to 2010. pH showed just the opposite trend to pCO_2 (Fig. 31).Vertical distribution also indicates higher pCO_2 values along T_W. A prominent feature is observed in the vicinity of the Crozet Island (46°S), wherein shoaling of subsurface waters is seen, adding to the pCO_2 in surface waters (Fig. 31).

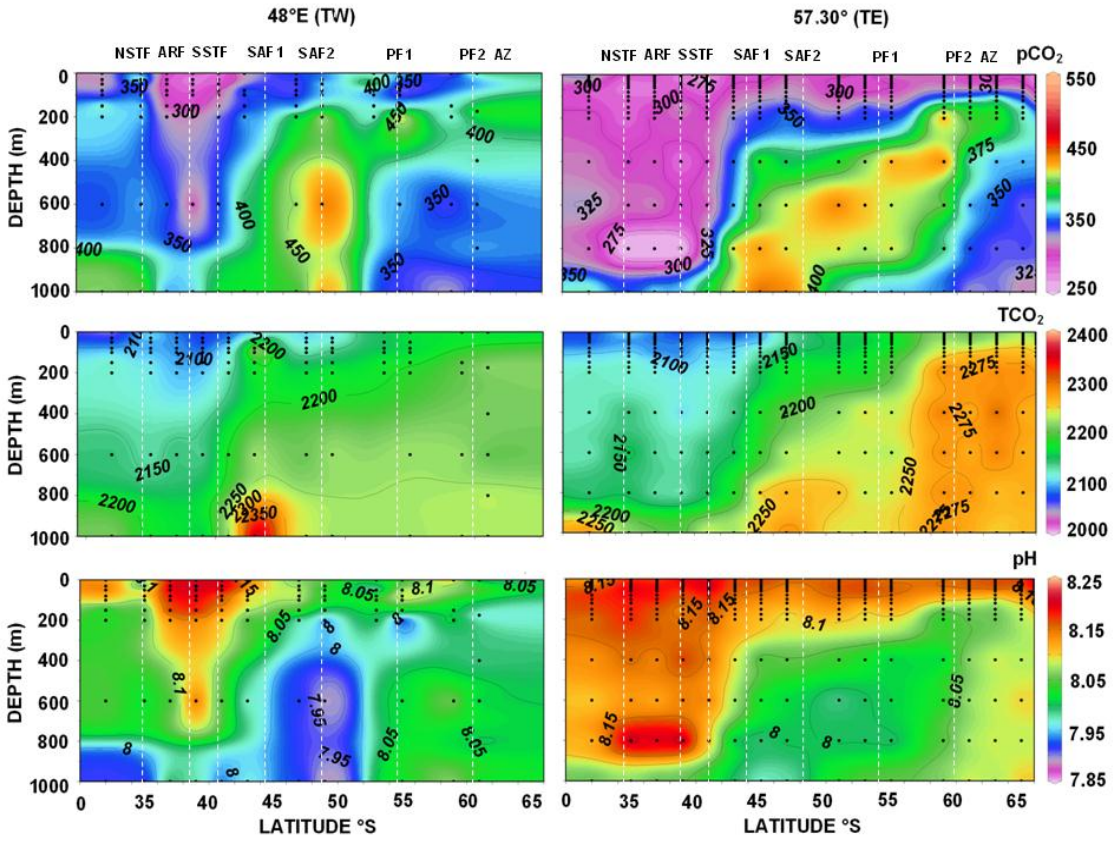

Fig.31. Vertical distribution of pCO_2 (µatm), TCO_2 (µM) and pH during March 2009 along the 2 transects TE (57.30°E) and TW (48°E). Various fronts identified have been marked in dashed lines.

During March 2009, TCO_2 ranged from 2020 µM to 2226 µM along the T_W, whereas it ranged from 1850 µM to 2230 µM along the T_E (Fig. 31). Along the two transects TCO_2 showed an increasing trend towards the south and increased with

depth (Fig. 31). TCO_2 is strongly negatively correlated with sea surface temperature with R^2=0.86 and 0.75, respectively, for T_W and T_E. TCO_2 concentrations increase with water depth (Fig. 31) and thus the vertical mixing plays an important role in pumping higher concentrations of TCO_2 to the surface waters.

The effect of Crozet Island is seen on the concentrations of chlorophyll *a*, showing elevated production along 48°E (Fig. 32).

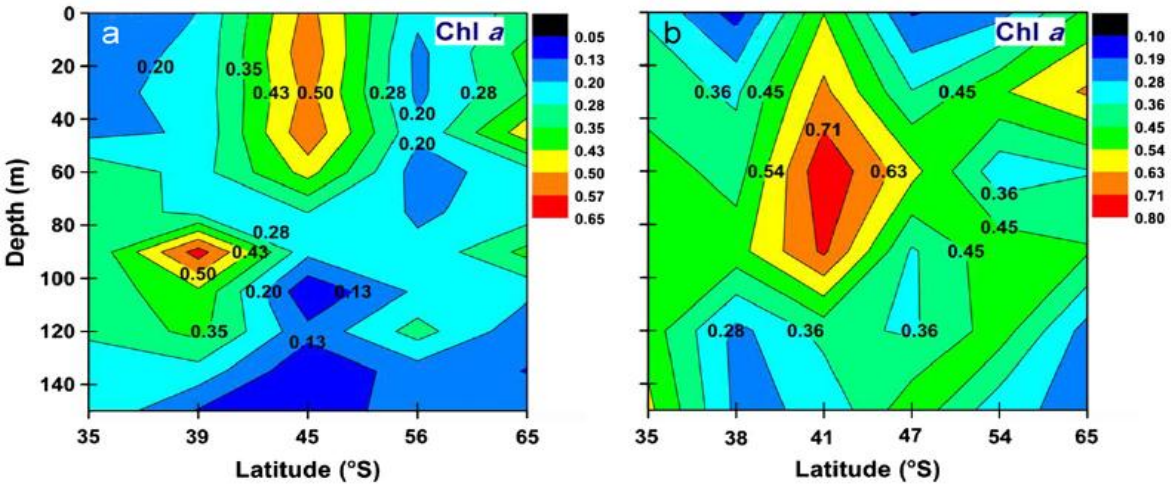

Fig. 32. Vertical distribution of chlorophyll *a* during 2009 along the 2 transects (a) T_E (57.30°E) and (b) T_W (48°E).

Table 14: Latitudinal variations in pCO_2 during March 2009, February 2010 and January 2012.

LATITUDE (°)	2009 (48° E)	2009 (57° 30'E)	2010 (48° E)	2010 (57° 30'E)	2012
30°S	367.6	331.3	236.5	238.6	-
31°S	334.2	314.5	238.0	230.4	-
32°S	333.7	339.8	235.7	281.5	-
33°S	333.5	343.2	241.0	235.7	-
34°S	323.8	293.1	249.1	240.9	-
35°S	351.2	288.9	258.0	238.6	-

36°S	256.1	353.5	253.8	248.3	-
37°S	277.0	341.0	223.2	362.6	-
38°S	328.1	272.3	242.6	263.5	212.0
39°S	304.9	270.8	270.0	259.0	288.4
40°S	261.0	264.1	248.4	254.5	282.8
41°S	256.8	251.4	318.3	259.8	256.9
42°S	275.9	274.8	321.3	250.8	285.1
43°S	333.4	289.5	348.6	253.3	253.0
44°S	372.3	406.4	326.9	250.9	-
45°S	352.5	291.7	342.8	271.9	290.1
46°S	387.8	320.3	248.8	335.7	295.8
47°S	345.8	294.3	293.0	282.5	392.2
48°S	339.5	352.4	330.4	252.6	321.8
49°S	399.1	332.4	267.6	290.6	
50°S	280.1	320.0	207.9	281.3	
51°S	314.6	342.9	252.0	257.9	296.4
52°S	391.8	336.4	322.2	255.3	281.9
53°S	369.6	276.3	369.0	261.3	300.1
54°S	422.8	322.5	389.6	237.4	298.2
55°S	368.8	329.9	367.4	275.3	317.4
56°S	361.1	343.9	346.3	281.6	313.2
57°S	439.5	318.9	349.3	345.6	271.0
58°S	303.9	306.2	316.0	281.9	282.9
59°S	289.9	310.0	332.6	344.1	312.9
60°S	371.3	353.3	320.8	334.0	267.1
61°°S	380.8	299.5	360.2	350.5	302.6
62°S	342.9	337.6	366.6	251.9	292.0
63°S	304.1	310.4	350.5	311.3	243.7
64°S		298.1	357.9	353.1	244.0
65°S	347.3	321.6	333.4	333.6	281.3
66°S	-	-	-	-	268.0

Table 15: Latitudinal variations in Dissolved oxygen (µM) during March 2009, February 2010 and January 2012.

LATITUDE (°S)	2009 (48° E)	2009 (57° 30'E)	2010 (48° E)	2010 (57° 30'E)	2012.0
30°S	224.6	218.4	255.6	277.9	-
31°S	225.1	223.7	289.0	305.7	-
32°S	215.3	228.7	222.3	289.0	-
33°S	219.7	223.7	239.0	289.0	-
34°S	222.0	228.7	239.0	277.9	-

35°S	231.3	218.4	272.3	289.0	-
36°S	226.9	233.6	166.7	277.9	-
37°S	235.4	238.9	272.3	-	-
38°S	237.1	233.6	227.9	277.9	278.4
39°S	232.2	243.8	277.9	277.9	289.3
40°S	230.9	228.7	344.6	277.9	283.9
41°S	251.9	243.8	333.4	277.9	294.8
42°S	272.0	242.5	344.6	289.0	322.0
43°S	299.2	249.2	344.6	289.0	343.8
44°S	303.2	272.9	333.4	316.8	-
45°S	282.3	264.4	339.0	333.4	338.3
46°S	-	290.7	350.1	333.4	343.8
47°S	299.2	299.7	339.0	333.4	343.8
48°S	307.3	305.9	350.1	350.1	360.1
49°S	318.4	306.4	405.7	355.7	-
50°S	320.7	310.8	389.0	416.8	-
51°S	318.0	305.0	383.5	394.6	376.5
52°S	329.1	314.0	405.7	372.4	387.4
53°S	332.3	305.0	389.0	372.4	387.4
54°S	338.5	312.2	355.7	377.9	403.7
55°S	338.5	305.0	366.8	377.9	403.7
56°S	343.4	310.4	372.4	383.5	392.8
57°S	335.8	332.7	405.7	377.9	403.7
58°S	327.8	325.1	400.1	394.6	398.3
59°S	-	320.2	400.1	377.9	398.3
60°S	339.9	322.9	-	382.3	409.2
61°°S	359.5	335.4	383.5	383.2	403.7
62°S	347.5	317.5	383.5	385.0	398.3
63°S	391.7	340.3	389.0	382.3	409.2
64°S	-	336.7	389.0	388.5	414.6
65°S	394.3	325.1	400.1	388.1	409.2
66°S	-	340.3	389.0	392.1	403.7

4.3.2.1 Enderby Basin

The average pCO_2 was 368 µatm, 340 µatm and 181 µatm during March 2009, February 2010 and January 2012 respectively.pCO_2 ranged from 245-558 µatm, 218-596 µatm and 117-237 µatm in March 2009, February 2010 and January 2012 respectively (Fig.33). During 2012, most of the stations had under saturated pCO_2 values. Chlorophyll *a* varied from 0.05-0.25 mg/m^3 under the ice cover during

March 2009, 0.3-3 mg/m^3 in the ice free area of February 2010. TOC ranged from 44-173 µM in March 2009, 96-232 µM in February 2010, and 110-252 µM in January 2012 respectively. TCO_2 ranged from 2154-2270 µM, 2019-2218 µM and 2099-2310 µM in March 2009, February 2010 and January 2012 respectively. pH ranged from 7.85-8.25, 7.96-8.3 and 8.25-8.52 in March 2009, February 2010 and January 2012 respectively (Fig. 33).

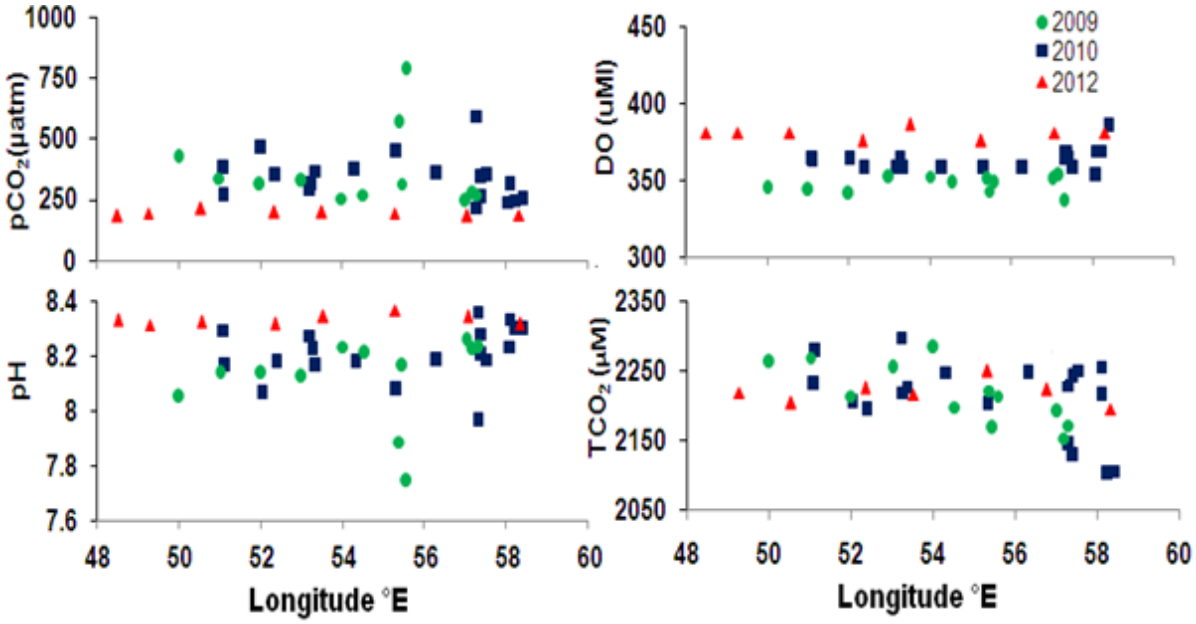

Fig. 33. Spatial distribution of *p*CO_2 and related parameters along coastal Antarctica during March 2009, February 2010 and January 2012.

Differences between the areas east and west of 55°E

There is a large variation between areas east and west of 55°E. During 2012, the mean *p*CO_2 west of 55°E was 175 µatm, whereas east of 194 µatm. Figure 34, shows the variation in *p*CO_2, collected during 2010 in open oceanic waters, outside the Antarctic Continental shelf (ACS) region between 60-66°S. The two transects are T_W (all stations west of 55°E) and T_E (all stations east of 55°E). The averaged *p*CO_2 values during 2009 were lower along T_W, than T_E and averaged 323 and 411

µatm respectively. The averaged pCO_2 values during 2010 (within ACS) were lower along T_W,

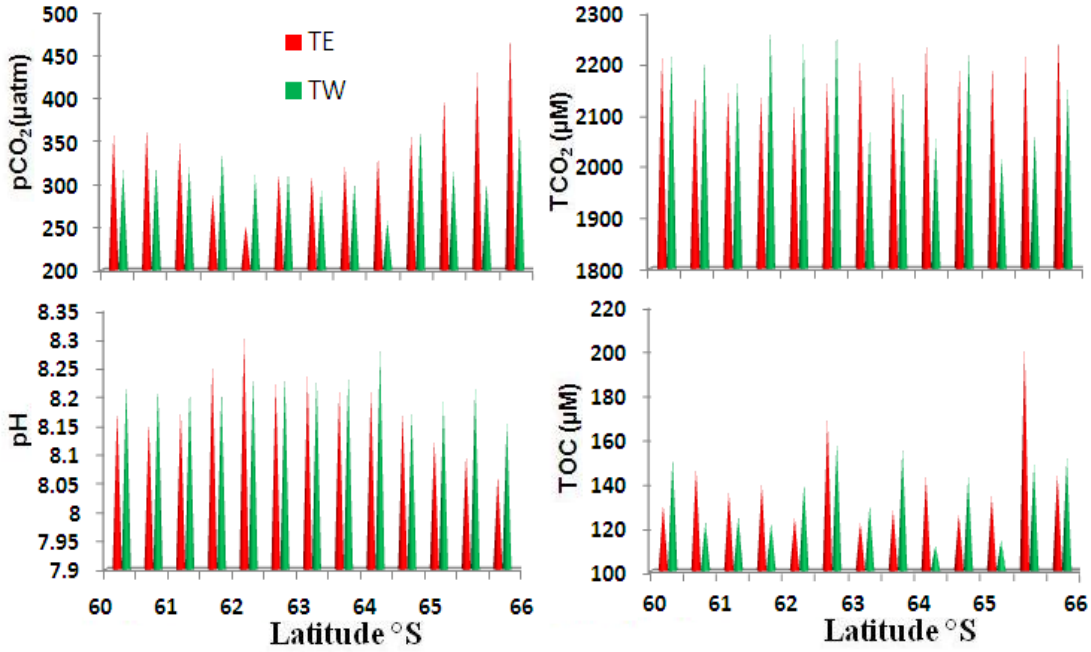

Fig.34.Variation in physicochemical parameters during 2010 (60-66°S) along the two transects T_E and T_W.

than T_E and averaged 337 and 350 µatm respectively. The averaged pCO_2 values were 334 and 342 µatm along T_W and T_E during 2010 (outside ACS), whereas pH showed just the opposite trend (Fig. 34). Averaged Chlorophyll *a* concentrations were 1.5 mg/m^3 along T_E, as compared to 1.1 mg/m^3 along T_W. TOC averaged 142 µM along T_E, whereas along T_W average TOC was only 133 µM, reflecting the variations in the biological production along the two transects. Despite having higher primary productivity along T_E as indicated by the Chlorophyll *a* and TOC values, the pCO_2 values are high indicating that the biological processes may not be the primary control over pCO_2, and that the physical processes might be the dominant force. Similar results are observed during 2012, wherein pCO_2 is high east of 55°E, but after 70°E (Prydz bay), there is drawdown in pCO_2 values (Fig. 35).

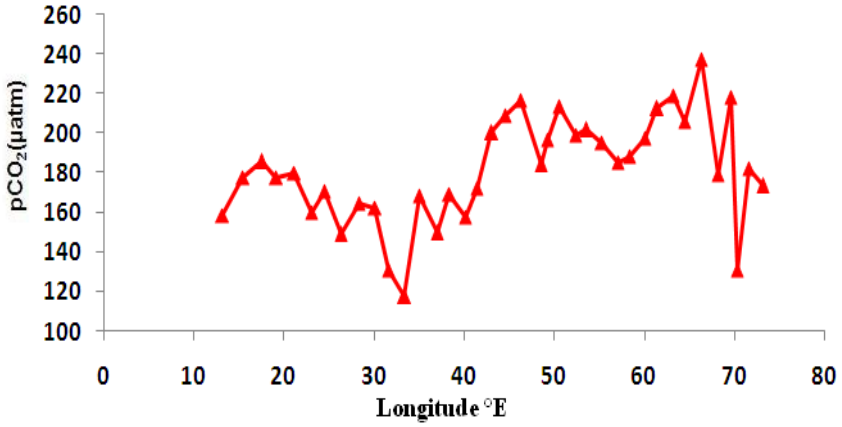

Fig.35. Spatial distribution of *p*CO_2 along coastal Antarctica during January 2012 between Larsemann Hills and Schirmacher Oasis.

Difference between stations within and outside Antarctic continental shelf (ACS) during February 2010

The averaged *p*CO_2 values in stations outside ACS were lower to those within the shelf waters. The averaged *p*CO_2 values were 337 and 342 µatm, outside and inside the ACS respectively. Wind speed averaged 5.9 and 8.8 m/s at the open waters and ACS waters respectively during 2010, clearly justifying the 5 µatm elevated pCO_2 values in the ACS waters. *p*CO_2 and wind speed showed positive correlation (r = 0.48 and 0.31) at ACS and open ocean waters respectively. The difference in *p*CO_2 is also reflected in the biological production, the averaged Chlorophyll *a* in the ACS was 1.3 mg/m^3, whereas in the open waters it was just 0.1 mg/m^3. Averaged TOC values in the open waters were 117 µM, whereas in coastal waters the TOC averaged 152 µM. Average N/P ratio was 10.6 and 12.5 at shelf and open ocean region.

Table 16: Longitudinal variations in physicochemical parameters during March 2009.

STATION	Latitude (°S)	Longitude (°E)	Temp (°C)	Salinity	PO_4 (µM)	SiO_4 (µM)	NO_3 (µM)	TCO_2 (µM)	pH	pCO_2 (µatm)	DO (uM)	wind(m/s)	TOC (uM)
1	66.1	57.31	-2.5	33.6	2.7	33.3	27.3	2173.2	8.2	272.0	341.5	4.8	39.2
2	66.08	57.18	-2.0	33.4	2.2	20.5	11.9	2154.6	8.2	275.0	358.3	8.0	37.5
3	65.54	57.02	-2.0	33.7	3.1	25.6	15.3	2192.3	8.3	245.0	355.7	8.0	170.0
4	65.29	55.56	-1.5	33.8	1.8	46.2	30.4	2214.5	7.7	790.0	353.7	7.7	110.0
5	65.44	55.45	-2.0	33.5	1.0	26.8	16.6	2169.3	8.2	318.0	348.1	2.8	23.3
6	65.45	55.38	-2.0	33.8	2.7	37.4	26.3	2222.8	7.9	571.0	356.2	2.8	150.0
7	65.33	54.53	-1.5	33.7	1.6	31.6	24.2	2199.1	8.2	273.0	353.2	4.0	131.7
8	65.3	54	-1.0	33.8	1.7	37.6	26.7	2284.3	8.2	258.0	357.8	4.0	173.0
9	65.32	53	-1.0	33.6	1.6	22.2	17.1	2256.5	8.1	327.0	357.3	12.0	35.8
10	65.28	52	-0.5	33.5	2.7	42.7	30.3	2215.1	8.1	315.0	346.6	7.5	48.3
11	65.28	51	-0.5	33.9	2.7	28.8	19.7	2270.5	8.1	341.0	349.1	11.8	75.8
12	65.3	50	-0.5	34.0	1.4	27.7	23.3	2263.7	8.1	429.0	350.1	14.5	80.8

Table 17: Longitudinal variations in physicochemical parameters during February 2010.

STATION	Latitude (°S)	Longitude (°E)	Temp (°C)	Salinity	PO_4 (µM)	SiO_4 (µM)	NO_3 (µM)	TCO_2 (µM)	pH	pCO_2 (µatm)	DO (uM)	wind(m/s)	TOC (uM)
1	60.26	57.3	1.5	33.7	3.7	23.4	22.7	2218.2	8.2	360.2	358.5	3.0	130.1
2	60.46	57.3	1.5	33.3	3.5	23.4	23.3	2145.5	8.2	366.6	358.5	2.0	146.6
3	61.1	57.3	1.5	33.2	3.7	22.4	25.0	2150.0	8.2	350.5	364.0	3.8	136.0
4	61.36	57.3	1.5	33.0	2.9	28.0	31.8	2145.5	8.3	289.2	365.0	2.5	139.6
5	62	57.3	1.5	33.7	3.2	23.0	25.1	2123.6	8.3	251.9	375.1	2.5	124.3
6	62.22	57.3	1.5	33.7	1.9	39.5	22.8	2172.7	8.2	312.8	364.0	3.3	169.3
7	62.47	57.3	1.5	33.6	3.8	28.4	30.1	2213.6	8.2	311.3	364.0	5.0	122.1
8	63.9	57.3	1	33.7	4.6	28.5	32.2	2181.8	8.2	323.3	352.9	5.7	127.9
9	63.34	57.3	1	33.7	2.0	38.9	24.9	2248.2	8.2	333.2	352.9	4.2	142.7
10	63.5	57.3	1	33.7	2.1	48.9	29.2	2194.5	8.2	357.9	358.5	4.5	126.0
11	64.11	57.3	1.5	33.7	2.7	17.8	19.1	2203.6	8.1	403.1	352.9	6.5	134.2
12	64.35	57.3	1.5	33.7	1.8	38.6	21.6	2218.2	8.1	433.4	347.4	6.3	201.9
13	65	57.3	1	33.9	2.1	46.2	26.9	2259.1	8.1	477.6	369.6	7.2	144.5
14	65.25	57.3	1	33.8	3.2	22.7	20.9	2230.9	8.0	596.5	375.1	8.5	95.6
15	65.41	57.4	-1.5	32.6	2.6	21.0	19.2	2129.1	8.3	263.1	369.6	4.6	107.2
16	65.39	57.3	-1.5	32.8	2.0	55.2	25.3	2145.5	8.4	218.0	369.6	0.8	232.3
17	65.59	58.08	0.5	33.6	1.9	39.4	27.2	2216.4	8.3	242.4	375.1	6.3	111.8
18	66.18	58.24	-0.5	33.1	1.8	29.2	21.4	2103.6	8.3	249.4	375.1	4.4	161.1
19	66.34	58.4	1	33.8	1.8	29.2	14.0	2107.3	8.3	252.9	391.8	2.6	144.0
20	66.03	58.09	1	33.8	1.9	36.1	20.1	2257.3	8.2	313.9	358.5	1.2	112.6

21	65.54	57.54	-0.5	33.5	2.0	40.5	23.0	2251.8	8.2	352.3	354.0	8.7	135.1
22	65.34	57.39	-0.5	33.0	1.7	30.2	16.4	2242.7	8.2	342.7	375.1	14.1	108.9
23	65.31	56.3	0.5	33.5	1.9	38.2	22.2	2247.3	8.2	358.5	354.0	11.4	136.3
24	65.28	55.32	0	33.0	1.9	29.5	16.9	2202.7	8.1	449.7	354.0	14.0	132.6
25	65.24	54.31	0	33.9	4.0	40.1	20.0	2249.1	8.2	375.0	354.0	19.1	156.9
26	65.19	53.35	0	33.9	2.0	36.5	21.8	2228.2	8.2	371.5	354.0	19.5	119.5
27	65.21	52.37	0	33.8	2.5	45.0	25.0	2194.5	8.2	350.8	354.0	18.0	96.8
28	65.21	52.02	0	33.8	2.3	52.2	32.4	2206.4	8.1	466.6	369.6	13.4	108.6
29	65.48	51.12	0	33.7	1.4	4.0	21.5	2280.0	8.2	380.6	369.6	4.2	123.3
30	65.49	51.09	0	33.8	2.2	44.2	19.9	2231.8	8.3	268.7	368.9	1.3	103.8
31	65.27	53.26	-0.9	33.1	2.0	58.1	26.8	2220.0	8.2	315.0	369.6	3.2	110.8
32	64	53.21	0.9	33.5	1.8	43.1	17.1	2299.1	8.3	294.3	354.0	11.8	114.6
33	65.17	54.15	0	33.7	1.7	53.3	32.9	2223.6	8.2	317.1	320.7	6.9	151.8
34	64.49	53.56	0.5	33.7	1.7	34.4	21.0	2215.5	8.2	322.2	347.4	6.5	122.4
35	64.2	53.36	1	33.5	1.9	44.2	22.5	2170.9	8.2	322.2	341.8	5.1	124.8
36	64	53.21	1	33.5	2.7	39.1	64.8	2275.5	8.2	337.9	347.4	4.5	121.7
37	63.45	53.1	0.5	33.6	2.2	46.5	42.8	2245.5	8.2	311.3	352.9	5.1	139.8
38	63.14	52.5	0.5	33.7	2.5	20.8	30.1	2269.1	8.2	314.3	352.9	5.8	158.8
39	62.5	52.34	1	33.3	2.5	17.9	17.8	2069.1	8.2	293.4	352.9	5.9	129.9
40	62.28	52.2	0.5	32.5	2.5	16.4	26.3	2157.3	8.2	302.2	352.9	5.1	155.6
41	62.04	52.04	1	33.6	2.4	15.4	16.9	2055.5	8.3	257.4	375.1	7.5	111.5
42	61.33	51.45	1	33.2	1.5	15.7	18.5	2231.8	8.2	365.6	375.1	9.0	143.0
43	61.09	51.29	1	32.7	1.9	16.3	38.0	2019.1	8.2	316.7	369.6	10.5	113.8
44	60.4	51.12	0.5	32.9	2.1	19.6	53.2	2067.3	8.2	302.7	369.6	4.8	148.8
45	60.3	51.05	1.5	33.6	2.8	22.6	64.1	2157.3	8.2	367.6	375.1	12.0	151.8
46	60.05	50.5	1.5	33.6	3.5	18.3	19.7	2121.8	8.1	397.7	358.5	13.2	116.6

Table 18: Longitudinal variations in physicochemical parameters during January 2012													
STATION	Latitude (°S)	Longitude (°E)	Temp (°C)	Salinity	PO_4 (µM)	SiO_4 (µM)	NO_3 (µM)	TCO_2 (µM)	pH	pCO_2 (µatm)	DO (uM)	wind(m/s)	TOC (uM)
1	68.15	73.17	1	34.0	0.6	40.8	15.4	2148.4	8.4	173.5	419.5	14.8	132.0
2	67.44	71.57	0	34.1	0.8	36.8	16.9	2171.6	8.4	182.3	408.6	15.7	156.6
3	67.1	70.34	-1.5	33.7	1.4	55.0	21.6	2168.9	8.5	131.1	403.2	20.4	146.0
4	66.5	69.54	-1.5	33.3	1.0	58.1	22.5	2306.7	8.3	218.4	392.3	17.7	149.6
5	66.36	68.14	-1	33.3	0.9	50.4	22.6	2189.3	8.4	179.2	392.3	21.9	134.3
6	66.27	66.33	-0.5	33.6	1.0	49.1	23.3	2225.8	8.3	237.7	392.3	14.1	179.3
7	66.18	64.47	0	34.0	1.4	60.9	24.6	2215.1	8.3	206.3	381.4	8.5	153.0
8	66.08	63.16	1	34.0	1.4	52.5	24.4	2256.9	8.3	219.0	381.4	10.4	137.9
9	65.57	61.41	0.5	33.8	1.9	58.2	22.9	2271.1	8.3	212.7	381.4	7.9	152.7
10	65.46	60.08	0	33.7	1.8	54.1	22.9	2160.0	8.3	197.5	381.4	9.8	136.0
11	65.36	58.32	0	33.9	1.2	30.8	13.5	2196.4	8.3	188.7	386.8	9.2	144.2
12	65.29	57.06	0	33.9	1.7	53.8	20.6	2287.1	8.4	185.6	386.8	13.7	171.0
13	65.28	55.27	-1	33.4	1.7	50.0	19.4	2276.4	8.3	195.3	381.4	4.3	154.5
14	65.23	53.51	-0.5	33.8	1.5	37.7	14.0	2217.8	8.3	201.8	392.3	13.3	105.6
15	65.22	52.34	-1	34.0	1.9	55.5	21.2	2226.7	8.3	199.1	381.4	17.5	117.2
16	65.26	50.54	0	33.9	2.0	65.4	22.2	2310.2	8.3	213.7	386.8	3.0	175.0
17	65.32	49.27	0	33.9	1.9	50.3	18.7	2220.4	8.3	196.9	386.8	19.3	121.8
18	65.43	48.5	0.5	34.0	1.8	40.2	14.8	2224.0	8.4	184.3	386.8	14.0	171.1
19	65.48	46.27	0.5	34.0	2.3	56.9	22.4	2241.8	8.3	217.1	386.8	12.2	154.0
20	65.56	44.55	0.75	34.0	1.9	49.5	20.7	2220.4	8.3	209.0	452.2	9.9	122.6
21	66.06	43.06	1	34.0	1.5	48.7	18.7	2273.8	8.3	200.3	397.7	13.6	145.1
22	66.12	41.44	1	34.0	1.7	47.0	17.6	2177.8	8.4	172.5	381.4	7.3	118.9
23	66.2	40.15	0	34.0	1.4	33.3	14.1	2099.6	8.4	157.6	381.4	10.4	146.3
24	66.29	38.36	0	34.0	2.1	56.1	21.1	2239.1	8.4	169.4	392.3	10.7	133.0

25	66.37	37.01	-0.5	33.8	1.9	57.5	19.3	2153.8	8.4	149.9	392.3	14.1	166.9
26	66.47	35.02	-0.5	33.5	1.9	65.7	21.7	2224.0	8.4	168.8	386.8	14.4	129.5
27	66.54	33.39	-1	33.6	1.6	63.7	18.6	2162.7	8.5	117.7	408.6	14.4	106.8
28	67.02	31.59	-1	33.7	2.1	50.7	16.8	2287.1	8.5	131.3	435.9	11.5	118.6
29	67.11	30.11	-0.5	33.9	2.0	75.4	21.4	2216.0	8.4	162.5	392.3	9.5	133.3
30	67.2	28.3	-0.5	34.0	2.0	74.3	22.4	2217.8	8.4	165.0	386.8	3.1	105.0
31	67.29	26.35	-0.5	34.0	2.0	68.0	20.9	2267.6	8.5	149.1	408.6	4.7	139.0
32	67.36	24.54	-0.5	34.0	1.9	69.2	22.0	2294.2	8.4	171.1	392.3	7.2	124.6
33	67.45	23.09	-0.5	34.0	1.7	61.2	20.9	2199.1	8.4	160.0	392.3	11.0	161.8
34	67.55	21.16	0	34.0	1.4	29.8	11.0	2336.0	8.4	180.2	392.3	12.8	132.4
35	68.03	19.19	-1	34.1	2.3	81.2	42.2	2238.2	8.4	177.6	386.8	10.8	145.0
36	68.11	17.49	-1	34.1	1.7	63.6	19.1	2305.8	8.4	185.7	386.8	9.7	131.7
37	68.24	15.48	-1	34.2	1.5	43.1	13.1	2256.9	8.4	177.8	381.4	8.1	149.8
38	69.04	13.21	-2.5	33.3	1.8	72.9	21.2	2210.7	8.4	158.6	403.2	9.0	168.8

4.3.1.2 Under Sea Ice

Chemistry under the 2 m thick sea ice was the most interesting data showing very high productivity (chlorophyll *a* 6mg/m^3) and this resulted in pCO_2<50µatm, whereas Dissolved oxygen and pH were extremely high, 629 µM and 9.2 respectively (Fig. 36).

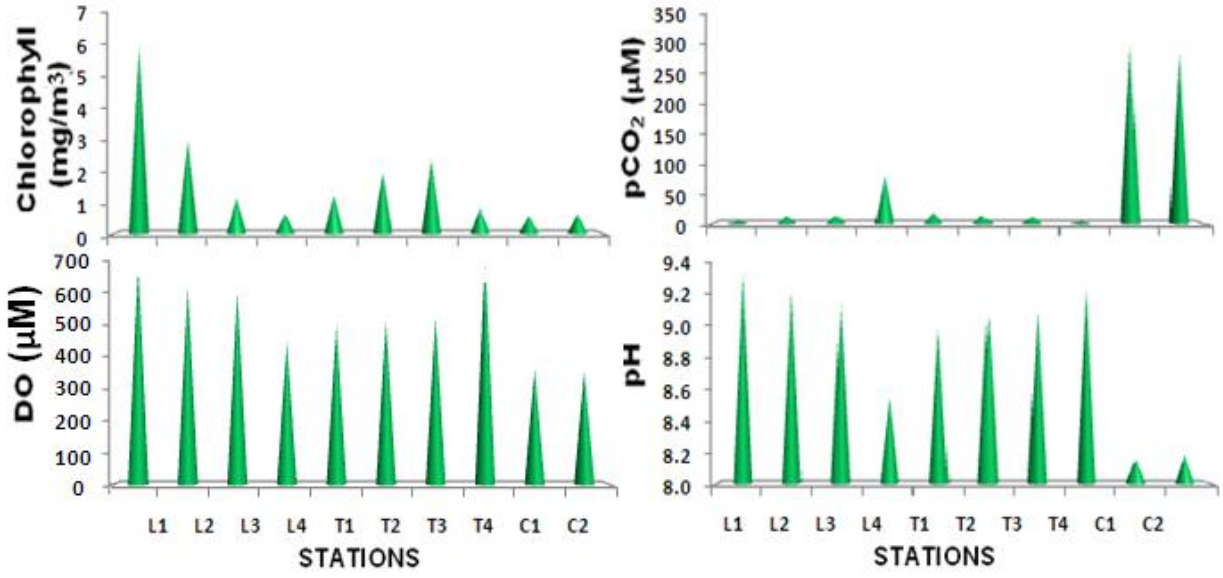

Fig.36. Variations in physicochemical parameters under the sea ice. C1 and C2 are stations collected from ice free region at 67°S and 69°S respectively.

Table 19: Variations in physicochemical parameters under Antarctic land fast Sea ice.

STATION	TCO_2 (µM)	pH	pCO_2 (µatm)	Chl a (mg/m^3)	Salinity	DO (uM)
L1	484.4	9.3	4.2	6.0	7.5	611.8
L2	992.0	9.2	12.4	3.0	6.7	544.9
L3	1160.0	9.2	12.7	1.1	23.4	531.5
L4	1448.9	8.6	79.6	0.6	24.8	393.0
T1	842.7	9.0	17.2	1.2	13.3	442.1
T2	805.3	9.1	13.0	2.0	15.3	451.1
T3	748.4	9.1	10.5	2.4	16.9	460.0
T4	274.7	9.2	3.5	0.8	3.7	629.7

4.3.2 Bay of Bengal

4.3.2.1 Coastal Bay of Bengal

Dissolved oxygen concentrations were high at the surface and were above 175 µM at all stations. Maximum concentration was found at Thamnapatnam (station 16) reaching upto 260 µM (Fig. 37). Concentration decreased rapidly with depth and an intense oxygen minimum zone (OMZ) is seen between 150-500 m. But at Thamnapatnam the OMZ starts from 75 m. Surface pH was greater than 8.3 at all stations and decreased with depth. pCO_2 was less than 300 µatm at all stations except Thamnapatnam, maximum pCO_2 was 376 µatm.

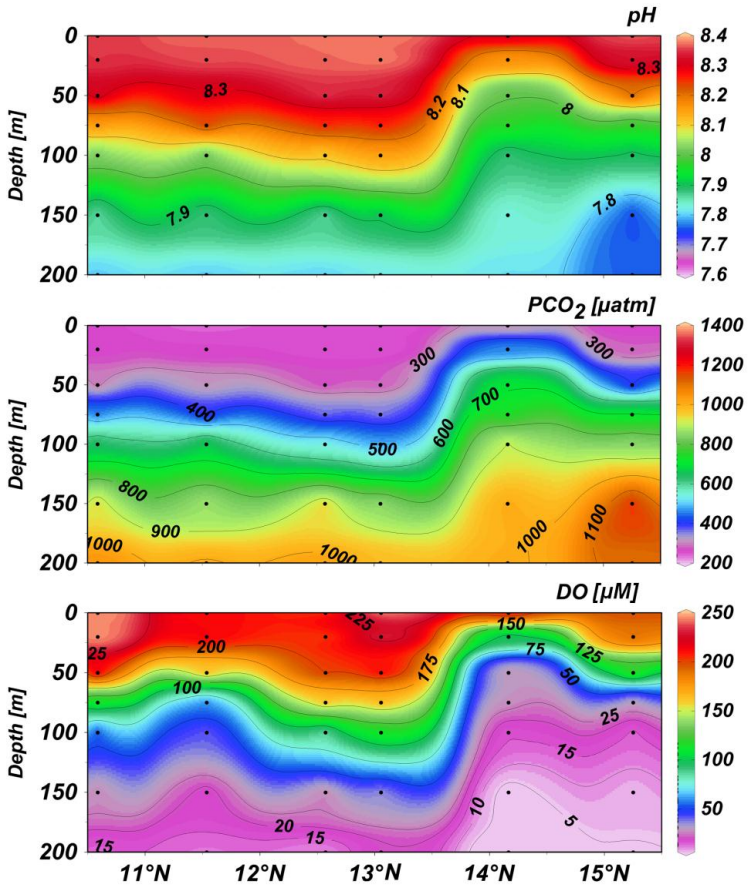

Fig.37. Vertical distribution of pCO_2, pH and Dissolved oxygen in coastal Bay of Bengal.

Table. 20: Latitudinal variations in physicochemical parameters along coastal western Bay of Bengal.

Station no.	Latitude	Longitude	SiO_4 (µM)	PO_4 (µM)	pH	Temp (°C)	Salinity	Wind (m/s)	TCO_2 (µM)	pCO_2 (µatm)	NO_3 (µM)	DO (uM)
1	10.60393	80.11622	5.4	0.4	8.3	29.1	34.1	7.6	1938.4	265.2	1.2	232.8
2	10.58783	80.19695	2.5	0.3	8.4	29.3	34.0	4.3	1930.2	231.4	0.0	247.7
3	10.61512	80.34663	3.8	0.3	8.5	29.7	33.5	3.9	2013.6	206.4	0.1	226.8
4	10.58977	80.52747	2.5	0.7	8.3	30.1	33.4	10.1	1900.0	235.0	0.2	226.8
5	10.58668	80.60625	1.6	0.3	8.4	30.3	33.5	7.5	1893.1	255.5	0.1	248.8
6	11.60047	79.91215	1.4	0.4	8.3	28.7	34.0	4.8	1952.6	273.9	0.3	216.3
7	11.554	79.9659	1.0	0.4	8.4	29.2	34.1	2.5	1982.0	257.2	0.0	216.3
8	11.5312	79.98088	2.0	0.3	8.3	29.5	33.6	7.3	1929.5	280.5	0.0	229.3
9	11.5323	80.04	1.0	0.4	8.3	29.7	33.7	6.0	2008.4	284.4	0.1	222.8
10	11.53628	80.14787	1.2	0.2	8.4	29.6	33.6	8.3	1889.2	240.6	0.1	214.6
11	12.54797	80.40715	0.9	0.2	8.4	29.5	34.0	5.0	1922.9	257.0	0.1	221.5
12	12.53783	80.59677	1.4	0.2	8.1	30.3	33.5	4.6	1930.0	237.0	0.1	214.4
13	12.48738	80.59083	1.6	0.2	8.4	30.2	33.6	6.0	1946.4	223.1	0.1	213.1
15	12.57157	80.68967	1.2	0.2	8.4	30.1	33.5	9.1	1921.4	245.4	0.1	202.5
16	13.115	80.4479	1.3	0.4	8.3	28.8	34.4	9.2	1997.6	279.5	0.0	263.0
17	13.10733	80.5315	0.8	0.3	8.4	28.6	34.3	8.5	1990.4	257.0	0.1	235.6
18	13.04522	80.61975	1.3	0.3	8.4	29.5	34.0	8.7	1983.8	238.2	0.1	227.8
20	13.05522	80.7585	1.5	0.3	8.4	29.8	33.8	7.7	1966.3	243.4	0.1	253.5
21	14.15875	80.3649	1.9	0.5	8.2	26.1	34.6	5.5	2114.5	376.2	4.1	171.1
22	14.15992	80.40377	1.5	0.6	8.2	26.2	34.6	2.9	2095.1	373.1	3.9	175.6
23	14.1585	80.41095	0.2	0.3	8.3	27.2	34.6	7.2	2001.3	276.5	0.1	228.4
24	14.16407	80.44907	1.0	0.4	8.3	27.3	34.5	7.5	2069.6	352.9	1.1	194.5
25	14.1659	80.47265	0.6	0.5	8.3	27.3	34.5	7.7	2038.9	305.2	0.5	212.6
26	15.24823	80.4029	1.1	0.2	8.4	28.7	34.4	3.1	1966.2	240.5	0.0	221.5
27	15.24907	80.48092	1.3	0.3	8.4	28.9	34.4	2.2	1966.3	234.4	0.2	224.7
28	15.24648	80.52252	1.1	0.3	8.4	29.5	34.3	6.5	1965.7	241.8	0.3	212.3
29	15.24903	80.551	0.5	0.4	8.4	28.8	34.4	5.0	2015.1	253.3	1.0	201.1
30	15.25185	80.6769	0.5	0.4	8.4	29.6	34.3	3.3	1956.9	254.0	0.0	199.7

4.3.2.2 Central Bay of Bengal

The average sea surface pCO_2 within a cyclonic eddy was 356 µatm, whereas outside the eddy average pCO_2 was 286 µatm. Maximum pCO_2 at surface was 445 µatm, which suggests that eddy play such an important role in elevating the already rising pCO_2 values due to anthropogenic activities (Fig. 38). Similar trend is followed by TCO_2, showing higher values within the eddy. Whereas pH showed opposite trend to pCO_2 and was higher outside the eddy.

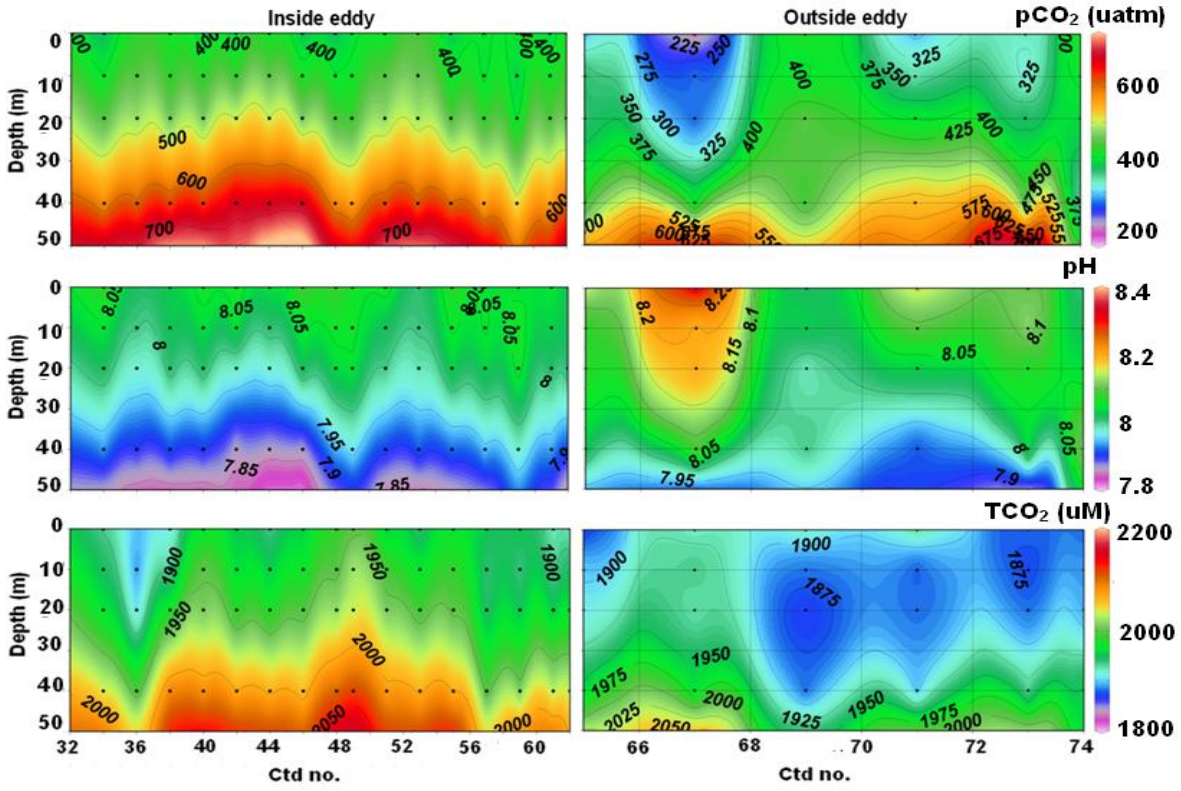

Fig.38. Vertical distribution of pCO_2, pH and TCO_2 within and outside a cyclonic eddy.

Table 21: Variations in physicochemical parameters Outside-EDDY										
Station no.	Depth (m)	Latitude (°N)	Longitude (°E)	Temp (°C)	Salinity	pH	TCO_2 (µM)	pCO_2 (µatm)	PO_4 (µM)	SiO_4 (µM)
65	0	15.4	87.2	27.7	33.3	8.2	1858.7	270.5	0.0	2.0
65	10	15.4	87.2	27.7	33.3	8.0	1897.0	378.2	2.1	3.4
65	20	15.4	87.2	27.7	33.3	8.1	1907.7	351.9	1.0	2.5
65	40	15.4	87.2	27.8	33.5	8.1	1923.2	368.7	0.9	2.0
65	60	15.4	87.2	26.2	34.4	7.9	2099.5	641.5	1.8	6.8
65	80	15.4	87.2	22.9	34.6	7.8	2127.2	822.5	2.2	16.0
65	100	15.4	87.2	20.2	34.7	7.7	2210.9	1079.0	3.2	19.1
65	120	15.4	87.2	18.6	34.8	7.7	2203.3	993.3	2.8	24.3
65	150	15.4	87.2	16.1	34.8	7.7	2241.8	1059.5	4.0	28.4
65	200	15.4	87.2	13.5	34.9	7.6	2283.1	1352.1	4.9	34.5
65	300	15.4	87.2	11.5	35.0	7.6	2279.2	1324.8	3.3	33.2
67	0	15.4	87.2	27.6	33.3	8.4	1915.8	167.9	0.7	2.0
67	10	15.4	87.2	27.6	33.3	8.2	1939.9	287.8	0.8	1.5
67	20	15.4	87.2	27.6	33.4	8.2	1916.0	244.9	0.9	1.9
67	40	15.4	87.2	27.7	33.6	8.2	1923.0	287.9	1.0	1.5
67	60	15.4	87.2	24.7	34.5	7.7	2144.1	924.3	2.4	8.9
67	80	15.4	87.2	21.9	34.7	7.7	2205.3	896.2	2.6	14.5
67	100	15.4	87.2	19.9	34.8	7.7	2177.2	999.5	2.8	15.8
67	120	15.4	87.2	18.3	34.8	7.6	2208.8	1288.9	3.1	23.6
67	150	15.4	87.2	15.6	34.9	7.6	2172.9	1341.9	4.4	24.3
67	200	15.4	87.2	13.2	35.0	7.4	2223.6	1730.9	3.2	25.6
67	300	15.4	87.2	11.4	35.0	7.6	2228.7	1206.2	3.7	31.3
69	0	15.4	87.2	27.7	33.5	8.0	1929.2	427.0	0.1	1.7
69	10	15.4	87.2	27.6	33.5	8.1	1879.5	366.3	0.3	1.8
69	20	15.4	87.2	27.6	33.5	8.0	1853.1	473.7	0.5	1.8
69	40	15.4	87.2	27.6	33.6	8.0	1850.1	384.1	0.7	2.0
69	60	15.4	87.2	27.6	33.9	7.9	1962.9	505.3	0.8	4.1
69	80	15.4	87.2	23.4	34.6	7.7	2117.1	898.9	1.8	13.3
69	100	15.4	87.2	21.0	34.8	7.6	2124.6	1082.7	2.1	18.3
69	120	15.4	87.2	18.8	34.7	7.7	2167.2	1034.9	2.2	20.8
69	150	15.4	87.2	15.8	34.9	7.6	2176.7	1224.9	2.5	27.1
69	200	15.4	87.2	13.4	34.9	7.6	2222.3	1233.4	2.6	30.4
69	300	15.4	87.2	11.5	35.0	7.5	2226.8	1412.3	4.1	29.2
71	0	15.4	87.2	27.6	33.5	8.2	1942.2	277.8	0.1	1.7
71	10	15.4	87.2	27.6	33.5	8.1	1862.3	311.5	0.2	1.8
71	20	15.4	87.2	27.6	33.5	8.0	1879.6	413.0	0.4	2.1
71	40	15.4	87.2	27.6	33.5	7.9	1846.7	538.6	0.9	2.0
71	60	15.4	87.2	24.6	34.5	7.9	2089.9	539.9	1.7	10.6
71	80	15.4	87.2	21.8	34.8	7.7	2171.3	877.3	2.3	16.5
71	100	15.4	87.2	19.7	34.7	7.7	2172.2	1039.4	2.2	19.7
71	120	15.4	87.2	17.6	34.8	7.7	2172.1	1038.9	3.1	24.8

71	150	15.4	87.2	15.3	34.9	7.6	2193.2	1322.1	3.1	27.7
71	200	15.4	87.2	13.2	35.0	8.2	2229.4	284.1	2.9	31.2
71	300	15.4	87.2	11.6	35.0	8.0	2272.2	462.8	2.8	34.8
73	0	15.4	87.2	27.6	33.5	8.1	1882.8	334.7	0.3	1.8
73	10	15.4	87.2	27.6	33.5	8.2	1861.8	283.1	0.4	2.1
73	20	15.4	87.2	27.6	33.5	8.0	1878.6	386.9	0.2	1.6
73	40	15.4	87.2	27.6	33.6	8.1	1895.9	313.5	0.5	1.9
73	60	15.4	87.2	26.0	34.4	7.7	2079.9	997.2	1.3	6.6
73	80	15.4	87.2	22.6	34.6	7.7	2199.2	933.6	2.1	15.2
73	100	15.4	87.2	20.6	34.7	7.6	2140.9	1249.3	2.2	18.7
73	120	15.4	87.2	19.3	34.7	7.6	2137.2	1355.0	2.4	21.0
73	150	15.4	87.2	16.5	34.8	7.6	2159.0	1297.0	2.6	25.8
73	200	15.4	87.2	13.8	34.9	7.6	2301.5	1392.9	2.3	29.6
73	300	15.4	87.2	11.5	35.0	7.5	2239.0	1412.1	2.9	35.8
74	0	15.4	87.2	27.8	33.5	8.0	1875.4	418.3	0.0	1.9
74	10	15.4	87.2	27.8	33.5	8.0	1888.7	410.9	0.1	2.0
74	20	15.4	87.2	27.8	33.5	8.0	1883.2	386.5	0.0	1.9
74	40	15.4	87.2	27.8	33.5	8.2	1959.4	284.9	0.0	2.0
74	60	15.4	87.2	26.7	34.2	8.0	1912.3	395.0	0.0	2.3
74	80	15.4	87.2	22.3	34.7	7.7	2147.9	924.3	1.7	16.2
74	100	15.4	87.2	20.1	34.8	7.7	2167.1	966.0	2.2	20.7
74	120	15.4	87.2	18.4	34.8	7.6	2198.8	1206.0	2.1	23.3
74	150	15.4	87.2	16.2	34.8	7.6	2250.2	1254.7	2.3	28.1
74	200	15.4	87.2	13.4	34.9	7.6	2265.2	1346.1	2.4	31.8
74	300	15.4	87.2	11.4	35.0	7.5	2264.7	1435.8	2.5	37.3

Table 22: Variations in physicochemical parameters inside-EDDY										
Station no.	Latitude (°N)	Longitude (°E)	Depth (m)	Temp (°C)	Salinity	pH	TCO_2 (µM)	pCO_2 (µatm)	PO_4 (µM)	SiO_4 (µM)
34	17.48	87.31	0	27.6	33.4	8.1	1891.1	300.8	0.2	5.0
34	17.48	87.31	10	27.6	33.4	8.1	1903.5	347.1	0.1	0.3
34	17.48	87.31	20	27.6	33.4	8.1	1905.2	361.7	0.2	1.0
34	17.48	87.31	40	27.8	33.7	8.1	1936.6	378.0	0.2	1.6
34	17.48	87.31	60	24.5	34.5	7.7	2102.8	865.7	1.4	10.7
34	17.48	87.31	80	21.5	34.8	7.7	2167.2	966.7	2.0	17.1
34	17.48	87.31	100	19.3	34.8	7.7	2138.0	1061.4	2.2	21.5
34	17.48	87.31	120	18.0	34.8	7.7	2127.8	995.7	2.4	26.5
34	17.48	87.31	150	15.6	34.9	7.6	2122.1	1076.8	2.4	27.3
34	17.48	87.31	200	13.3	35.0	7.6	2144.3	1190.3	2.9	32.8
34	17.48	87.31	250	12.1	35.0	7.6			2.5	32.8
34	17.48	87.31	300	11.3	35.0	7.5	2197.8	1416.1	2.8	34.8
34	17.48	87.31	400	10.5	35.0	7.5			2.8	37.7
34	17.48	87.31	500	9.8	35.0	7.5			2.8	43.6
36	17.48	87.31	10	27.4	33.3	8.0	1817.9	371.6	0.1	3.1
36	17.48	87.31	20	27.4	33.7	8.0	1784.6	411.5	0.4	5.6
36	17.48	87.31	40	27.9	34.0	8.0	1854.0	445.5	0.4	5.2
36	17.48	87.31	60	23.5	34.7	7.8	2029.9	792.7	1.7	13.5
36	17.48	87.31	80	20.9	34.8	7.7	1998.6	956.8	1.8	21.3
36	17.48	87.31	100	18.8	34.8	7.6	2103.9	1103.8	1.9	23.3
36	17.48	87.31	120	17.0	34.8	7.6	2101.2	1095.9	2.2	27.4
36	17.48	87.31	150	15.1	34.9	7.6	2061.2	1175.1	2.3	29.5
36	17.48	87.31	200	13.0	35.0	7.5	2151.9	1300.7	2.4	33.9
36	17.48	87.31	300	11.2	35.0	7.5	2206.9	1366.0	2.7	33.6
38	17.48	87.31	0	27.4	33.5	8.0	1847.2	387.2	0.3	2.3
38	17.48	87.31	10	27.4	33.5	8.1	1822.9	355.2	0.1	3.2
38	17.48	87.31	20	27.4	33.5	8.1	1911.2	315.1	0.2	1.8
38	17.48	87.31	40	27.3	34.1	8.0	2044.2	434.7	0.8	3.8
38	17.48	87.31	60	23.3	34.7	7.7	2101.9	996.7	1.7	16.5
38	17.48	87.31	80	21.1	34.8	7.7	2151.6	936.7	2.0	18.7
38	17.48	87.31	100	19.0	34.8	7.6	2151.2	1235.5	2.1	22.9
38	17.48	87.31	120	17.2	34.3	7.6	2220.5	1192.5	2.2	27.3
38	17.48	87.31	150	15.1	35.0	7.6	2196.6	1237.6	2.5	29.8
38	17.48	87.31	200	13.2	35.0	7.5	2224.1	1365.8	2.4	33.3
38	17.48	87.31	300	11.5	35.0	7.5	2243.6	1351.6	2.6	38.2
40	17.48	87.31	0	27.3	33.5	8.1	1887.5	321.4	0.2	1.4
40	17.48	87.31	10	27.3	33.5	8.1	1983.4	367.1	0.2	1.5
40	17.48	87.31	20	27.4	33.5	8.1	1907.6	325.8	0.3	5.5
40	17.48	87.31	40	26.7	33.2	8.0	1948.1	476.1	0.9	12.3
40	17.48	87.31	60	23.0	34.7	7.7	2103.0	1022.3	1.9	15.0
40	17.48	87.31	80	20.6	34.8	7.8	2239.8	891.9	2.1	18.4
40	17.48	87.31	100	18.9	34.8	7.6	2178.9	1133.6	2.4	21.7

40	17.48	87.31	120	17.0	34.8	7.6	2158.9	1087.4	2.3	17.4
40	17.48	87.31	150	15.2	34.9	7.7	2189.4	957.7	1.9	26.8
40	17.48	87.31	200	12.8	35.0	7.6	2220.2	1329.8	2.6	30.4
40	17.48	87.31	300	11.3	35.0	7.5	2270.3	1382.0	2.6	2.4
42	17.48	87.31	0	27.4	33.4	8.1	1900.0	321.6	0.1	3.4
42	17.48	87.31	10	27.4	33.4	8.2	1889.8	261.9	0.3	1.9
42	17.48	87.31	20	27.4	33.4	8.0	1879.8	463.6	0.9	9.1
42	17.48	87.31	40	27.5	34.0	7.8	1941.4	785.8	1.6	13.7
42	17.48	87.31	60	24.5	34.6	7.8	2120.8	823.7	1.8	20.1
42	17.48	87.31	80	22.3	34.8	8.1	2145.1	395.0	0.3	3.3
42	17.48	87.31	100	20.2	34.8	7.6	2127.5	1099.3	2.3	24.8
42	17.48	87.31	120	17.9	34.8	7.6	2147.2	1108.0	2.2	30.2
42	17.48	87.31	150	15.7	34.9	7.6	2193.9	1117.9	2.5	34.4
42	17.48	87.31	200	13.6	35.0	7.6	2233.0	1303.6	2.7	40.4
42	17.48	87.31	300	11.3	35.0	7.6	2239.6	1220.9	2.6	45.0
44	17.48	87.31	0	27.4	33.4	8.1	1868.1	342.5	0.1	3.5
44	17.48	87.31	10	27.4	33.4	8.1	1888.9	367.7	0.1	2.8
44	17.48	87.31	20	27.4	33.4	8.0	1885.4	413.8	0.2	8.3
44	17.48	87.31	40	27.0	33.9	7.8	1942.4	638.9	0.9	13.6
44	17.48	87.31	60	24.0	34.6	7.8	2091.8	789.9	1.5	19.7
44	17.48	87.31	80	21.6	34.8	7.6	2168.0	1157.1	1.9	26.9
44	17.48	87.31	100	19.8	34.8	7.6	2159.8	1145.3	2.1	30.5
44	17.48	87.31	120	17.4	34.8	7.6	2196.1	1155.5	2.3	34.2
44	17.48	87.31	150	14.9	34.9	7.5	2223.2	1442.1	2.3	39.3
44	17.48	87.31	200	13.0	35.0	7.5	2192.4	1489.7	2.4	14.5
44	17.48	87.31	300	11.2	35.0	7.7	2279.2	939.8	1.7	3.4
46	17.48	87.31	0	27.4	33.3	8.2	1890.4	287.0	0.2	3.4
46	17.48	87.31	10	27.4	33.3	8.1	1895.6	334.3	0.1	1.8
46	17.48	87.31	20	27.3	33.0	8.2	1917.0	278.9	0.1	7.4
46	17.48	87.31	40	27.1	34.0	7.8	1908.8	719.0	1.2	11.7
46	17.48	87.31	60	23.2	34.7	7.7	2023.4	955.5	2.0	17.8
46	17.48	87.31	80	21.1	34.8	7.8	2174.3	867.8	2.0	19.1
46	17.48	87.31	100	18.9	34.8	7.6	2225.5	1158.2	2.2	21.8
46	17.48	87.31	120	17.5	34.8	7.6	2240.1	1273.3	2.2	25.4
46	17.48	87.31	150	15.4	34.9	7.6	2248.9	1130.5	2.5	30.1
46	17.48	87.31	200	13.3	34.9	7.5	2276.1	1432.6	2.5	32.6
46	17.48	87.31	300	11.4	35.0	7.5	2292.1	1355.5	2.6	38.4
48	17.48	87.31	0	27.3	33.4	8.2	1917.0	294.1	0.0	1.9
48	17.48	87.31	10	27.3	33.4	8.1	1901.9	360.9	0.1	1.7
48	17.48	87.31	20	25.3	33.4	8.1	1901.3	312.4	0.3	2.3
48	17.48	87.31	40	27.1	33.2	8.0	1988.7	428.5	1.6	3.6
48	17.48	87.31	60	24.3	34.7	7.8	2099.8	781.6	1.8	13.1
48	17.48	87.31	80	21.3	34.8	7.7	2176.1	1039.4	2.1	17.6
48	17.48	87.31	100	18.8	34.8	7.6	2184.9	1108.5	2.2	23.1

48	17.48	87.31	120	17.4	34.8	7.7	2168.0	1013.8	2.2	23.1
48	17.48	87.31	150	15.3	34.9	7.5	2238.5	1415.6	2.4	28.5
48	17.48	87.31	200	13.3	34.9	7.6	2233.9	1211.1	2.5	33.4
48	17.48	87.31	300	11.5	35.0	7.5	2271.8	1370.9	1.7	38.7
49	17.48	87.31	0	27.2	33.5	8.0	1924.6	395.3	0.1	0.8
49	17.48	87.31	10	27.2	33.5	8.1	2009.2	379.6	0.1	0.7
49	17.48	87.31	20	27.2	33.5	8.2	1929.8	281.3	0.3	0.8
49	17.48	87.31	40	27.5	34.1	8.1	2037.8	334.4	1.6	1.7
49	17.48	87.31	60	24.1	34.4	7.8	2138.3	746.1	1.9	11.7
49	17.48	87.31	80	22.0	35.8	7.8	2175.8	774.8	2.0	15.8
49	17.48	87.31	100	20.1	35.8	7.6	2225.3	1134.5	2.1	20.2
49	17.48	87.31	120	18.3	35.8	7.6	2171.1	1139.2	2.4	23.3
49	17.48	87.31	150	16.2	35.9	7.6	2232.1	1183.5	2.6	27.1
49	17.48	87.31	200	13.7	34.9	7.6	2258.9	1231.7	2.9	31.7
49	17.48	87.31	300	11.5	35.0	7.5	2253.9	1572.8	2.9	37.0
51	17.48	87.31	0	27.3	33.4	8.2	1855.3	304.7	0.3	2.1
51	17.48	87.31	10	27.3	33.4	8.0	1938.1	435.7	0.4	1.4
51	17.48	87.31	20	27.3	33.4	8.1	1917.6	361.2	0.2	1.2
51	17.48	87.31	40	27.4	34.0	8.0	1948.6	481.4	0.9	7.3
51	17.48	87.31	60	23.6	34.8	7.7	2132.8	1016.9	1.6	12.3
51	17.48	87.31	80	20.9	34.7	7.7	1917.1	834.8	2.2	17.4
51	17.48	87.31	100	19.1	34.8	7.7	2200.6	990.0	2.4	23.0
51	17.48	87.31	120	17.6	34.9	7.9	2237.7	646.0	2.2	24.8
51	17.48	87.31	150	15.0	34.9	7.6	2266.8	1161.3	2.5	30.2
51	17.48	87.31	200	13.0	35.0	7.5	2255.1	1371.9	2.6	33.6
51	17.48	87.31	300	11.2	35.0	7.5	2301.5	1488.5	2.6	39.6
53	17.48	87.31	0	27.2	33.5	8.0	1858.7	439.8	0.4	1.7
53	17.48	87.31	10	27.3	33.5	8.0	1897.0	397.7	0.4	1.5
53	17.48	87.31	20	27.3	33.5	8.0	1907.7	407.0	0.4	1.3
53	17.48	87.31	40	27.2	33.9	8.0	1923.2	382.7	0.6	3.0
53	17.48	87.31	60	23.8	34.5	7.7	2099.5	934.5	2.2	12.9
53	17.48	87.31	80	21.6	34.6	7.6	2127.2	1125.0	2.3	16.6
53	17.48	87.31	100	19.7	34.8	7.6	2210.9	1205.9	2.3	20.6
53	17.48	87.31	120	18.2	34.8	7.6	2203.3	1125.9	2.2	24.0
53	17.48	87.31	150	15.8	34.9	7.6	2241.8	1333.5	2.6	26.4
53	17.48	87.31	200	13.5	35.0	7.6	2283.1	1362.5	2.7	31.0
53	17.48	87.31	300	11.3	35.0	7.6	2279.2	1312.7	2.8	37.8
55	17.48	87.31	0	27.1	33.5	8.1	1915.8	308.1	0.5	1.1
55	17.48	87.31	10	27.1	33.5	8.1	1939.9	344.4	0.4	1.4
55	17.48	87.31	20	27.1	33.5	8.1	1916.0	301.5	0.3	1.8
55	17.48	87.31	40	27.2	33.8	8.0	1923.0	453.0	0.5	4.1
55	17.48	87.31	60	24.4	34.7	7.7	2144.1	931.4	1.7	11.1
55	17.48	87.31	80	21.9	34.7	7.8	2205.3	877.0	2.0	17.0
55	17.48	87.31	100	19.8	34.8	7.7	2177.2	897.5	2.1	13.3

55	17.48	87.31	120	18.2	34.8	7.6	2208.8	1178.4	2.2	22.2
55	17.48	87.31	150	15.9	34.9	7.6	2172.9	1094.8	2.3	28.1
55	17.48	87.31	200	13.2	35.0	7.5	2223.6	1394.8	2.5	32.6
55	17.48	87.31	300	11.2	35.0	7.5	2228.7	1562.3	2.6	37.3
57	17.48	87.31	0	27.3	33.5	8.0	1929.2	422.7	0.2	2.0
57	17.48	87.31	10	27.3	33.5	8.1	1879.5	310.1	0.4	1.6
57	17.48	87.31	20	27.3	33.5	8.1	1853.1	331.3	0.5	1.4
57	17.48	87.31	40	26.8	33.7	8.1	1850.1	359.1	0.9	3.6
57	17.48	87.31	60	26.6	33.4	7.7	1962.9	835.0	1.9	14.1
57	17.48	87.31	80	21.9	34.8	7.7	2117.1	1030.6	2.1	15.3
57	17.48	87.31	100	20.0	34.8	7.7	2124.6	849.5	2.2	18.8
57	17.48	87.31	120	17.8	34.8	7.5	2167.2	1365.3	2.4	22.2
57	17.48	87.31	150	15.8	34.9	7.6	2176.7	1178.3	2.4	27.4
57	17.48	87.31	200	13.6	34.9	7.6	2222.3	1232.9	2.6	31.2
57	17.48	87.31	300	11.6	35.0	7.5	2226.8	1421.6	2.9	35.7
59	17.48	87.31	0	27.4	33.5	8.0	1942.2	445.3	0.1	1.7
59	17.48	87.31	10	27.4	33.5	8.1	1862.3	313.1	0.1	1.5
59	17.48	87.31	20	27.3	33.5	8.2	1879.6	277.7	0.1	1.2
59	17.48	87.31	40	27.1	33.6	8.0	1846.7	367.5	0.2	1.6
59	17.48	87.31	60	25.0	34.3	8.0	2089.9	492.9	0.7	5.1
59	17.48	87.31	80	22.0	34.7	7.7	2171.3	971.6	2.0	15.8
59	17.48	87.31	100	19.3	34.7	7.7	2172.2	1027.9	2.1	20.6
59	17.48	87.31	120	17.4	34.8	7.6	2172.1	1158.1	2.4	22.9
59	17.48	87.31	150	15.6	34.9	7.6	2193.2	1191.4	2.4	26.5
59	17.48	87.31	200	13.5	34.9	7.5	2229.4	1383.5	2.6	30.2
59	17.48	87.31	300	11.3	35.0	7.5	2272.2	1518.0	2.9	35.1
61	17.48	87.31	0	27.4	34.4	8.1	1882.8	343.0	0.3	2.8
61	17.48	87.31	10	27.4	33.4	8.0	1861.8	373.1	0.4	2.1
61	17.48	87.31	20	27.4	33.4	8.1	1878.6	346.7	0.1	2.0
61	17.48	87.31	40	27.2	33.6	8.0	1895.9	425.3	0.9	5.1
61	17.48	87.31	60	24.5	34.4	7.9	2079.9	605.3	1.5	10.7
61	17.48	87.31	80	21.8	34.7	7.7	2199.2	992.7	1.9	15.4
61	17.48	87.31	100	19.8	34.8	7.7	2140.9	990.7	2.2	18.7
61	17.48	87.31	120	18.2	34.8	7.7	2137.2	1056.7	2.2	21.7
61	17.48	87.31	150	16.0	34.9	7.6	2159.0	1286.5	2.6	26.2
61	17.48	87.31	200	13.6	35.0	7.5	2301.5	1406.2	2.6	29.7
61	17.48	87.31	300	11.3	35.0	7.6	2239.0	1291.9	3.0	21.8
62	17.48	87.31	0	27.4	33.4	8.0	1875.4	414.8	0.0	1.7
62	17.48	87.31	20	27.4	33.4	8.1	1883.2	304.8	0.2	1.3
62	17.48	87.31	40	27.0	33.7	8.0	1959.4	494.6	1.0	7.1
62	17.48	87.31	60	25.5	34.0	7.7	1912.3	825.8	1.7	12.0
62	17.48	87.31	80	23.1	34.7	7.7	2147.9	904.8	2.0	18.3
62	17.48	87.31	100	24.0	34.9	7.7	2167.1	1059.3	2.4	19.4
62	17.48	87.31	120	18.8	34.8	7.7	2198.8	1041.3	2.2	21.7

62	**17.48**	**87.31**	**150**	**16.3**	**34.8**	**7.6**	**2250.2**	**1176.8**	**2.3**	**28.6**
62	**17.48**	**87.31**	**200**	**13.8**	**34.9**	**7.5**	**2265.2**	**1404.7**	**2.5**	**32.3**
62	**17.48**	**87.31**	**300**	**11.6**	**35.0**	**7.6**	**2264.7**	**1170.3**	**2.7**	**40.2**

4.4 Carbon Fluxes

4.4.1 CO_2 Fluxes

4.4.1.1 Southern Ocean

The average air-sea flux was –9.2 and –18 mmol $m^{-2}d^{-1}$ on T_W and T_E, respectively during 2009, whereas it was -15.3 and -25 mmol $m^{-2}d^{-1}$ on T_W and T_E, respectively during 2010 (Fig. 39). The average fluxes during 2012 were -30 mmol $m^{-2}d^{-}1$. Therefore the Southern Ocean acted as a mean sink during all the 3 years. The averaged wind speed was 8.8 m/s (T_E) and 11.5 m/s (T_W) during 2009, and 8.3 m/s (T_E) and 10.2 m/s (T_W) during 2010. During 2012 the wind speed averaged 11m/s.

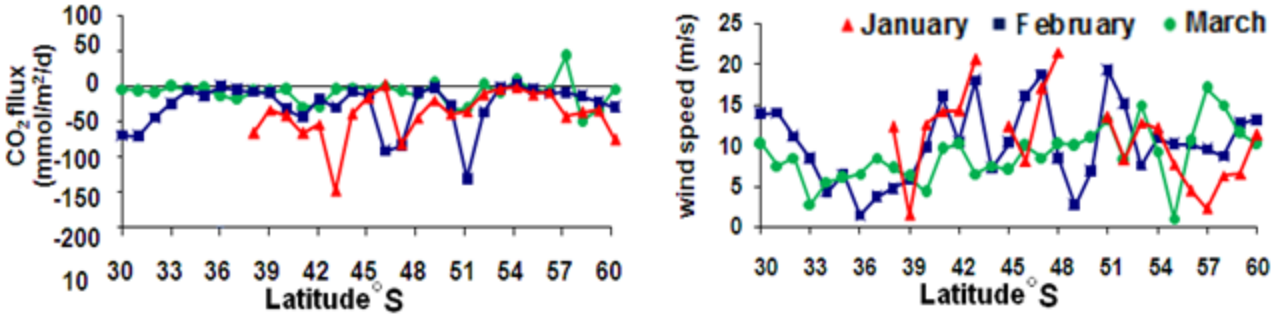

Fig.39.Spatial variations in CO_2 flux during March 2009, February 2010 and January 2012 in Indian sector of Southern Ocean.

4.4.1.1.1 Enderby Basin

Due to the strong wind forcing in the coastal regions upwelling in particular plays a significant source of atmospheric CO_2 with high flux densities. The sea-air CO_2 fluxes showed that in March 2009, the Enderby basin absorbed atmospheric CO_2 at a rate ranging from -26 to 60 mmol $m^{-2}d^{-1}$, whereas in February 2010, it absorbed from -34 to 41.3 mmol $m^{-2}d^{-1}$ and during January 2012 it was -4 to -169

mmol $m^{-2}d^{-1}$. Averaged CO_2 fluxes suggest that the Enderby Basin acts as a weak sink of

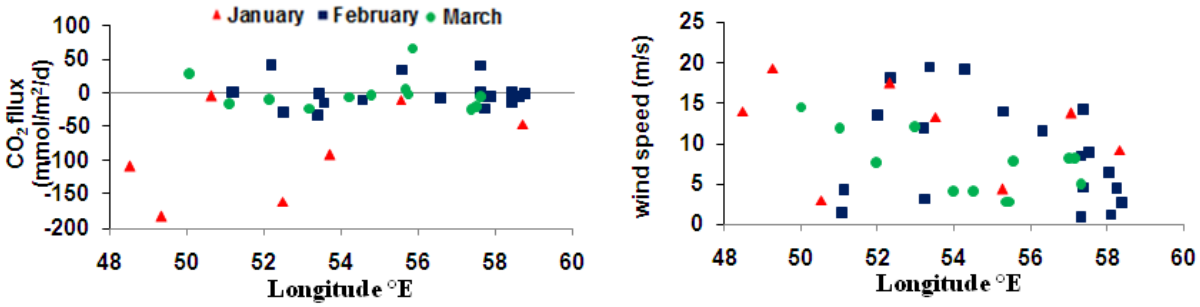

Fig.40. Spatial variation in CO_2 flux during March 2009, February 2010 and January 2012 in Indian sector of Southern Ocean along Antarctic coast.

CO_2 to the atmosphere, -1.7 and -2.4 mmol $m^{-2}d^{-1}$ during March 2009 and February 2010, respectively and acts as a strong sink -81 mmol $m^{-2}d^{-1}$ during January 2012 (Fig. 40). Fluxes depict the dynamic nature of coastal ecosystem, wherein we can see rapid changes within very short distances. Such high flux densities (-20 mmol $m^{-2}d^{-1}$) were also reported in coastal Antarctic waters by Louanchi et al., 2001. Carbon dioxide fluxes in different regions have been given in Table: 23.

Table 23: Comparison of sea–air fluxes of CO_2 in the present study with the CO_2 fluxes from previous studies.

Region	Period	Flux (mmol $m^{-2}d^{-1}$)	References
Enderby Basin, Antarctic Coastal region, Indian Sector	March 2009 February 2010 January 2012	-1.7 -2.4 -81	Present study
Antarctic Ocean (Indian Sector)	winter	-20	Louanchi et al., 2001

Antarctic Ocean (Atlantic Sector)	**Summer**	**-3 to + 7**	**Stoll et al., 2002**
Arctic Ocean	**Summer**	**-7.7**	**Murata and Takizawa (2003)**
Chukchi Sea		**-12**	
Canadian Coast	**Year**	**-16.8**	**Murata et al., (2008)**

The CO_2 fluxes (with in ACS) averaged 2.4 and 0.1 mmol $m^{-2}d^{-1}$ along T_E during 2009 and 2010 respectively, whereas along T_W, CO_2 fluxes averaged -5.9 and -6.8 mmol $m^{-2}d^{-1}$ during 2009 and 2010 respectively. These findings indicate that the eastern region acted as a source, whereas the western region acted as a sink for atmospheric CO_2. Higher extreme values of CO_2 fluxes were observed chiefly in 2009. Whereas during 2012, it acted as a strong sink throughout the transect.

4.4.1.2 Bay of Bengal

4.4.1.2.1 Coastal Bay of Bengal

The average CO_2 flux in Bay of Bengal along east coast of India was -12.8 mmol $m^{-2}day^{-1}$(Fig. 41). Whereas at Thamnapatnam the CO_2 flux was -3.9 mmol m^{-2} day^{-1}. The negative sign indicates that the region is a sink for atmospheric CO_2 and the capacity to act as a sink decreased at Thamnapatnam.

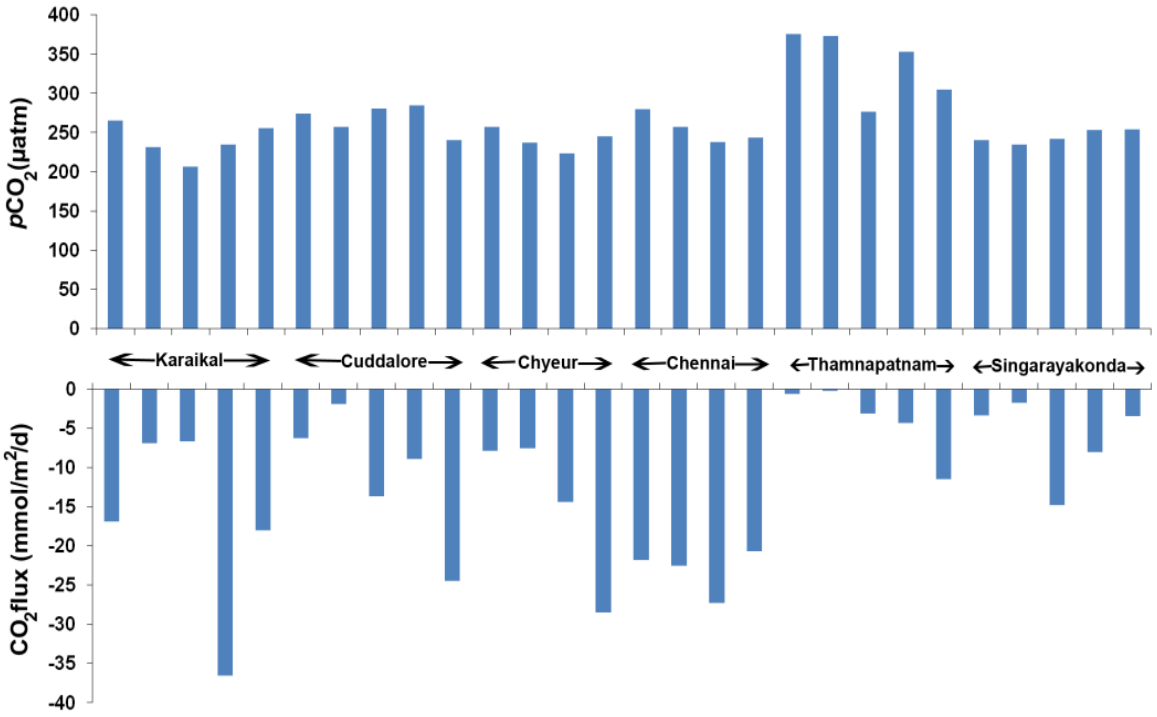

Fig.41. Station wise distribution of *p*CO_2 and CO_2 flux in Bay of Bengal along east coast of India.

4.4.1.2.2 Open Bay of Bengal waters

The average CO_2 flux in Bay of Bengal outside eddy was -7.8 mmol m^{-2} day^{-1}. Whereas within eddy the CO_2 flux was -2.2 mmol $m^{-2}day^{-1}$ (Fig. 42). The capacity to act as a sink decreases within an eddy. Also, few stations within the eddy act as a source of CO_2 to the atmosphere.

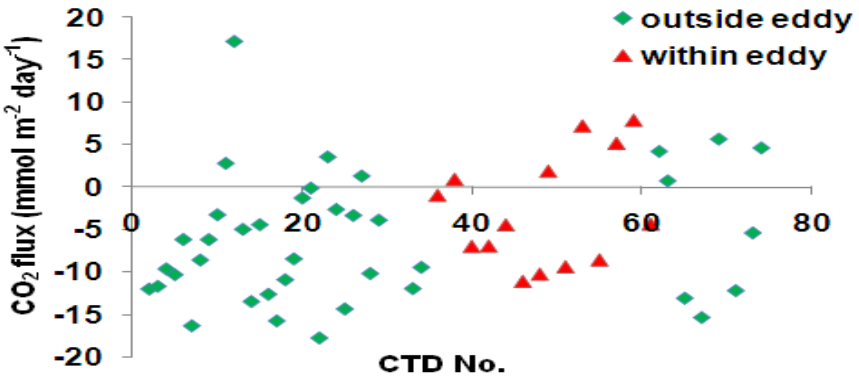

Fig.42. Station wise distribution of carbon dioxide flux in Bay of Bengal within and outside a cyclonic eddy.

4.4.2 Carbon Fluxes

The net effect of the biological pump on draw-down of atmospheric CO_2 depends on three main characteristics. Firstly, the mode and speed of particle sinking determines the depth to which particles are exported and the degree to which they are remineralised in the water column. Empirical studies have yielded algorithms linking primary production to particulate organic carbon (POC) flux and water depth (Suess, 1980; Pace et al., 1987; Berger et al., 1987) that are useful to calculate the fraction of productivity that is exported (i.e. the Export Ratio, ER= POC Flux/Primary Production). There are significant regional differences in ER normalised to a single depth (e.g. ER2000m by Lampitt and Antia, 1997; ER1000m by Fischer et al., 2000). Yet little is known of regional and temporal variations in the degree of decrease of POC flux with depth that results from differences in the mode of export and composition of sedimentary particles.

Secondly, the draw-down of atmospheric CO_2 is a function not just of the organic tissue pump but results from the ratio of organic (POC) to inorganic carbon (PIC=calcite+aragonite) in export, termed the rain ratio (RR=POC:PIC), since photosynthesis and calcification have opposing effects on pCO_2 of the surface

water that is in contact with the atmosphere (Frankignoulle et al., 1994; Archer and Meier-Reimer, 1994). The Rain Ratio is thus a measure of the "efficiency" of biological carbon sequestration.

4.4.2.1 Southern Ocean

Primary productivity (PP) was high in the subtropical front as compared with the SAF, PF or Antarctic zone (ANZ). Among the 3 months of sampling, January had the highest productivity. MLD integrated PP was 442, 248, 162 and 92 mgC/m^2/d during March, 506, 383, 254 and 155 mgC/m^2/d during February and was 809, 466, 461 and 371 mgC/m^2/d during January in the STF, SAF, PF and AZ respectively. Primary productivity (PP) was high in the subtropical front as compared with the SAF, PF or Antarctic zone (AZ). The modelled PP values were comparable with the *insitu* PP values for the study area during same time period as described in Gandhi et al., 2012. Carbon fluxes were calculated using equations given by Pace et al., 1987, and Suess 1980. POC fluxes were high at the STF and decreased towards south. POC fluxes at the bottom of MLD were

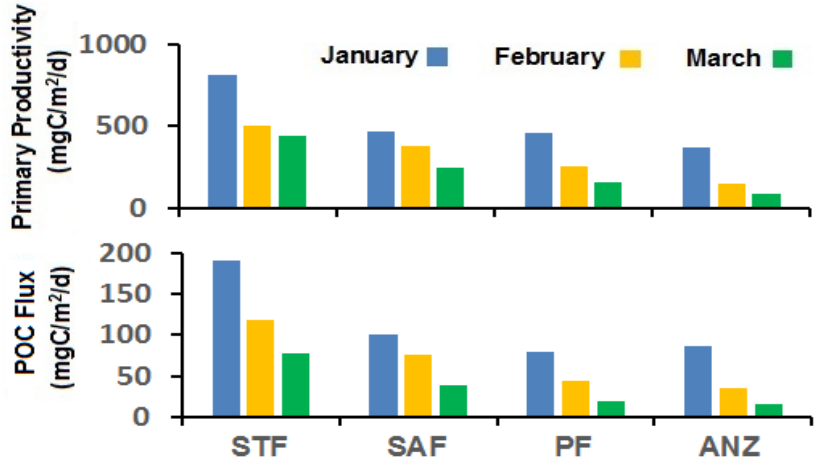

Fig.43. Primary productivity and Particulate organic carbon flux at bottom of MLD, during March 2009, February 2010 and January 2012 in different fronts.

190, 100, 80, 87 mgC/m^2/d during January, 118, 76, 44, 36 mgC/m^2/d during February, 77, 38, 19, 16 mgC/m^2/d during March along STF, SAF, PF and AZ respectively (Fig.43). POC fluxes at 1000m also followed similar trend as that of PP and averaged 11.6, 7.1 and 5.1 mgC/m^2/d during January, February and March respectively. The export ratio was 0.02 at 1000m, whereas at 100m it was 0.11, thus indicating a lowering in downward POC flux at deeper depths, due to remineralization. Inorganic carbon flux was calculated using equation of Martin et al., 1993, at 1000 m depth. The organic carbon flux to inorganic carbon flux ratio (Co/Ci) was calculated, and the ratio varied from 0.19 to 0.93 during March, 0.32 to 1.06 during February, and 0.78 to 1.7 during January. The Co/Ci decreased from STF towards the AZ for all the 3 years. Co/Ci was maximum in the STF (1.7) during January and the lowest in the AZ (0.73) during March.

4.4.2.2 Bay of Bengal

The integrated primary production within the cyclonic eddy was 480 mgC/m^2/d, whereas outside eddy it was 287 mgC/m^2/d. The POC flux at 1000 m were 10.6 mgC/m^2/d and 6.3 mgC/m^2/d within the cyclonic eddy and outside the eddy respectively. The Co/Ci at 1000 m was 1 and 0.6, within the cyclonic eddy and outside the eddy respectively. The *insitu* integrated primary productivity within the cyclonic eddy was 430 mgC/m^2/d, whereas outside eddy it was 203 mgC/m^2/d (Singh et al., 2015), POC flux at 1000 m were 9.5 mgC/m^2/d and 4.5 mgC/m^2/d

within the cyclonic eddy and outside the eddy respectively. The Co/Ci at 1000 m was 0.9 and 0.42, within the cyclonic eddy and outside the eddy respectively.

Along the coastal Bay of Bengal during May 2009, the integrated primary productivity at Thamnapatnam was 2005 mgC/m^2/d, whereas at karaikal it was 900.4 mgC/m^2/d. The carbon fluxes at 1000 m were 44.3 and 19.9 mgC/m^2/d. The Co/Ci at 1000 m was 4.3 and 1.9, at Thamnapatnam and Karaikal respectively.

4.5 Phytoplankton Distribution

4.5.1. Phytoplankton in Southern Ocean

Diatoms were the most dominating Phytoplankton group and its abundance was high during February and January as compared to March. Maximum abundance was seen during January reaching upto 15.3 x 10^3 cells/l at 51°S (Fig. 44). Average diatom abundance was also high during January (3.2 x 10^3 cells/l) which decreased to 2.4 x 10^3 cells/l during February and 0.49 x 10^3 cells/l during March. Despite having maximum abundance of Diatoms during January, but still the species diversity was maximum during February. The Shannon-Weaver Diversity Index (H') was 7.6, 5.8 and 3.5 for February, January and March respectively. The most common Diatom species found were *Trichotoxon, Thalassiothrix antarctica, Nitzschia species, Pseudonitzschia lineola, Dactyliosolen species, Corethron pennatum, Chaetoceros species, Proboscia alata, Navicula species, Coscinodiscus*

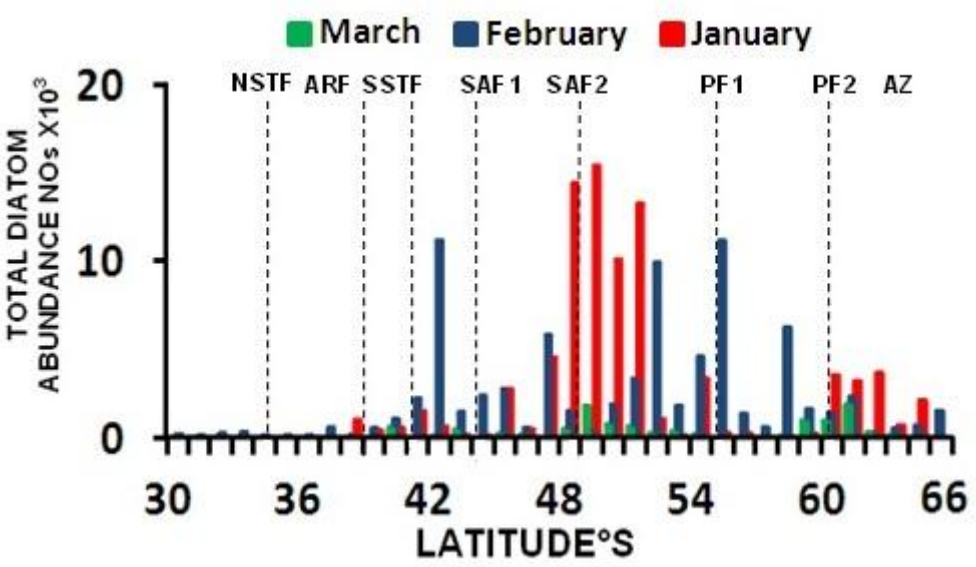

Fig. 44: Latitudinal variations in Diatom abundances during January, February and March in Indian sector of Southern ocean.

species, Actinocyclus species, Fragillariopsis kerguelensis, Ephemera planamembrane, Membraneis challergeri Thalassiosira species, A. parvulus, Rhizosolenia antena f semispina, Eucampia antarctica, R.polydactylus, A. hyalinus and *F. cylindres* (Fig 45).

F. kerguelensis was the most dominant diatom species in Indian sector of Southern Ocean for all the 3 studied months of respective years. *F. kerguelensis* was followed by thinly silicified species *Corethron criophillum and then by Chaetoceros species.* Some species like the sea ice diatom species *F. cylindres* were found only in January 2012 which also coincides with the maximum sea ice extent for all the 3 studied months. *Phaeocystis antarctica*, a haptophyte known to grow in low light and deeper mixed layers was not found, probably because *P. antarctica* is reported to decline by mid-late December (Kaufman et al., 2014).

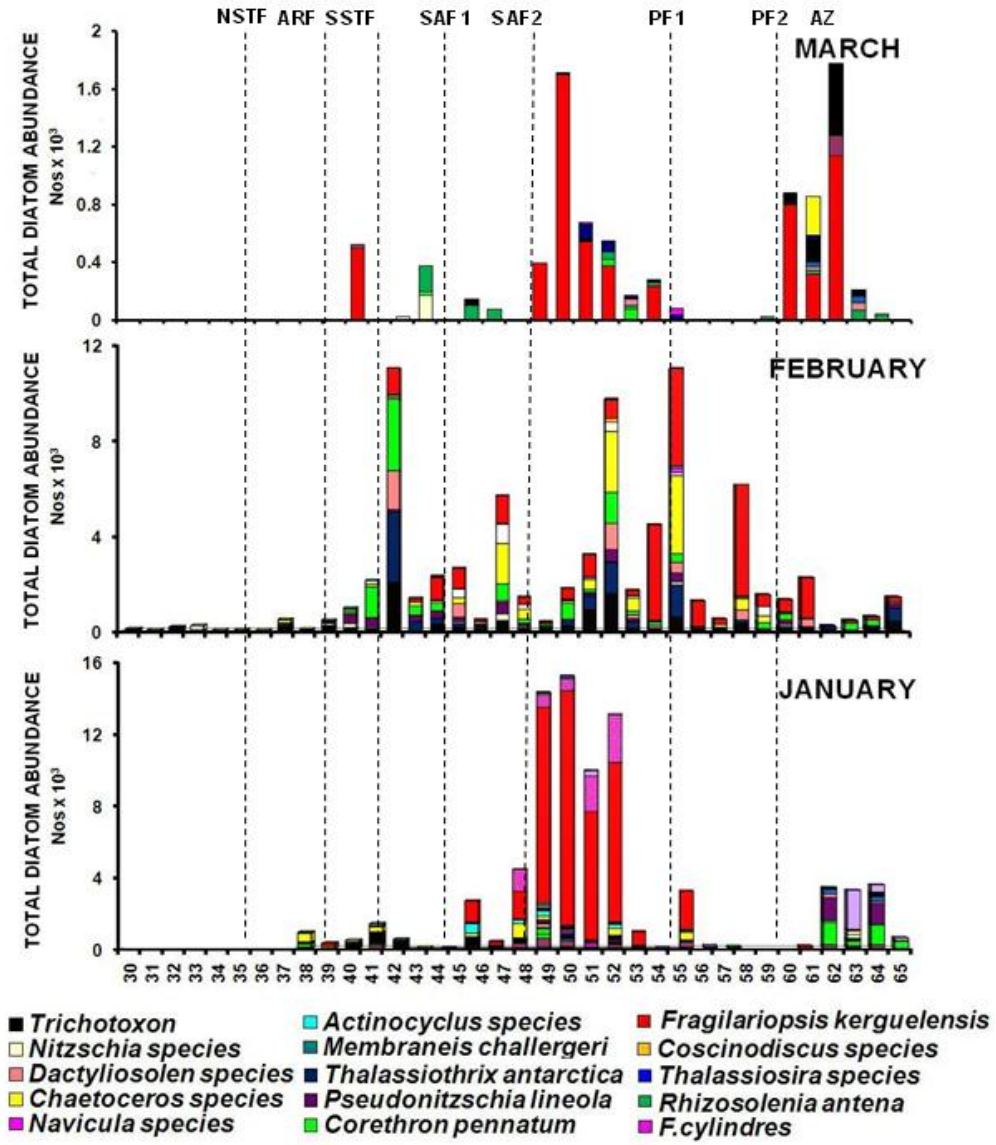

Fig. 45: Latitudinal variations in Diatom species abundances during January, February and March in Indian sector of Southern ocean.

4.5.1.1 Phytoplankton in Antarctic coastal region

Phytoplankton were dominated by diatoms, with minor presence of cyanobacteria, and silicoflagellates. Dominating diatom comprised of genera: *Corethron, Fragillariopsis, Chaetoceros, Rhizosolenia, Proboscia*, *Nitzschia*, *Dactyliosolen*, *Thallasiothrix*, *Trichotoxon*, *Astromphalus, Paralia,* and *Actinocyclis. Corethron*

criophilum was the most dominant diatom species and its abundance varied from 0 to 30x10^4 cells/l, however it was either absent or low in abundance along transect TE. Abundance of upwelling indicator diatom *Chaetoceros dichaeta* increases along TE. Figure 46, clearly shows the decrease in Total diatom abundance and *Corethron criophilum* with increase in abundance of cyanobacteria *Nostoc commune* east of 55°E.

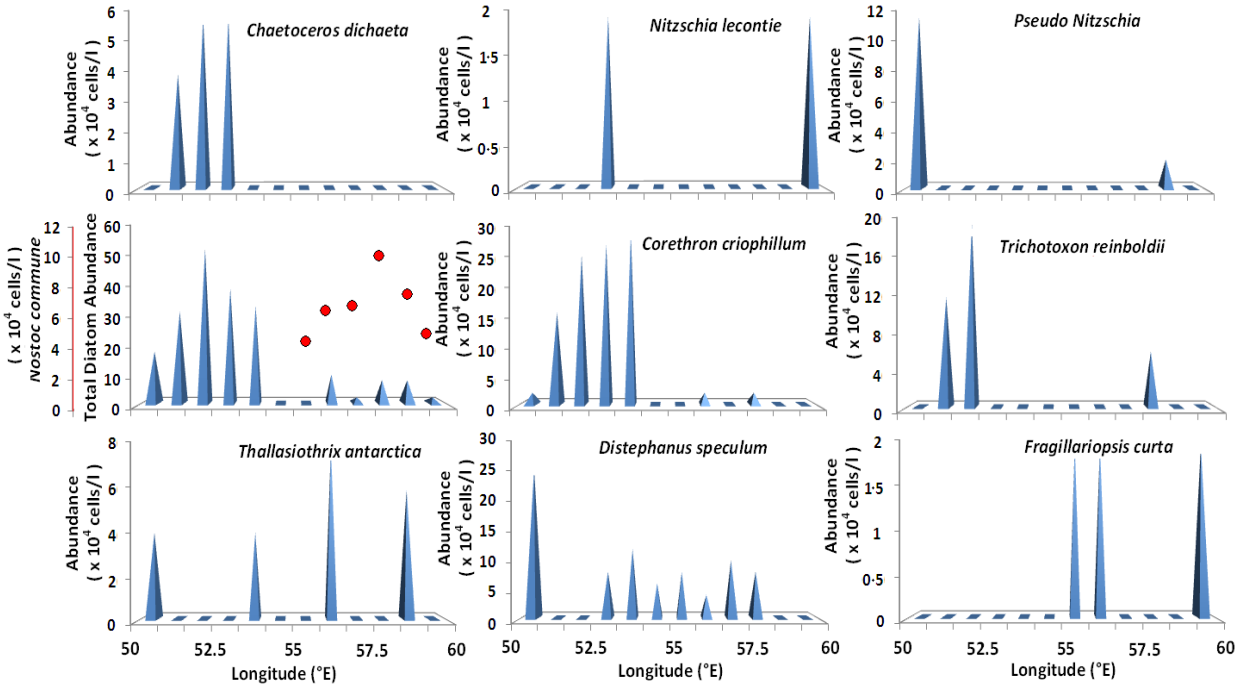

Fig. 46: Longitudinal variations in phytoplankton abundance in Antarctic coastal region.

Live cyanobacteria (*Nostoc commune*) were found attached on the icebergs (fig 47a & b) and in few coastal stations along transect TE (fig. 47 c & d), and its abundance varied from 1.5x10^{4}cells/l to 10.1x10^{4}cells/l. Abundance was high at stations having low salinity and high pCO_2.

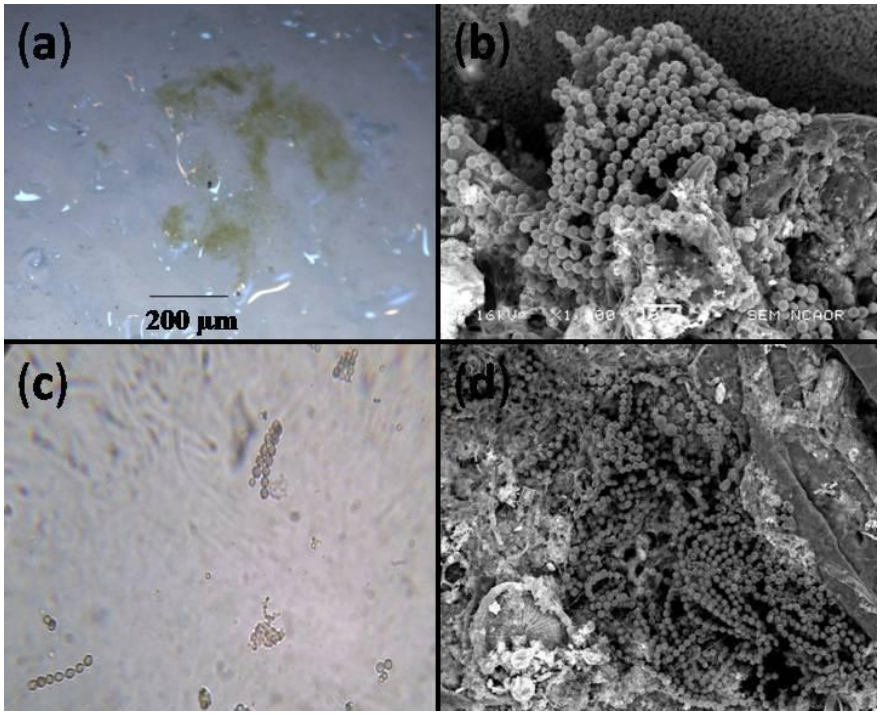

Fig. 47: Light microscopic image and Scanning electron micrograph of *Nostoc sp.,* from iceberg (a & b) and (c & d) Antarctic coastal region respectively.

4.6 Statistical Analysis

4.6.1 Correlation

Correlation between the biogeochemical parameters is given in table 24, 25 and 26 showing how the parameters behave with respect to other parameters. During March 2009, chlorophyll showed positive correlation with SST, PAR, Upwelling, SiO_4 and PO_4, whereas it was negatively correlated with pCO_2. During February 2010, Chlorophyll showed positive correlation with PAR, pCO_2, TOC, SiO_4 and SSS. However it was negatively correlated with SST, Upwelling velocity, NO_3 and PO_4. The negative correlation with upwelling is indicative of reduction in role of upwelling in supplying nutrients in summer. During January 2012, chlorophyll *a* is positively correlated with PAR, upwelling velocity, TOC and wind, whereas it's negatively correlated with SST, SSS, pCO_2 and nutrients. The strong negative correlation with pCO_2 is indicative of reduction in pCO_2 via biological activities.

Table 24: Pearsons correlation coefficient for physicochemical parameters during March 2009 (n=12)

Variables	Chlorophyll	SST	PAR	SST (BT)	SSS	pCO_2	TOC	wind	pH	SIO_4	PO_4	NO_3
Chlorophyll	1	0.331	0.162	0.222	-0.003	-0.174	0.230	-0.297	0.076	0.070	0.085	-0.006
SST	0.331	1	-0.186	0.384	0.564	0.363	0.490	0.184	-0.385	0.335	-0.022	0.256
PAR	0.162	-0.186	1	-0.628	-0.160	0.083	0.192	-0.779	-0.071	0.073	-0.389	0.082
Upwelling	0.536	0.110	-0.153	0.289	-0.027	-0.344	0.186	0.010	0.271	-0.319	0.089	-0.387
SST (BT)	0.222	0.384	-0.628	1	0.442	0.027	-0.023	0.634	-0.090	0.144	-0.184	0.220
SSS	-0.003	0.564	-0.160	0.442	1	0.401	0.540	0.364	-0.404	0.240	-0.049	0.341
pCO_2	-0.174	0.363	0.083	0.027	0.401	1	0.153	0.053	-0.990	0.576	-0.112	0.470
TOC	0.230	0.490	0.192	-0.023	0.540	0.153	1	-0.264	-0.130	0.328	0.220	0.246
wind	-0.297	0.184	-0.779	0.634	0.364	0.053	-0.264	1	-0.074	-0.348	-0.019	-0.234
pH	0.076	-0.385	-0.071	-0.090	-0.404	-0.990	-0.130	-0.074	1	-0.568	0.113	-0.478
SIO_4	0.070	0.335	0.073	0.144	0.240	0.576	0.328	-0.348	-0.568	1	0.127	0.926
PO_4	0.085	-0.022	-0.389	-0.184	-0.049	-0.112	0.220	-0.019	0.113	0.127	1	0.069
NO_3	-0.006	0.256	0.082	0.220	0.341	0.470	0.246	-0.234	-0.478	0.926	0.069	1

Table 25: Pearsons correlation coefficients for physicochemical parameters during February2010 (n=46)

Variables	Chlorophyll	SST	PAR	SST (BT)	SSS	pCO_2	TOC	wind	pH	SIO_4	PO_4	NO_3
Chlorophyll	1	-0.588	0.250	-0.431	0.121	0.035	0.054	0.172	-0.014	0.379	-0.293	-0.101
SST	-0.588	1	-0.057	0.503	-0.034	0.155	0.127	-0.125	-0.191	-0.282	0.443	0.244
PAR	0.250	-0.057	1	-0.449	-0.109	0.142	-0.067	0.294	-0.113	0.084	-0.034	-0.055
Upwelling	-0.108	0.252	0.247	-0.258	-0.337	-0.007	0.052	-0.076	0.081	-0.043	0.028	-0.163
SST (BT)	-0.431	0.503	-0.449	1	0.365	0.215	-0.037	-0.157	-0.255	-0.354	0.356	0.148
SSS	0.121	-0.034	-0.109	0.365	1	0.321	-0.184	0.160	-0.270	0.239	0.120	-0.071
pCO_2	0.035	0.155	0.142	0.215	0.321	1	-0.159	0.420	-0.984	-0.033	0.127	-0.020
TOC	0.054	0.127	-0.067	-0.037	-0.184	-0.159	1	-0.251	0.170	0.125	-0.096	0.092
wind	0.172	-0.125	0.294	-0.157	0.160	0.420	-0.251	1	-0.437	0.052	0.006	-0.058
pH	-0.014	-0.191	-0.113	-0.255	-0.270	-0.984	0.170	-0.437	1	0.092	-0.139	-0.014
SIO_2	0.379	-0.282	0.084	-0.354	0.239	-0.033	0.125	0.052	0.092	1	-0.250	0.066
PO_4	-0.293	0.443	-0.034	0.356	0.120	0.127	-0.096	0.006	-0.139	-0.250	1	0.134
NO_3	-0.101	0.244	-0.055	0.148	-0.071	-0.020	0.092	-0.058	-0.014	0.066	0.134	1

Table 26: Pearson's correlation coefficients for physicochemical parameters during January 2012 (n=38).

Variables	Chlorophyll	SST	PAR	SST (BT)	SSS	pCO_2	TOC	wind	pH	SiO_4	PO_4	NO_3
Chlorophyll	1	-0.316	0.071	-0.204	-0.125	-0.651	0.357	0.194	0.689	-0.018	-0.097	-0.104
SST	-0.316	1	0.215	0.643	0.484	0.430	-0.033	-0.224	-0.457	-0.437	-0.081	-0.129
PAR	0.071	0.215	1	-0.224	-0.195	0.160	-0.061	0.006	-0.131	0.045	-0.340	0.222
Upwelling	0.221	0.043	-0.079	-0.061	-0.009	-0.207	-0.177	0.280	0.185	-0.328	-0.149	-0.242
SST (BT)	-0.204	0.643	-0.224	1	0.528	0.383	-0.055	-0.131	-0.405	-0.404	-0.063	-0.182
SSS	-0.125	0.484	-0.195	0.528	1	0.059	-0.165	-0.253	-0.077	-0.127	0.213	-0.060
pCO_2	-0.651	0.430	0.160	0.383	0.059	1	-0.335	-0.041	-0.984	-0.188	-0.164	0.160
TOC	0.357	-0.033	-0.061	-0.055	-0.165	-0.335	1	0.272	0.297	-0.291	-0.272	-0.318
wind	0.194	-0.224	0.006	-0.131	-0.253	-0.041	0.272	1	0.016	-0.291	-0.445	-0.063
pH	0.689	-0.457	-0.131	-0.405	-0.077	-0.984	0.297	0.016	1	0.227	0.207	-0.147
SIO_4	-0.018	-0.437	0.045	-0.404	-0.127	-0.188	-0.291	-0.291	0.227	1	0.561	0.730
PO_4	-0.097	-0.081	-0.340	-0.063	0.213	-0.164	-0.272	-0.445	0.207	0.561	1	0.332
NO_3	-0.104	-0.129	0.222	-0.182	-0.060	0.160	-0.318	-0.063	-0.147	0.730	0.332	1

4.6.2 Principal component analysis

4.6.2.1. March 2009

Principal component analysis of environmental parameters indicates three major factors that account for ~66.8% of variance in the data (Table 27; Fig.48).

Table 27: Factor Loadings for Physico chemical parameters during 2009

	F1	F2	F3
Chlorophyll	**-0.020**	**0.074**	**0.811**
PAR	**0.014**	**-0.837**	**0.236**
Upwelling	**0.293**	**0.401**	**0.666**
SST (BT)	**-0.302**	**0.803**	**0.049**
SSS	**-0.662**	**0.407**	**0.114**
pCO_2	**-0.819**	**-0.148**	**-0.303**
TOC	**-0.454**	**-0.053**	**0.630**
wind	**-0.025**	**0.866**	**-0.450**
pH	**0.820**	**0.102**	**0.250**
SIO_4	**-0.814**	**-0.298**	**0.068**
PO_4	**0.017**	**0.079**	**0.208**
NO_3	**-0.778**	**-0.240**	**-0.020**
Eigen Value	**3.830**	**2.749**	**2.112**
Variability (%)	**29.462**	**21.144**	**16.243**
Cumulative %	**29.462**	**50.606**	**66.848**

The first factor accounts for 29.46% of the variance (eigen value=3.83) and is strongly loaded on SST, SSS, pCO_2, pH and NO_3 (Table 27). Based on these loadings, particularly the strong loadings of pCO_2 and pH, we interpret this factor as Nutrient Availability.

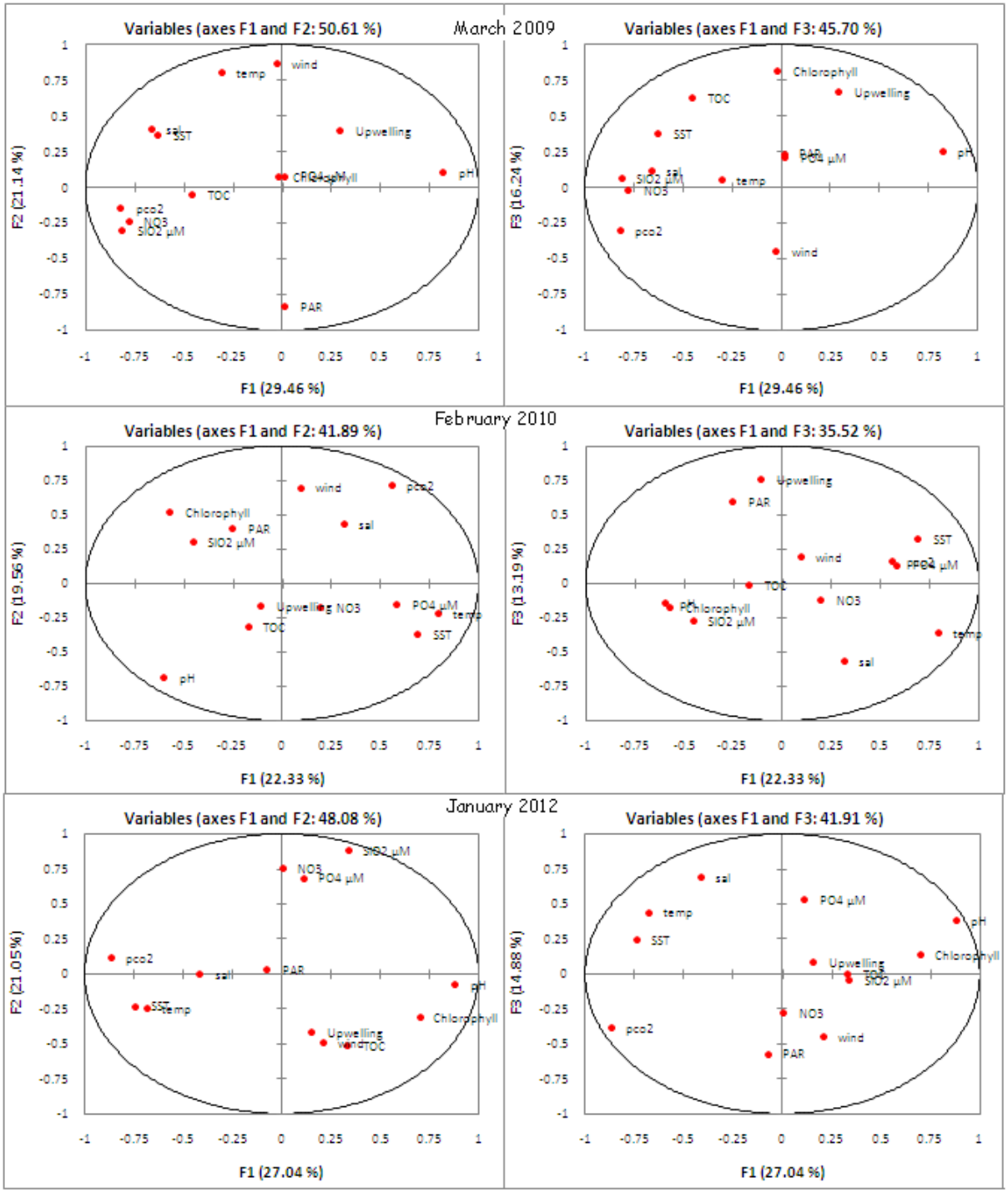

Fig. 48: PCA plots for various physicochemical parameter factor loadings during March 2009, February 2010 and January 2012.

The second factor, accounting for 21.1% of the total variance (eigen value = 2.7), is positively loaded on only two variables — SST and wind. These characteristics indicate that Factor 2 is Solar Insolation. The third factor accounts for 16.24% of the total variance in the data (eigen value = 2.11). It is strongly loaded on chlorophyll, upwelling and TOC. On the basis of these loadings we interpret Factor 3 as Biological productivity & vertical mixing.

4.6.2.2 February 2010

Principal component analysis of environmental parameters indicates three major factors that account for ~55.07% of variance in the data (Table 28; Fig. 48).

Table 28: Factor Loadings for Physico chemical parameters during 2010

	F1	F2	F3
Chlorophyll	**-0.572**	**0.516**	**-0.179**
PAR	**-0.253**	**0.394**	**0.595**
Upwelling	**-0.107**	**-0.167**	**0.758**
SST (BT)	**0.794**	**-0.222**	**-0.365**
SSS	**0.314**	**0.428**	**-0.568**
pCO_2	**0.560**	**-0.716**	**0.159**
TOC	**-0.172**	**-0.321**	**-0.010**
wind	**0.096**	**0.697**	**0.192**
pH	**-0.599**	**0.690**	**-0.144**
SiO_2	**-0.450**	**0.297**	**-0.279**
PO_4	**0.584**	**-0.155**	**0.132**
NO_3	**0.198**	**-0.180**	**-0.121**
Eigen value	**2.903**	**2.543**	**1.715**
Variability (%)	**22.327**	**19.559**	**13.189**
Cumulative %	**22.327**	**41.886**	**55.076**

The first factor accounts for 27.03% of the variance (eigen value=3.51) and is strongly loaded on chlorophyll, SST, pCO_2, pH and PO_4 (Table 28). Based on these loadings, particularly the strong loadings of pCO_2 and pH, we interpret this factor as Temperature

effect. The second factor, accounting for 19.55% of the total variance (eigen value = 2.54), is positively loaded on only three variables — Chlorophyll *a*, pH and wind. These characteristics indicate that Factor 2 is Biological productivity. The third factor accounts for 13.18% of the total variance in the data (eigen value=1.71). It is strongly loaded on PAR, upwelling and salinity. On the basis of these loadings we interpret Factor 3 as Sea ice melting.

4.6.2.3 January 2012

Principal component analysis of environmental parameters indicates three major factors that account for ~62.95% of variance in the data (Table 29; Fig. 48).

Table 29: Factor Loadings for Physico chemical parameters during 2012

	F1	F2	F3
Chlorophyll	**0.702**	**-0.308**	**0.136**
PAR	**-0.072**	**0.028**	**-0.572**
Upwelling	**0.154**	**-0.418**	**0.085**
SST (BT)	**-0.680**	**-0.251**	**0.439**
SSS	**-0.413**	**0.001**	**0.688**
pCO_2	**-0.865**	**0.118**	**-0.385**
TOC	**0.332**	**-0.516**	**-0.001**
wind	**0.210**	**-0.489**	**-0.453**
pH	**0.883**	**-0.076**	**0.379**
SIO_2	**0.341**	**0.885**	**-0.045**
PO_4	**0.112**	**0.684**	**0.529**
NO_3	**0.006**	**0.757**	**-0.278**
Eigen value	**3.515**	**2.736**	**1.934**
Variability (%)	**27.035**	**21.046**	**14.877**
Cumulative %	**27.035**	**48.081**	**62.958**

The first factor accounts for 27.03% of the variance (eigen value=3.51) and is strongly loaded on chlorophyll, SST, pCO_2 and pH (Table 29). Based on these loadings, particularly the strong loadings of pCO_2 and pH, we interpret this factor as Biological

Productivity. The second factor, accounting for 21.04% of the total variance (eigen value = 2.73), is positively loaded only on Nutrients. These characteristics indicate that Factor 2 is Nutrient Availability. The third factor accounts for 14.87% of the total variance in the data (eigen value=1.93). It is strongly loaded on PAR, SSS and PO_4. On the basis of these loadings we interpret Factor 3 as Sea ice-cover.

Chapter 5

Discussion

5.1. Factors controlling water column pCO_2 in Southern Ocean and Bay of Bengal

5.1.1. Southern Ocean (Open Oceanic Region)

In the SO, macronutrient concentrations are rarely the limiting factor for phytoplankton growth. Micro nutrients, solar irradiance, ozone and surface temperatures could directly or indirectly limit phytoplankton growth and contribute to ocean carbon variability. In order to examine the role of biogeochemical processes on variations in pCO_2 in the sub-tropical and polar front, the contributions of different effects on pCO_2 during March, February and January were estimated following Louanchi et al. (1996) model. The contribution of changes in pCO_2 due to biological process (biological effect), mixing with subsurface waters (mixing effect), variations in temperature (thermal effect) and variations in fluxes at sea–air interface (flux effect) were evaluated (Fig. 49 A). This analysis suggested that biological processes like primary production, respiration and calcification were dominant controlling factors followed by thermal, mixing, and fluxes. Both biological and thermal effects decreased pCO_2 by 18 to 108 µatm and 1 to 34 µatm respectively whereas mixing increased pCO_2 by 2 to 23 µatm at different oceanic fronts sampled. Effect of flux on pCO_2 was negligible except during January where it increased pCO_2 by 2 µatm. Calculation of mixing and thermal contributions during January 2012 were not possible due to lack of data.

5. 1.1.1 Mixed Layer Depth (MLD)

The MLD was greater in March than in January or February. During February increased solar heating and lower salinity of the surface water lead to more stable density stratification, thereby reducing the penetration of wind-driven mixing to 45 m.

Because seawater is denser just before freezing, cooling over the ocean during March not only reduces stable stratification, allowing for deeper penetration of wind-driven turbulence but also generates turbulence that can penetrate to greater depths upto 110 m in the PF. Also, the pCO_2 is higher in March because the temperatures are low and mixing is high, as also the carbon fluxes at the bottom of MLD are low. The mixed layer is also important as its depth determines the average level of light obtained for marine organisms. In deep mixed layers as in March, the phytoplankton are unable to get enough light to maintain their metabolism. The deepening of the mixed layer in March is therefore associated with a strong decrease in surface chlorophyll *a* as a result of light limitation (Fig. 49 B) and matches with results of DeBoyer-Montégut, 2004, Fauchereau et al., 2011 and Comiso et al., 1993.

5.1.1.2 Biological production

Figure 49(A), clearly shows that during January and February biological processes dominated pCO_2 concentrations, whereas during March mixing and thermal effects become equally important. Highest biological drawdown of pCO_2 was during January, decreasing pCO_2 by 108 µatm and this is supported by high abundance in diatom and dissolved oxygen concentrations in January. The seasonal variations in phytoplankton biomass in the SO have been typically attributed to changes in the light limitation in the framework of the critical depth hypothesis (Sverdrup, 1953). The high PP during January could be related with higher irradiance (60 Einsteins/m^2/day), and high Nutrient concentrations. This difference in PP between January and March is also reflected in the total diatom count of $0.2x10^3$ cells/l in March to 2 $x10^3$ cells/l in

February and 3.2 x10^3 cells/l in January. Chlorophyll *a* averaged 0.2mg/m^3 in March, 0.39 in February and

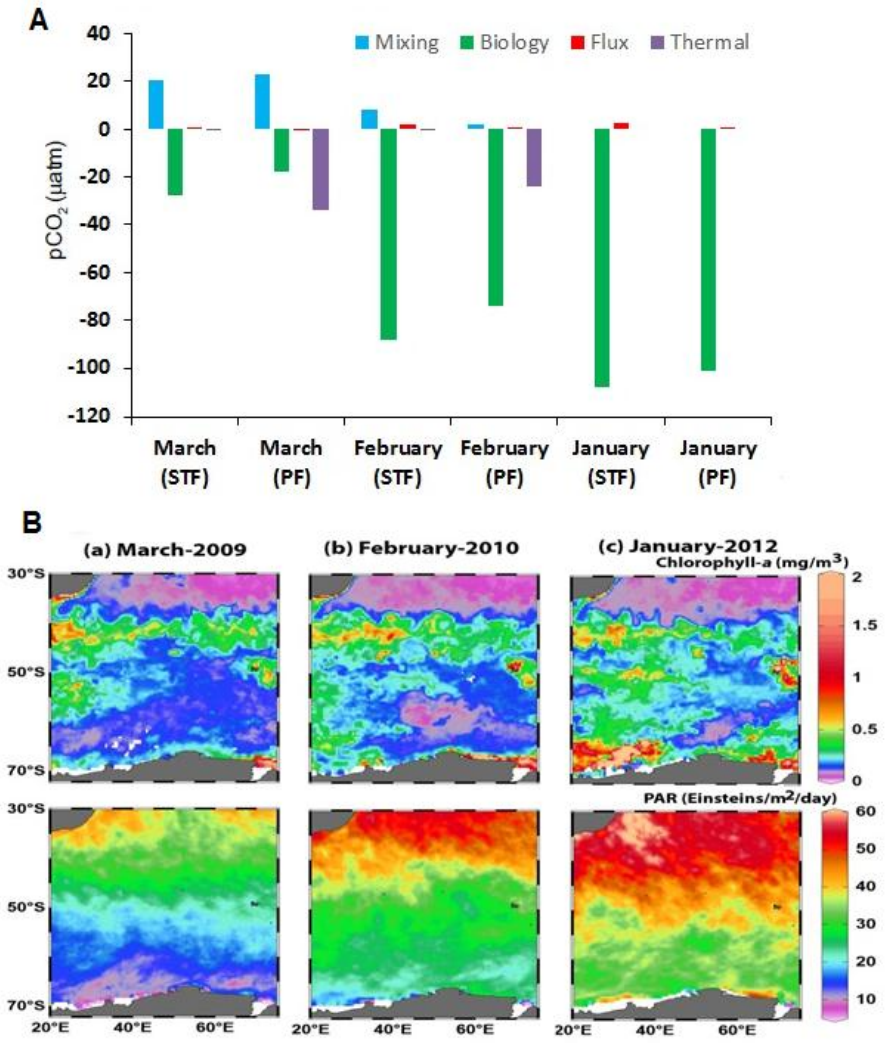

Fig. 49: (A) Effects of biological, mixing, thermal and flux on *p*CO_2 distribution at STF and PF during January, February and March. (B) Observation of Aqua-MODIS derived chlorophyll-*a*, and photo-synthetically active radiation in Southern Ocean during (a) March-2009, (b) February-2010 and (c) January-2012.

0.59 mg/m^3 in January. Similar trend was seen by LeFevre, 2000 through SeaWIFS composite imagery showing higher values in December 1998 (1–2 mg/m^3) and decreasing in January-February 1999 (0.3–0.5 mgm^3). Irradiance varied from >60 Einstein /m^2/day during January to <10 Einstein /m^2/day during March (Fig. 49). As seen from Figure 49, during January, irradiance was in fact the sole factor that limited the phytoplankton production, as nutrients were abundant (Fig. 17). From summer (January) to early winter (March) the average values of SiO_4 decreased and this would have limited algal production during March. However, our observations of low light during March as a co-limitation of iron and light influence phytoplankton processes (Moore et al., 2007). Nitrate uptake is particularly sensitive to lower light and it gets worsened by any iron stress (Glibert and Garside, 1992). Also, the PF had high pCO_2 and low diatom counts which may be the result of deeper MLD in this region. The deepening of the MLD during March (60m) and (110m in PF) further aggravates the light deficiency during March due to low irradiance. Our results are consistent with earlier studies by Joubert et al., 2014; Sakshaug and Holm-Hansen, 1986 and Cassar et al., 2011 that support low production when MLD exceeds 50m. The dominant diatom in our study was *F. keguelensis* which is known to grow under shallow MLD and high irradiance and this species was absent at stations with deeper MLD, especially in the PF.

During the late Austral summer, growth of the larger diatoms becomes limited due to low silicate concentrations (Tréguer and Jacques, 1992). During March, the nutrient concentrations were lower than in February, whereas January witnessed the highest

silicate. During February the N/P ratio was 10.2 whereas during March the N/P ratio was 6.1 depicting greater utilization of nutrients by phytoplankton in March. N/P ratio in the SSTF front are <1 in all the 3 months indicating nitrate limitation in the SSTF leading to low primary productivity. Also, the Si/N ratio indicates utilization of SiO_4 by phytoplankton during March as compared to January. The decreased nutrient concentrations in seawater or changes in the nutrient ratios can restrict phytoplankton growth and abundance (Dortch and Whitledge, 1992). A previous study by Smetacek et al., 2002 during early summer (December–January) showed the abundance of larger and slow growing phytoplankton species, which build their biomass by sequestrating available nutrients. But due to their large size, they are less affected by grazing, whereas in low-nutrient conditions smaller phytoplankton species get more reflected in the phytoplankton community (Fiala et al., 1998). Pavithran et al., 2011 reported high grazing pressure due to large size copepods within the polar front resulting in low primary productivity in Indian sector of SO. This could have resulted in the low diatom counts in the PF in this study.

Low pCO_2 was observed despite high temperature in January. Similar finding was reported by Jan et al., 2004, in the western Indian POOZ (50–57°S, 65°E) where a large CO_2 sink (oceanic pCO_2 <330μatm) was observed during a warm period and was attributed to high biological production. In large areas between 40-70°S in the SO the biology effect exceeds the temperature effect (Takahashi et al., 2006). This feature has been demonstrated by the extensive pCO_2 data obtained between 40-65°S during different seasons in the Atlantic, Indian and Pacific sectors of the SO.

The method adopted by Takahashi et al., 2006, was used to differentiate between Biological and Temperature effect on pCO_2. After following the equation:

$$T/B = \Delta pCO_2 temp - \Delta pCO_2 bio$$

T/B = 0.47 for March, 0.5 for February and 0.92 for January, thus suggesting that biology was the dominant factor over temperature in regulating pCO_2. Despite high biological productivity and the lowering in pCO_2, we still did not get a negative correlation with DO, as the correlation coefficient (r) was 0.4, 0.5 and 0.1 for March, February and January, respectively. It may be attributed to the fact that the sea surface pCO_2 is buffered by the marine carbonate system, while DO is not associated with any buffer system. Therefore the relationship between the pCO_2 and DO variation in the euphotic zone may differ between different biogeochemical settings (DeGrandpre et al., 1997; 1998), and the different pCO_2-DO relationship may have different implications on metabolic status.

5.1.1.3 Island Mass Effect

While the SO is the largest HNLC region in the global ocean, high marine productivity does occur during the summer near frontal systems, downstream of islands and over shallow topography in the Antarctic Circumpolar Current (Tyrrell et al., 2005). Numerous studies have shown enhanced nutrient concentrations and productivity around islands, known as the “island mass effect” (Boden 1988). The rotational tendency of the water and the shifting of the oceanic fronts around the Crozet Island

are attributed to sea-bed topography (Anilkumar et al., 2006). The present study suggests that the regions around the Crozet Island, where fronts are known to merge, can act as a source of atmospheric CO_2. Merging of oceanic front's results in an increased vertical mixing that pumps pCO_2 to the surface waters. Average pCO_2 was higher along 48°E compared to 57.30°E by 24µatm and 41 µatm during March and February respectively, indicating stronger convective mixing towards the west of the Crozet Island and near the Crozet Plateau (Fig 31). Similarly, the maxima of NO_3 and SiO_4 were higher by 2µM and 3µM, respectively, along the western side of the Crozet Island (Fig 19).

Phytoplankton blooms have also been reported earlier in the vicinity of the Crozet Island (Bakker et al., 2007, Fielding et al., 2007). Average TOC and chl *a* was higher by 3 µM and 0.3 mg/m^3along 48°E which is in vicinity of Crozet Island than at 57.30°E which is away from Crozet island. The presence of Crozet Island provides some micronutrients along 48°E (Gandhi et al., 2012). Although, most of the Fe entering World Ocean is through Aeolian dust, in case of a shallow plateau with water depth of only several hundreds of meters in open waters, Fe from the deep may become available in surface waters (Blain et al., 2001). However, apart from bringing micro nutrients, the vertical mixing also brings elevated pCO_2 waters to the surface. Thus the island mass effect could be responsible for the regions in the vicinity of the Crozet Island to be a source of CO_2 rather than a sink. Jouandet et al., 2011 studied the high productive area localized over the Kerguelen plateau with the surrounding HNLC waters. The core of the bloom was characterized by low sea surface CO_2 fugacity in seawater (fCO_2, 320 µatm), representing a large CO_2 sink for the atmosphere (ΔfCO_2

= 5-50 µatm) and was in contrast with the near equilibrium conditions observed outside the bloom.

5.1.1.4 Southern Annular Mode Effect

In the last few decades both greenhouse gas accumulation and stratospheric ozone depletion have led to the strengthening of southern winds (Lenton and Matear 2007) and induced significant thermal contrast in the Southern Hemisphere (Thompson and Solomon, 2002). This changed the meridional atmospheric pressure gradients, leading to more positive state of the so-called Southern Annular Mode (SAM) (Marshall, 2003). In such a positive SAM state, stronger westerly winds south of 40°S cool the surface ocean and increase vertical mixing (Sengupta and England, 2006) and increase the import of CO_2 to surface waters. A direct link between the SAM and the decadal reduction of the SO carbon sink has been suggested from the *in situ* ocean carbon dioxide observations of Metzl, 2009. Lovenduski and Gruber, 2005 examined how the SAM, a dominant mode of local atmospheric variability, is related to observed variability in primary production; they speculate that the biological response to SAM would largely compensate the supply of DIC resulting from SAM-induced changes in ocean circulation. More recent modelling studies, however, suggest that SAM drives about a third of regional CO_2 air-sea flux variability on interannual timescale, primarily due to changes in the physical circulation (Lovenduski et al., 2007). To test the effect of SAM on pCO_2 and phytoplankton distribution, the SAM Index was plotted following the NOAA website. During March 2009, the SAM was in positive phase (SAM Index = +1), whereas during February

2010 SAM was in negative phase (SAM Index = -0.8) (Fig. 50). Both these observations support the theory that positive SAM leads to elevated pCO_2 values and vice versa. However during January 2012 when we got undersaturated pCO_2 values, SAM was in positive phase (SAM Index = +1) (Fig. 50), thus suggesting that SAM may not have major impact on pCO_2, or the effect of

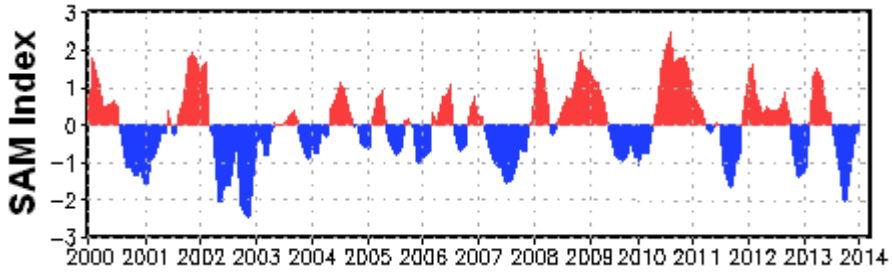

Fig. 50: Standardized 3 month running mean SAM Index

SAM may have been nullified by the biological productivity. During January the MLD was 50m, which was higher than February (45m) despite having higher temperature in January, and this could be related with the positive SAM generating higher wind speed that increased mixing. The higher MLD during January was also associated with high productivity, irradiance, nutrients and low pCO_2. Although past studies have reported decline in productivity as a result of increased MLD, this study indicates that during summer when light availability is limiting factor, SAM could increase production due to macronutrient and iron supply via vertical mixing.

5.1.1.5 Co/Ci Ratio

The organic carbon flux to inorganic carbon flux ratio (Co/Ci) at 1000m during January was high as compared with February and March thus leading to drawdown of pCO_2 during January. Co/Ci ratio varied from 0.19 to 0.93 during March, 0.32 to 1.06 during

February, and 0.78 to 1.7 during January. Honda et al., 1997 found that pCO_2 in seawater decreased when the Co/Ci ratio of carbon flux was larger than 0.7 and the decrease in pCO_2 became larger with increasing Co/Ci ratio. They also suggested that, water temperature play an important role in the decrease in pCO_2. When the water temperature is 5°C, a carbon flux of approximately 150 $mgCm^{-2}day^{-1}$ with a Co/Ci ratio of 3 is needed in order to decrease pCO_2 by 40 ppm $year^{-1}$, while a carbon flux of 50 mg $m^{-2}day^{-1}$ is needed when the water temperature is 30°C. This means that biological activity in high latitude areas with high pCO_2 and low temperature, such as the PF, should be higher than that in low latitude areas in order to decrease pCO_2 by the same level. This could be the reason behind high pCO_2 in PF in this study. Again, the high Co/Ci ratio is mostly dependent on the POC flux which by itself is dependent on MLD.

5.1.1.6 Ultraviolet (UV) radiation

The harmful effects of UV radiations on phytoplankton growth (Larsen, 2005) are well documented. UVA-R (320 - 400 nm) accounts for most of the photoinhibition in the surface waters of Antarctica (Arrigo et al., 2003). Ultraviolet radiation is strongly influenced by stratospheric ozone. Changes in ozone concentrations are likely to influence UV radiation reaching the sea surface and could influence the net primary production. Total column ozone data were obtained from the Total Ozone Mapping Spectrometer satellite (http://ozoneaq.gsfc.nasa.gov/OMIOzone.md). Over the studied area the monthly mean of the total ozone varied from January 2012 to March 2009. The ozone concentrations at the sampling time at the sampling locations

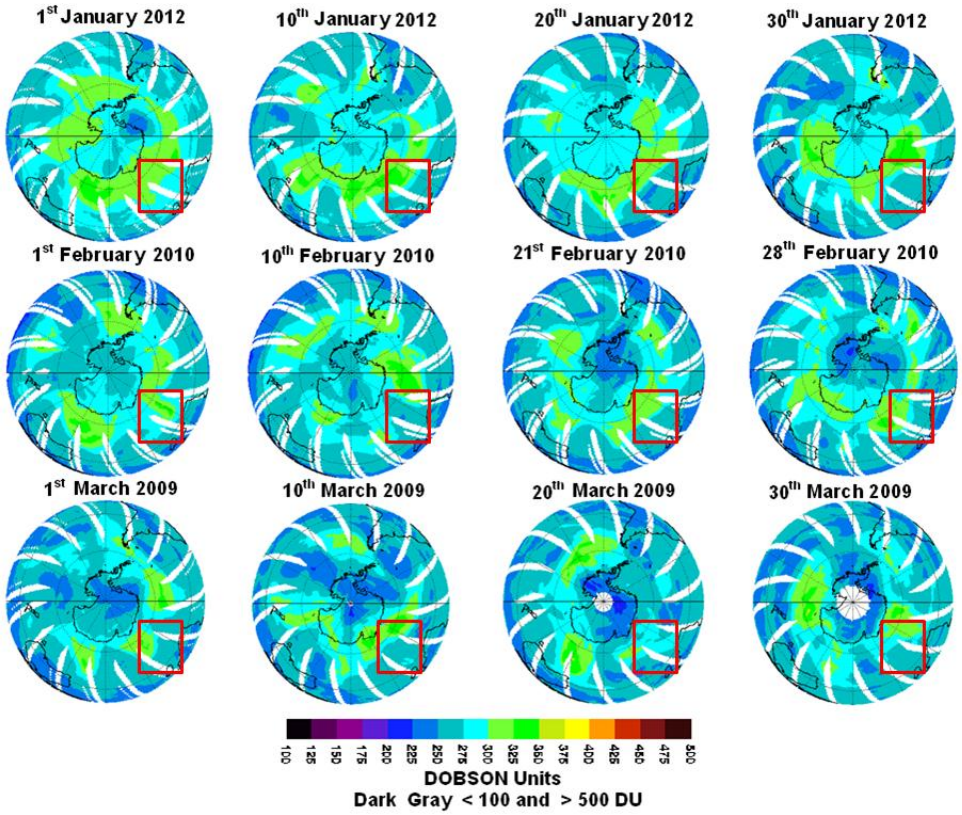

Fig. 51: Satellite images of Total Column Ozone during March 2009, February 2010 and January 2012.

shows that during January 2012, most of the samples had the total ozone 325 DU, whereas during March 2009 the total ozone was 275 DU (Fig. 51). The variations in total Ozone between studied periods makes it a likely contributor towards low productivity in March.

5.1.1.7 Dust storms and iron input

In HNLC regions such as southern ocean, iron limits primary production. A TOM's Aerosol optical depth (Fig. 52) (http://earthobservatory.nasa.gov/), does not show

elevated aerosol concentrations in the nearby continents during January 2012, thereby ruling out the possibility of an iron source that led to increased phytoplankton biomass and CO_2 drawdown in January 2012.

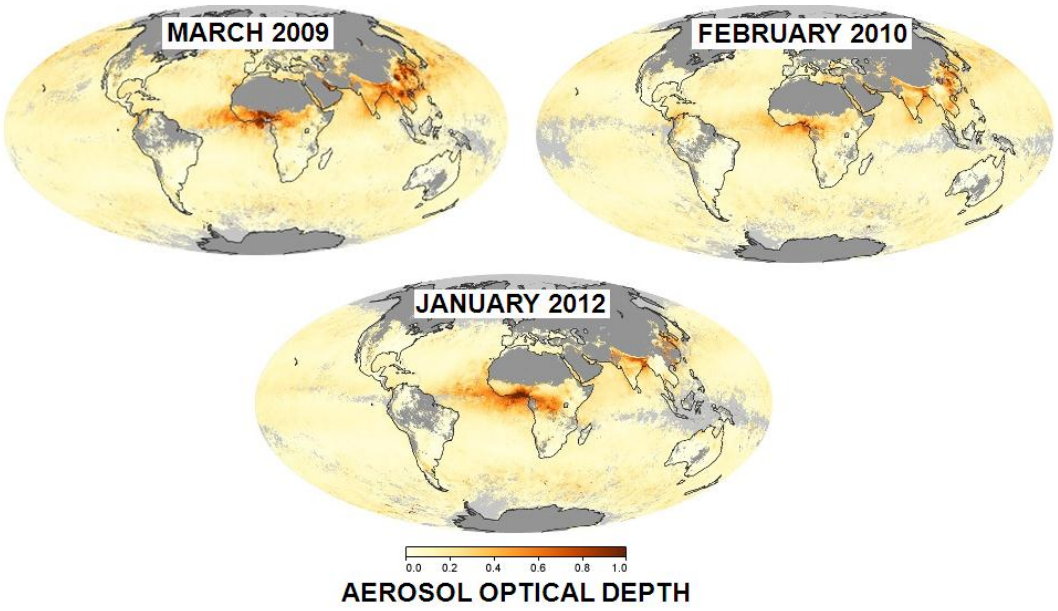

Fig. 52: Aerosol Optical Depth images taken from NASA website for the study period January 2012, February 2010 and March 2009.

However, observations of low light during March 2009 could have aggravated the role of Fe; as a co-limitation of iron and light influences phytoplankton processes (Moore et al., 2007). Nitrate uptake is particularly sensitive to lower light and it is worsened by any iron stress (Glibert and Garside, 1992). Low light and low Fe result in decreasing the pigment content and consequently light harvesting efficiency of the photosynthetic systems of microalgae (Timmermans et al., 2001) as well as decreases the photosynthetic electron transport capacity (Geider and LaRoche,1994).

5.1.2 Southern Ocean (Coastal region)

The magnitude of sea-air CO_2 exchange and the potential role of the Enderby Basin in transfer of atmospheric CO_2 during ice covered and ice free period is obtained. In this study, different factors dominate during the three studied months. During March 2009, Nutrient availability is the most important factor affecting biogeochemistry and nutrients get depleted during March. This is also supported by the factor loadings showing strong negative loadings for factor 1 for March 2009. Light availability is the second important factor, as during March it is the transition from summer to winter and figure 53 clearly shows the lower PAR during March 2009. The third important factor is vertical mixing and primary production. Figure 53 clearly shows higher upwelling velocities during March 2009, this is also evident from the positive loadings for factor 3 and upwelling velocities. Biological production does not play a major role during March 2009 as seen from the slight negative correlation between chlorophyll *a* and pCO_2. During February 2010, Temperature seems to be the most important factor as seen from positive loadings for Temperature on factor 1 and also from figure 53. In, the absence of sea ice cover, there is no albedo effect and hence SST is high. The second important factor is biological production, as seen from positive loadings for chlorophyll *a* on factor 2. The third important factor is sea ice melting, as seen from negative loadings for salinity on factor 3. Due to higher temperatures (Fig. 53) there is maximum of sea ice melting, as seen from sea ice extent, resulting in addition of fresh water which decreases the salinity. During January 2012, primary production is the most dominating factor, as seen from strong positive loadings for factor 1 on chlorophyll *a*. This is also seen from figure 53, showing high chlorophyll *a* and PAR

during January 2012. The positive loadings for Nutrients on factor 2 indicate that nutrients are available for primary production. The third important factor during January 2012 is Sea ice cover. January 2012 had the maximum sea ice extent indicating that brine rejection during sea ice formation increased the surface salinity.

Combining all the 3 years results, we can see a drastic change in the dominant factors affecting biogeochemistry from summer to early winter. Primary production, nutrient availability, light availability, temperature, sea ice melting and freezing and vertical mixing seem to be the most important factors. Irradiance and nutrients played significant role in the study region. Irradiance varied from >40 Einstein /m2/day during January to <10 Einstein /m2/day during March. As seen from figure 53, during January, irradiance is the only factor that limits the phytoplankton production, as nutrients are abundant relative to Phytoplankton requirements (Gosselin et al. 1990).

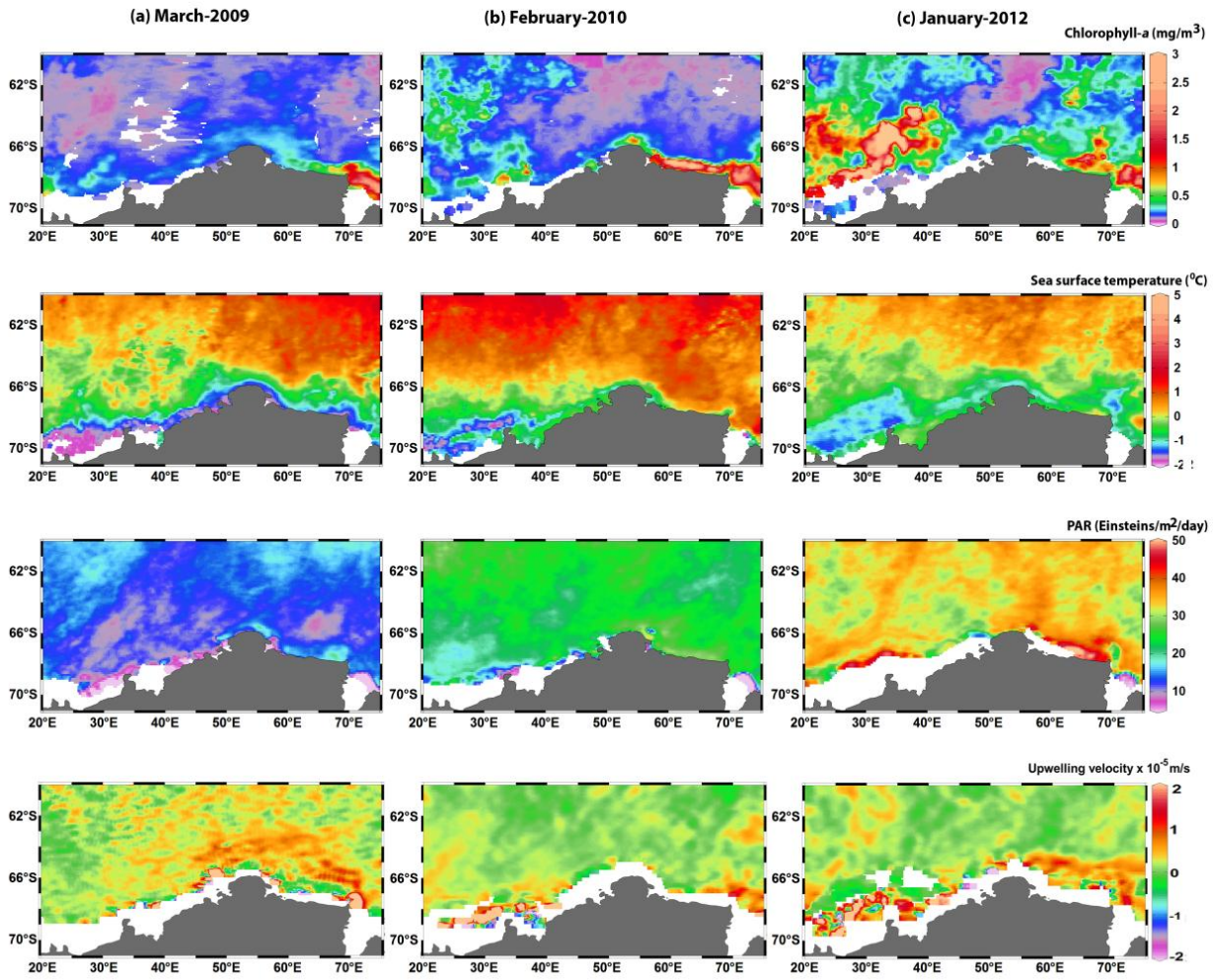

Fig.53.Observation of Aqua-MODIS derived chlorophyll-*a*, sea surface temperature and photo-synthetically active radiation, upwelling velocity along Antarctic coast during (a) March-2009, (b) February-2010 and (c) January-2012.

5.1.2.1 Nutrient Availability

The magnitude of primary production depends upon surface ocean nutrient supply which is strongly regulated by vertical mixing. Coastal upwelling such as the Oregon coast (Hales et al. 2005) tend to have high levels of nitrate and phosphate. Among the nutrients, nitrate and phosphate are the principal variables that limit the

phytoplankton growth. The nutrient concentrations are high, reaching a maximum value of 41.7µM, 3.8 µM and 58 µM for NO_3, PO_4 and SiO_4, respectively. At Enderby basin, the concentration of silicate is less than that of nitrate at most of the stations. This feature was previously described in Antarctic Ocean (Knox, 1994) and was related to the efficiency of nitrogen recycling over silicon recycling (TreHguer and Jacques, 1992). Nutrients found both in seawater and in ice and are supplied via brine rejection, regeneration or vertical diffusion. From summer (January) to early winter (March) the average values of SiO_4 decreased, however the average values of NO_3 and PO_4 show an increase, which may be a result of the increase in the MLD, which entrains subsurface nutrient-rich waters under the sea ice cover (Louanchi et al. 2001).

5.1.2.2 Biological productivity

Antarctic coastal regions exhibit high and variable biological productivity resulting in high spatial variations in pCO_2 as evident from our results. Biological processes clearly dominated the control of pCO_2 in January (fig 53). Photosynthetic uptake of DIC by phytoplankton would have resulted in the pCO_2 changes. Sea-ice covered the study site through January while pCO_2 decreased rapidly to below 150 µatm. The average pCO_2 during March was 368 µatm, whereas during January was 181 µatm. A drawdown of half pCO_2, is attributed to higher biological production (fig 52) which may be due to the phytoplankton blooms generated in spring during January (avg. Chlorophyll *a* 1.5 mg/m^3 & TOC=147µM), as compared to March (avg. Chlorophyll *a* 0.1 mg/m^3 & TOC=90 µM). This regulation of the pCO_2 values by the biological

production during January is reflected by the negative correlation between Chlorophyll *a* and TOC with pCO_2 (r = -0.65 and r = -0.33), whereas during March, pCO_2 shows slightly positive correlation with TOC (r = 0.15) and slight negative correlation with Chlorophyll *a* (r = 0.15). The end of summer was accompanied by sharp increases in pCO_2 and decrease in pH in March. Higher pCO_2 values during March can also be due to intensive decay of organic matter (Pipko et al. 2002). In March, the sea ice cover would have led to elevated CO_2 levels by preventing CO_2 produced organic matter degradation from diffusing into the atmosphere.

5.1.2.3 Upwelling Intensity

The advection of CO_2 rich deeper water under the ice cover is reflected by the increase in salinity at 56°E during 2009 (pCO_2 = 690 µM, Salinity = 34.01 psu). Anilkumar et al. 2010, have reported upwelling and CDW along 50°E and 60°E. Anderson et al. (2009) has also reported wind driven upwelling around Antarctica and its role in regulating CO_2 levels. Baker et al., 2008, based on the O_2 minima, suggested that upwelling of CDW occurs elsewhere around Antarctica, and is not limited to the Weddel Gyre. We observed high upwelling velocities in March 0.5–0.6 x $10^{-5}ms^{-1}$, whereas during January/February we found lower velocities ($0.1x10^{-5}ms^{-1}$). Comiso et al. (1993) reported high upwelling velocities (0.3–0.4 x $10^{-5}ms^{-1}$) during winter as compared to 0.1-10^{-5} x ms^{-1} in summer. Upwelling would have resulted in the higher pCO_2 during March 2009. Also, our comparison of the TW and TE showed elevated pCO_2 values along the TE, which again would be due to the upwelling and CDW, as these physical processes can overrule the reduction due to the biological

production at TE (Chlorophyll *a* 1.5 mg/m^3) as compared to TW (Chlorophyll *a* 1.1 mg/m^3).

5.1.2.4 Sea Ice Cover

Fluxes calculated, suggest that the Enderby Basin acts as a weak sink of CO_2 to the atmosphere, -1.7 and -2.4 mmol/m^2/d during March 2009 and February 2010, respectively. During 2009, due to the ice cover, the wind cannot have direct effect on the calculated flux. The gas exchange being restricted severely, the flux is then determined by the gas solubility and ΔpCO_2. The sea ice cover prevents release of CO_2 and other gases, which is evidenced by major super saturation of pCO_2 under the ice cover during March 2009.

In Antarctica ice melting first starts in December, in the presence of warm waters below the winter mixed layer (Bakker et al. 2008). Ice melting itself would reduce surface water TCO_2 through dilution. Our observations of high pCO_2 values below the ice cover during March with rapid transition to a biologically-mediated CO_2 under saturated waters during ice free zone (February), matches well with other data sets from the Antarctic region. Weiss et al. 1992 reported super saturation of pCO_2 by 40µatm in the southeastern Weddell Gyre in June-November, while strong under saturation of pCO_2 by 60 to 130µatm in February 1984.

This study indicates that with the expected loss of sea ice over the next century would decrease primary production in the Southern Ocean. Arrigo et al. 1999 reported

negative feedback to climate change as a result of phytoplankton community shift and greater utilization of nutrients. Sarmiento et al. 1998 reported increase in stratification leading to reduced nutrient supply, however they also report increase in wind speed as a result of less sea ice extend.

5.1.2.5 Ikaite Precipitation

Apart from the physical and biological processes, the chemical processes including the calcium carbonate chemistry could also play a role in the changes in pCO_2 from the sea ice covered region to ice free region. Earlier studies by Dieckmann et al., 2008, reported that ikaite($CaCO_3 \cdot 6H_2O$), precipitates within brines during sea ice thus increasing the pCO_2 (eq. 1).

$Ca^{2}+(aq) + 2HCO_3^- (aq) + 5H_2O(l) \leftrightarrow CaCO_3 \cdot 6H_2O(s)+ CO_2(aq)$. (1)

During summer, sea ice melts and ikaite is released into the water column and its dissolution would reduce pCO_2 of the water (Jones et al., 2010).

5.1.3 Southern Ocean (under 2m thick ice cover)

Under the thick packed sea ice of 2 m thickness, the results indicate very high primary productivity. The sea ice cover restricts the light penetrating into the surface waters and shields the phytoplankton from ultra violet radiations and it also gives a stable platform for the algae to attach and grow. Super saturation in dissolved oxygen concentrations was observed (616 µM), whereas pCO_2 was under-saturated. This was attributed to the algal biomass on the under flanks of ice. Chlorophyll *a* values reached 6 mg/m^3 and surface sediment organic carbon was >3.5%. The blooms were

dominated by sea ice diatoms *Berkelia adeliansis* (Fig. 54). Silicate was depleted under the sea ice, as a result of utilization by the high algal biomass, chlorophyll *a* (0.6-6.1 mg/m^3), whereas pCO_2 concentrations were as low as 3 to 9 µatm. pH was as high as 9.2. This study infers that biological production regulates pCO_2 concentrations under the ice covered region. The organic matter generated by seasonal blooms of diatoms, serve as essential food resource for grazers and most of the benthic organisms growing at deeper depths, thereby facilitating Carbon sequestration and its transfer to higher trophic levels (Legendre, 1992).

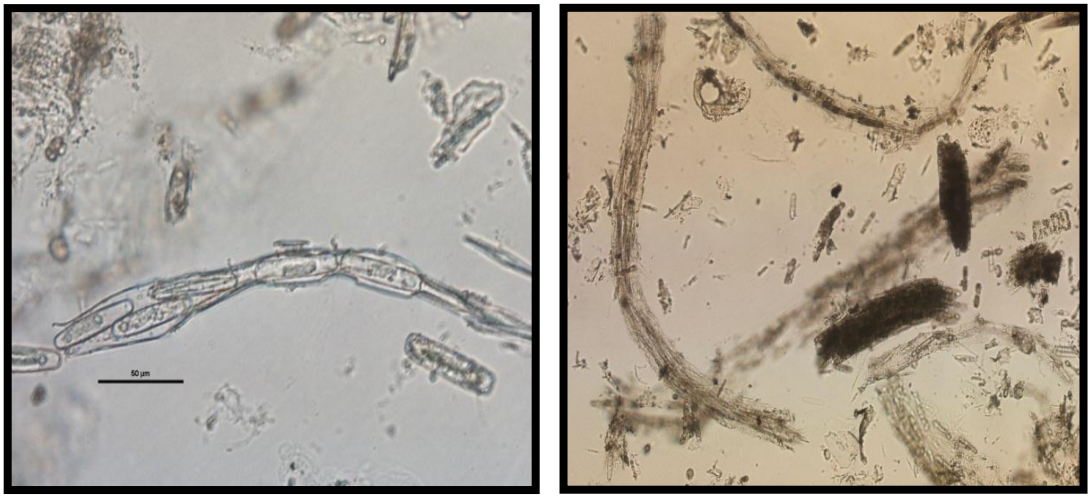

Fig.54: Tube forming diatoms from underneath the sea ice.

The very high biological production under the sea ice cover is still a mystery as to how the light penetrates under the thick ice cover, however from this study one new hypothesis could be proposed saying that the spicules on benthic siliceous sponges in the bottom could act as optical fibre for the little light that passes through the sea ice holes.

5.1.4 Bay of Bengal (Coastal region)

In coastal Bay of Bengal, the pCO_2 values are very low, except at Thamnapatnam. The region acted as a strong sink for atmospheric CO_2. Kumar et al., 2004, reported high average new production at coastal stations due to East India Coastal Current, which also brings cooler, more saline water with nutrients to the surface (Shetye et al., 1993). This current is best developed during our study period April-May and could be the signature seen at Thamnapatnam.

Although the Bay of Bengal is known for its low productivity, the region along the eastern coast of India during the study period showed very high productivity as seen from the satellite chlorophyll *a* image (Fig. 55).

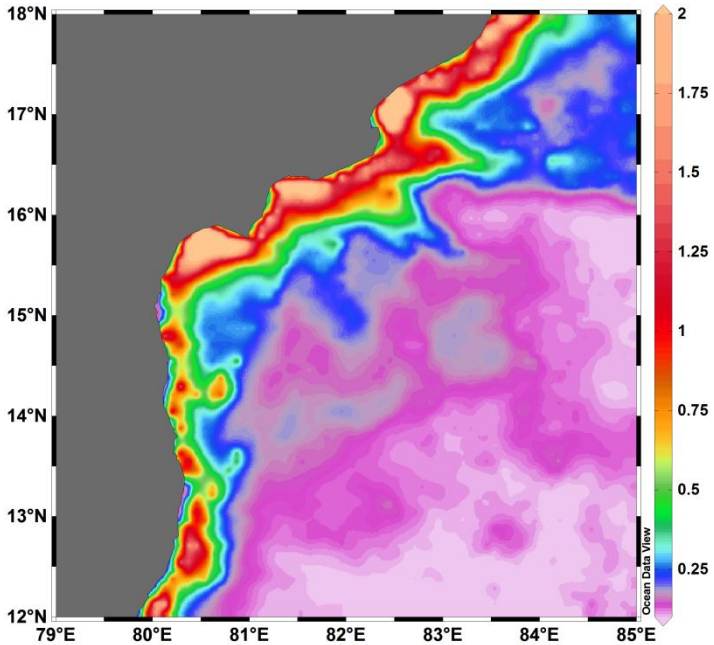

Fig.55. Satellite derived sea surface chlorophyll *a* along western Bay of Bengal.

At Thamnapatnam, the upliftment of thermocline, halocline and nutricline near 14°N is due to upwelling resulted from divergence of water masses. The upwelling induced cooling feature is well captured by NOAA AVHRR derived SST during 12th May 2009 (Fig. 56) and also reflecting in weekly composite product (9-16th May 2009) signifying persistency of the feature (Fig. 55). Satellite observations indicated lower SST (~27°C to ~27.5°C) and associated negative SSHA ranging from -0.1m to -0.2m near the bloom region off Thamnapatnam (Fig. 56). These features represent upwelling area where cold, high nutrient, dense waters are pushed to the surface, leading to phytoplankton bloom. Analysis indicated alongshore wind stress is favorable off Thamnapatnam to induce coastal upwelling (Fig. 56)**.**

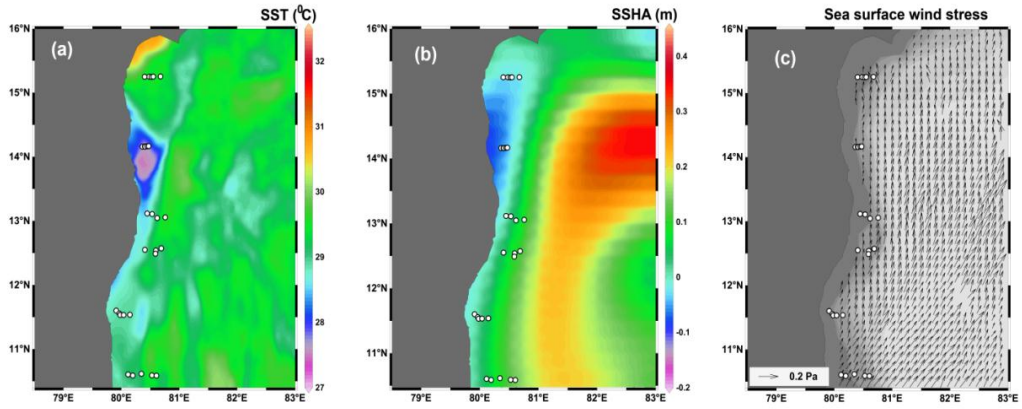

Fig.56. Satellite observations during 12th May 2009 illustrating (a) NOAA-AVHRR sea surface temperature (ºC), (b) Satellite altimetry based sea surface height anomaly (SSHA) in meter and (c) QuikSCAT measured wind stress vectors (Pa).

5.1.5 Bay of Bengal (open ocean)

The role of eddies in pCO_2 variations was explained in the central Bay of Bengal by conducting an Eddy experiment. Within the cyclonic eddy the average pCO_2 was 355 µatm, whereas outside the eddy it was 285 µatm,

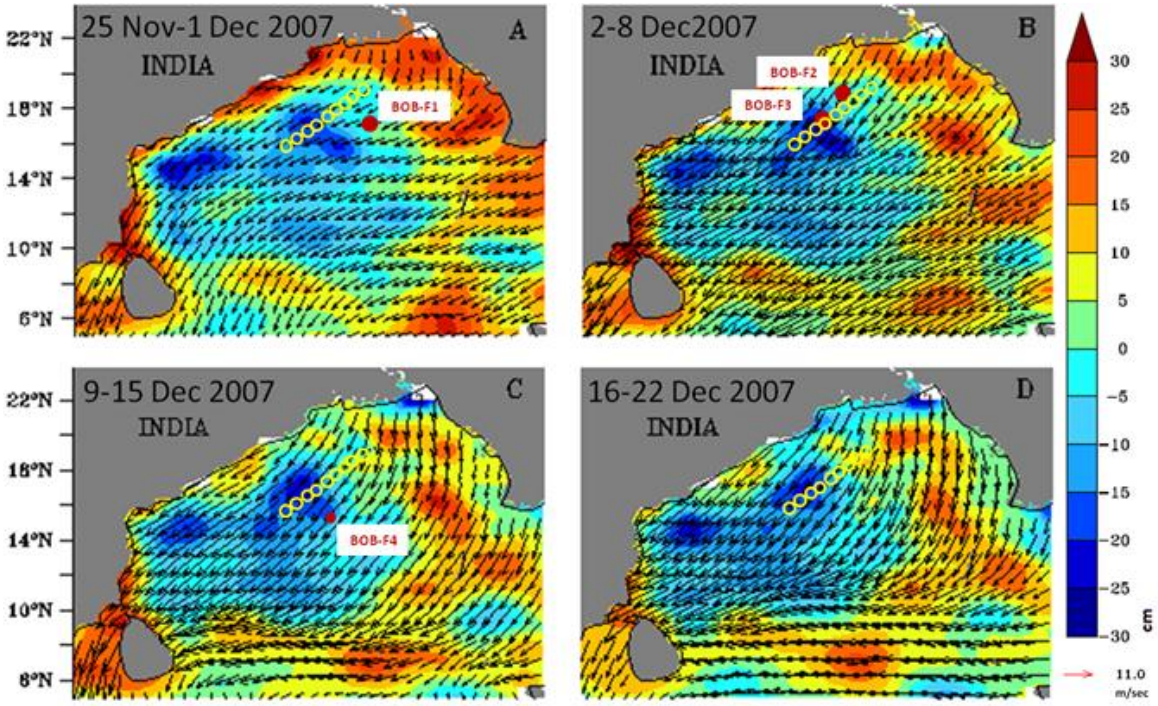

Fig.57. Sea surface height anomaly images overlaid with surface winds showing different evolutionary stages (A-D) of the eddy (close to 17.8N, 87.5E) during A- 25 November - 1 December, B- 2-8 December, C- 9-15 December, D- 16-22 December 2007 in the Bay of Bengal. Time series measurements were carried out at BOB-F3 (Inside eddy) and BOB-F4 (Outside eddy). Figure modified from Singh et al., 2014.

reflecting the role that the eddy play in elevating the surface pCO_2 values in Bay of Bengal. Despite having higher Primary productivity in the eddy (430 mgC/m^2/d) than the outside eddy stations (203 mgC/m^2/d) as also seen from the chlorophyll *a* image (Fig. 57), and higher Co/Ci ratio of 0.9 and 0.42 at 1000m within and outside eddy

respectively, the pCO_2 is higher at the cyclonic eddy as the physical pumping of pCO_2 by the eddy to the surficial layers is higher than the drawdown due to biological pump.

5.2 Comparison with previous studies

5.2.1 Southern Ocean

Biogeochemical processes caused high spatial variations in pCO_2 as it is evident from our results. The end of summer-time production was accompanied by sharp increases in pCO_2 and decrease in pH in March (pCO_2 = 337 µatm) and maximum pCO_2 was in PF. Fransson et al., 2004 found that the southern Atlantic Ocean near the PF was a weak source of atmospheric CO_2 and a sink for O_2 during the austral winter of 1997–1998. The decadal variability of the pCO_2 in south west Indian sector of Southern Ocean during the period 1991–was studied by Metzl 2009. The average annual rate of the atmospheric CO_2 was 1.72 ppm/yr, and oceanic pCO_2 increased at a rate of 2.11µatm/yr i.e. about 0.4 µatm/yr faster than in the atmosphere. Figure 58 shows the pCO_2 variation during this study following Metzl 2014.

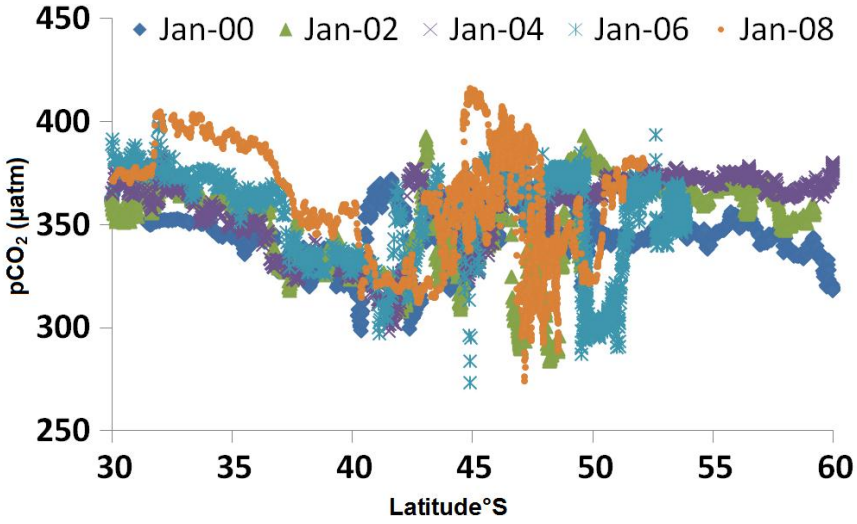

Fig. 58. Yearly sea surface pCO_2 variations in Indian sector of Southern Ocean (Metzl 2014).

Metzl also observed similar changes as observed in the present study wherein the sea surface pCO_2 was higher during January as compared to december (fig . 59). In the Indian Ocean sector between 50°S and 58°S, Metzl et al. (2006) measured pCO_2, TCO_2, alkalinity, and the concentrations of chlorophyll, silicate, and nitrate during January and August cruises in 2000, observing that the summertime seawater pCO_2 was lower than the atmospheric pCO_2 ($\Delta pCO2$ ~ –15 µatm) due to photosynthesis, and the winter pCO_2 was higher than the atmospheric (ΔpCO_2 ~ +10 µatm) due to the upwelling of high-CO_2 deep waters.

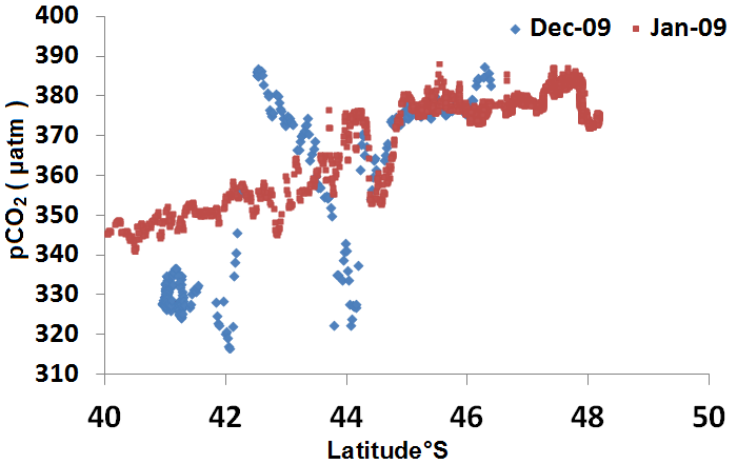

Fig. 59: Variations in sea surface pCO_2 during December and January 2009 taken from Metzl 2014.

The present study is also supported by the data of Poisson (2014) for the time period January and April 1992, where in he observed high pCO_2 in April as compared to January (Fig. 60). The average pCO_2 during January was 326 µatm, whereas during April it was 333 µatm.

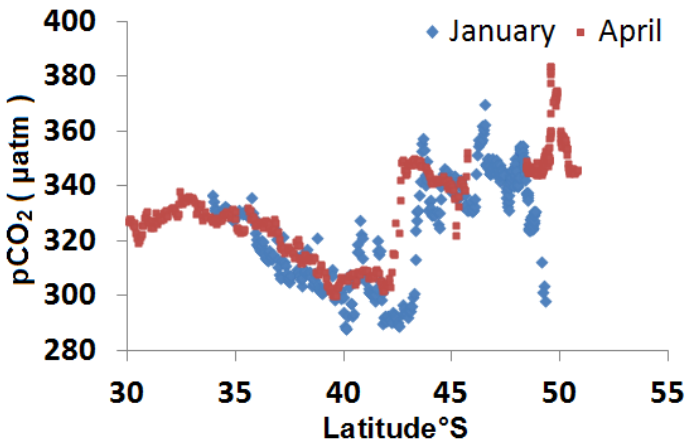

Fig. 60: Variations in sea surface *p*CO_2 during January and April 1992 taken from Poisson 2014.

Figure 61 displays monthly distribution maps for the climatologically mean sea-air *p*CO_2 difference for the reference year 2000 (Takahashi et al., 2012). The sea-air *p*CO_2 differences (ΔpCO_2) are computed using atmospheric *p*CO_2 values that are calculated from zonal mean atmospheric CO_2 concentrations in dry air for the year 2000 (GLOBALVIEW, 2006) and monthly mean values for barometric pressure and water vapour pressure at the sea surface. Figure 61 shows that a strong CO_2 sink zone (blue colour with negative ΔpCO_2) is located near 40°S during the austral summer months (November to February) and is attributed primarily to high productivity over the same latitudes.

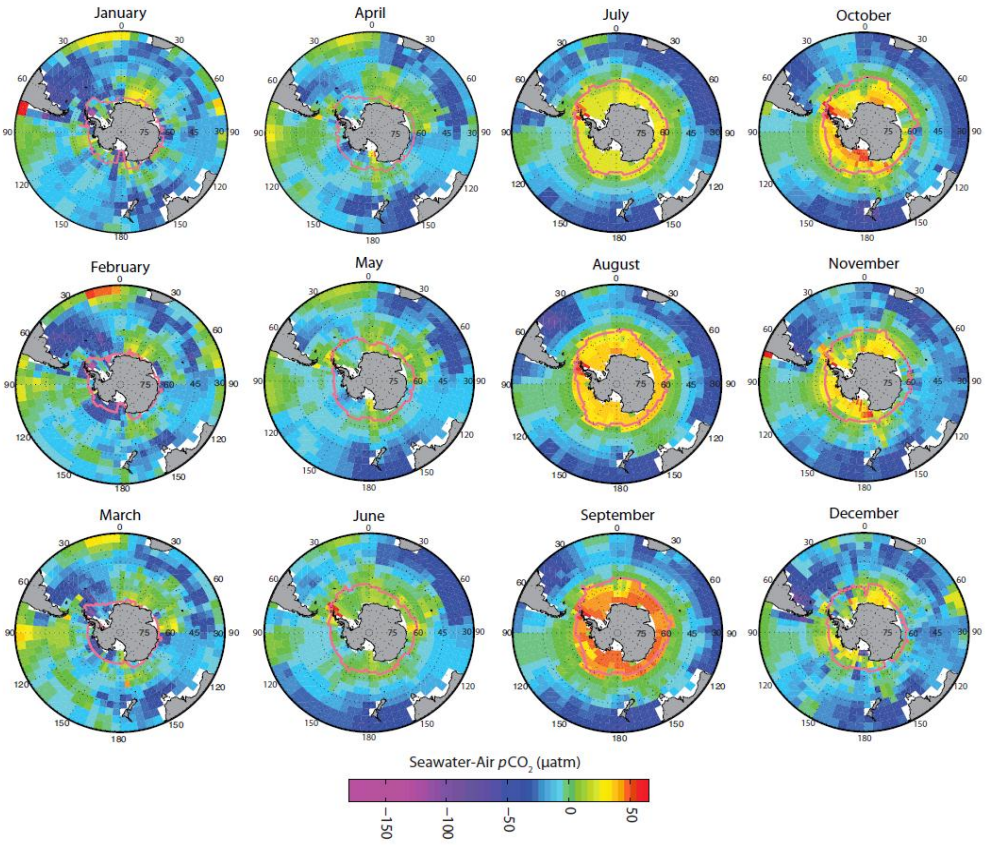

Fig. 61: Monthly distribution maps for the climatological mean sea-air pCO_2 difference (µatm) for the reference year 2000. The pink curves indicate the approximate locations of the northern edges of ice fields, and hence define the seasonal ice zone. The high pCO_2 values in the under-ice mixed layer are due to the upward mixing of high CO_2 Upper Circumpolar Deep Water (Takahashi et al., 2012).

In the permanently open ocean zone (POOZ) of the ACC between 50°S and 60°S, ΔpCO_2 is generally small (light blue and green in Figure 61) because of the competing effects of temperature and TCO_2 on seawater pCO_2: summertime photosynthesis reduces TCO_2 and pCO_2, counteracting pCO_2 increase due to warming, whereas

wintertime cooling counteracts the increasing effect on pCO_2 of upwelled high TCO_2 deep waters.

The coastal waters reflect the properties of upwelled waters modified by complex shelf processes, and they regulate the transfer of atmospheric CO_2 into the deeper layers and abyssal regimes (Takahashi and Chipman, 2012). In summer, the Ross and Weddell Seas and the coastal waters in the Amundsen and Bellingshausen Seas are strong CO_2 sinks with pCO_2 values as low as 170 µatm (~ 210 µatm below the air pCO_2) due to intense photosynthesis, whereas they are a strong source during winter with pCO_2 as high as 425 µatm due to upwelling of high-CO_2 deep waters (Bakker et al., 1997, 2008).

Whether the CO_2 sink intensity in the Southern Ocean has changed in recent decades in response to increasing atmospheric loading of CO_2 and climate change is an important question. This issue has been addressed actively in recent studies. Le Quere et al. (2007) inverted the atmospheric CO_2 concentration data from 12 stations located south of 30°S to obtain sea-air CO_2 flux, and observed that the Southern Ocean CO_2 sink weakened during 1981–2004. They attributed this weakening to the increase in upwelling of deep waters caused by stronger winds during this period. Their study yielded a mean decadal rate of ΔpCO_2 change of about 20 µatm/decade, which is about 4 µatm/decade faster than the mean atmospheric CO_2 increase rate of about 16 µatm/decade for their study period of 1981–2007. Lenton and Matear (2007) and Lovenduski et al. (2007) used Biogeochemistry-Ocean model to explore

the relationship between the SAM and changes in the Southern Ocean CO_2 flux. These investigators found that the southward shift and the intensification of zonal winds that occurred during the positive trend of SAM for the past several decades caused an increase in deepwater upwelling, which in turn increased surface water pCO_2 and decreased CO_2 sink intensity.

5.2.2. Bay of Bengal

Biogeochemistry of Bay of Bengal is poorly understood. Limited observations suggests maximal primary production of 1229 mg C m^{-2} d^{-1}, triggered by a cyclone (Madhu et al., 2002). Primary productivity does not vary seasonally in the Bay, unlike the Arabian Sea. Prasanna Kumar et al., 2007 reported eddy mediated enhancement in biological productivity in Bay of Bengal. A recent study suggests that 42% of the exportable carbon in the Bay of Bengal is accounted by eddies possibly via diatom bloom (Vidya and Prasanna Kumar, 2013).

Depth profiles of C uptake rates showed higher productivity near the surface and a gradual decrease with the depth (Singh et al., 2015). Although the annual minimum light in the Bay is during winter (Narvekar and Prasanna Kumar 2006), phytoplankton are limited rather by nutrients (Gomes et al., 2000). Even though the supply of nutrients by eddy-pumping is higher in the sub-surface (Prasanna Kumar et al., 2007). Euphotic-depth-integrated production was found to be more than twice at station within and outside eddy (Singh et al., 2015). This points to the role of eddy in enhancing productivity.

Gomes et al. (2000) found off-shore production of ~300 mg C m^{-2} d^{-1} during winter in a non-eddy area in the northern Bay of Bengal, which is consistent with that observed away from the eddy (Singh et al., 2015). Singh et al., 2015 reported that the productivity in the eddy was 35.8 ± 3.3 mmol C m^{-2} d^{-1} (430 ± 40 mg C m^{-2} d^{-1}), which is similar to values ~500 and ~425 mg C m^{-2} d^{-1} associated with an eddy during fall and spring in the central Bay of Bengal, respectively (Prasanna Kumar et al., 2007). From these observations it is clear that eddy does play a role in affecting the primary production by increasing the nutrient supply, but in this thesis it is observed that eddy also pumps high pCO_2 waters to the surface.

Sardessai et al., 2010 reported that during Southwest monsoon, the BOB acted as a strong sink of CO_2 (-20 mmol $m^{-2}d^{-1}$), during fall intermonsoon it acted as a weak sink (-4.69mmol $m^{-2}d^{-1}$) and during winter monsoon the BOB acted as a weak source (4.7 mmol $m^{-2}d^{-1}$). The present study was carried out during spring intermonsoon, and BOB acted as a strong sink (-12.8 mmol $m^{-2}d^{-1}$). However, at Thamnapatnam it acts as a weak sink (-3.9 mmol $m^{-2}d$).

5.2.3 Comparison between Southern Ocean and Bay of Bengal

In this thesis two study regions (Southern Ocean and Bay of Bengal) were studied. Both Southern Ocean and Bay of Bengal act as sink for atmospheric CO_2, however the sink capacity is decreasing in Southern Ocean in recent years. There are some regions which act as sources in Southern Ocean, especially near islands, and in Antarctic coast and especially in winter. In Bay of Bengal the region acts as source of CO_2 during winter. Although both the regions are sinks but the biogeochemistry in

both the regions is completely different and hence the factors affecting sea surface pCO_2 are totally different. In the Southern Ocean light intensity, temperature, productivity, UV radiations, Micronutrient Fe availability, Southern Annular Mode effect, sea ice cover, and upwelling intensity are important factors. In the Bay of Bengal, freshwater induced low salinity, eddies, stratification, nutrient availability, turbidity and productivity play an important role.

5.2 Ocean Acidification

5.3.1 Impacts on Foraminifera

Recently ocean acidification as a major threat for marine species has moved from a consensus statement into a much discussed and even challenged conception. Past studies on calcareous organisms suggest reduced calcification as a result of lowering in pH (Gattuso et al., 1998; Langdon et al., 2000, 2003; Riebesell et al., 2000). Different foraminiferal species have different response towards elevated pCO_2. Benthic foraminifera are known to be more resistant as compared to the planktic ones (Broecker 1984).

During March 2009, a high percentage of Antarctic forms of planktic foraminifera *N. pachyderma*, had damaged shells, with a few chambers to entire whorls missing (Fig. 62).

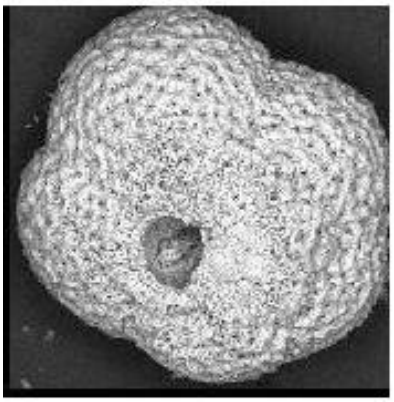

Fig.62. SEM micrographs showing dissolution of planktic Foraminiferal test.

This shell loss is attributed to dissolution due to low pH in the study area (Lowest pH 7.85). However, the effect was only seen on planktic foraminifera and the benthic species like *Quinqueloculina stalkeri, Elphidium excavatum and Pyrgo williamsoni* were not affected. Elevated pCO_2 would have decreased carbonate ion concentration, thus leading to the dissolution of calcareous foraminiferal tests at surface. Although it is quite possible that dissolution of $CaCO_3$ during March 2009 could play a minor role in the reduction of pCO_2, but that would be negligible when compared to the amount of pCO_2 that is pumped in the surface waters due to upwelling.

Earlier studies on planktic foraminifera reported decrease in shell mass due to acidification (Spero et al., 1997). Dissolution is indicated by absence, thinning, or weakness of the calcium carbonate tests in foraminifera (Corliss and Honjo, 1981). In the present study, thinning of foraminiferal shells in the water column was observed when compared with the same species within surface sediment. The shell weight decreased by 17% in water column as compared to surface sediment. The varied response of different species towards elevated pCO_2 may reflect resistance among the organisms and their ability to regulate pH at the site of calcification. Foraminifers

have the ability to increase their intracellular pH at the site of calcification by atleast one unit higher than the seawater pH (Nooijer et al., 2009). Since, calcareous foraminifera represent more than 50% of the total benthic assemblages (Ricketts et al., 2009) elevation of CO_2 will result in negative effects to benthic biota. Dissolution or decreased calcification would shift $CaCO_3$-dominated system to one dominated by organic algae (Kuffner et al., 2008). Future research on the reconstruction of oceanic paleotemperature and paleoproductivity should focus on developing strategies to determine when foraminiferal faunas are biologically, as opposed to thermally controlled and this would pave the road for robust progress in our understanding of how ocean acidification impacts biota of the ocean.

5.3.2 Impact on Diatoms

The dynamic nature of coastal Antarctic ecosystem, wherein rapid changes in biogeochemistry within very short distances and time was studied. Phytoplankton abundance was dominated by diatoms, with minor exception of cyanobacteria, and silicoflagellates. Dominating diatom species include *Corethron sp., Fragillariopsis sp., Chaetoceros sp., Rhizosolenia sp., Proboscia sp*., *Nitzschia* sp., *Dactyliosolen* sp., *Thallasiothrix sp.*, *Trichotoxon* sp., *Astromphalus sp., Paralia sp.,* and *Actinocyclis sp. Corethron criophilum* was the dominant diatom species and its abundance varied from 0 to $30x10^4$ cells/l (Fig 63a), however it was either absent or low in abundance along transect T_E. *Nitzschia* sp was abundant along T_E.

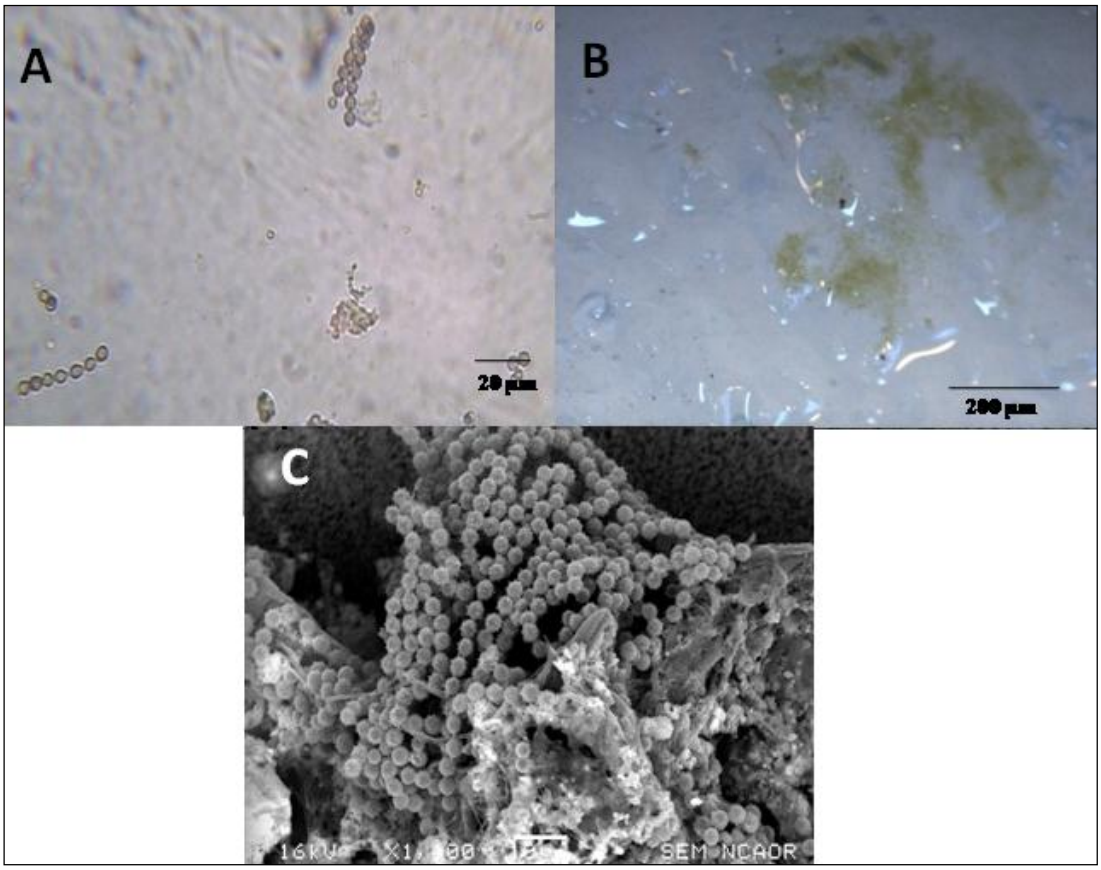

Fig.63. (a) & (b) Light microscopic image of *Nostoc sp* from iceberg (c) Scanning electron micrograph of *Nostoc sp.,* from Antarctic coastal waters.

Fresh water cyanobacteria (*Nostoc sp.,*) were found in few stations along transect T_E along the Antarctic coast (Fig. 63d), its abundance varied from $1.5x10^4$cells/L to $10.1x10^4$cells/L and was high at stations having low salinity and high pCO_2 (Fig 63 a). Silicoflagellates comprised of *Distephanus speculum.* EDS results of the iceberg samples showed iron (Fe) particles within the iceberg. Iron (Fe) was as high as 71%. Cyanobacteria (*Nostoc sp.*) attached on the icebergs were also found.

Recent study by Vernet et al., (2011) indicated presence of healthy phytoplankton cells in vicinity of iceberg. The current study reports presence of cyanobacteria over

icebergs, which indicates that apart from being a source of Iron (Fe), icebergs also act as a source of cyanobacteria to the marine environment. Cyanobacteria were abundant in surface waters along T_E at stations with salinity <33 and pCO_2 >325 µatm, whereas diatom *Corethron criophilum* dominated along T_W. The low abundance of diatoms in elevated pCO_2 and low saline waters in samples reflects the dominance of cyanobacteria over other phytoplankton in high CO_2, low saline region. This is reflected in the correlation of cyanobacteria with salinity (r= -0.25) and pCO_2 (r= 0.86) and the correlation of *Corethron criophilum* with salinity (r= 0.33) and pCO_2 (r= -0.15). Keating (1978) reported that cyanobacteria could limit the ability of diatom species to form bloom in high pCO_2 and low pH conditions. Tortell et al., (2002) recently suggested that the CO_2 concentration can potentially influence competition among phytoplankton species as CO_2 is a limiting factor for phytoplankton growth. Phytoplankton community shift could also play a key role in the cycling of nutrients.

Due to climate change, cyanobacterial growth will increase with warm water temperatures, lower salinity, increased CO_2 and abundant nutrients in future (Castle and Rodgers 2011). Cyanobacterial blooms have caused massive mass destruction in the Phanerozoic (Castle and Rodgers 2011). Warmer weather will likely extend the spatial and temporal influences of glacial meltwater and will also increase the spatial extent and importance of cyanobacteria with significant consequences for Antarctic food web dynamics and coastal biogeochemistry.

5.3.2 Impact on Sea urchin

The effect of future ocean acidification is projected to be particularly threatening to calcifying marine organisms in coldwater, high latitude seas, making tolerance data on these organisms a critical research need in Southern Ocean marine ecosystems. Due to a high magnesium (Mg) content of their calcitic hard parts, Sea urchins are especially vulnerable to dissolution stress from ocean acidification because they currently inhabit seawater that is barely at the saturation level to support biogenic calcification. Thus, cold-water, high latitude species with a high Mg-content in their hard parts are considered to be the 'first responders' to chemical changes in the surface oceans. How, the sea urchin would adapt towards dissolution of its shell is still an unanswered question, however recent study by Pespeni et al., 2013 has reported signatures of adaptation in the purple sea urchin, by altering the genetic material during larval stage. Taylor et al., 2013 have also suggested shoaling and contraction of bathymetric range in *Strongylocentrotus fragilis*, rather than its extinction.

This study, examines the effects of ocean acidification on Sea urchins in the coastal waters of Antarctica, the sea urchin *Sterechinus neumayeri*. Lab experiments were conducted on sea urchins by subjecting it to acidified seawater, to mimic the scenarios defined by IPCC models and by analyses of future acidification predicted for the Southern Ocean. Specimens were reared in 3 different pH conditions (pH 6, 7.8 and 8.1).

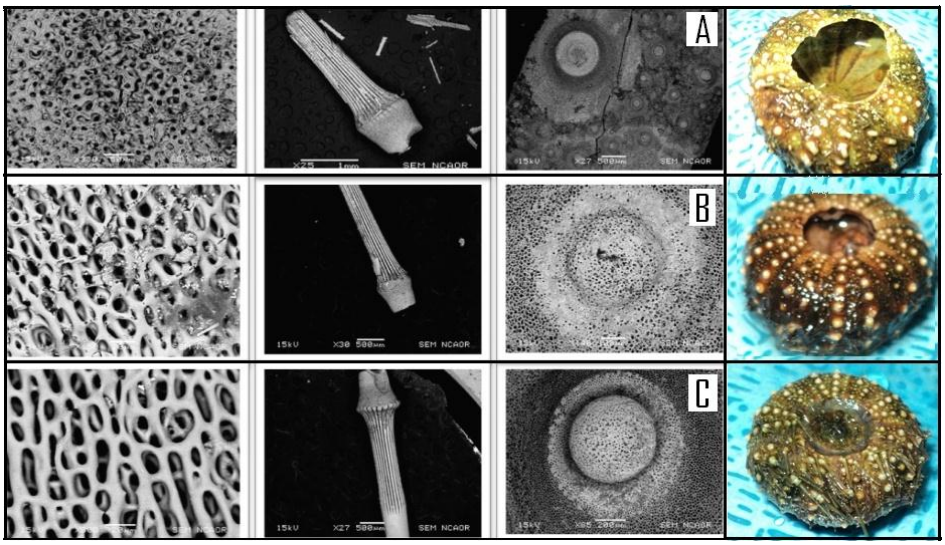

Fig.64. Acidification study on Sea-urchin collected from coastal Antarctica. (A) pH=6, (B) pH=7.8, (C) pH=8.1.

At pH 8.1 (current global oceanic average pH) the Sea urchin shell showed no effects, while at pH 7.8 (IPCC predicted global oceanic average pH by 2100) the shells showed dissolution as evidenced by the scanning electron micrographs (Fig. 64). Considering that the growth rate of oceanic pCO_2 is highest in the Indian sector of the Southern Ocean, this study rings alarm questioning the adaptability of Antarctic marine organisms and hence it is highly essential to anticipate the severity and consequences of future climate change. Future studies should conduct long-term multi-generational experiments to determine whether vulnerable sea urchin species have the capacity to adapt to elevations in atmospheric CO_2 over the next century.

5.4 Significance of this study and outlook

Indian initiates in CO_2 chemistry in Southern Ocean started from this study when pCO_2 was measured for the first time during 3rd Indian scientific expedition to Southern Ocean in March 2009. Also, Indian initiatives in Antarctic CO_2 chemistry started with this study when pCO_2 was measured for the first time during 31st Indian scientific expedition to Antarctica in January 2012. In total 3 years data was generated for the Indian Sector of Southern Ocean which covered wide area (30-66S). Considering that the growth rate of oceanic pCO_2 is maximum in the Indian sector of Southern Ocean, the data generated by this study would help in developing climate change models. As suggested by Dr. Nicolas Metzl the data generated from this study will be submitted to the Global CO_2 Data bank. These data sets would be used to develop long term models for climate change. The Nutrient data generated from this study has already been useful to correlate with various phytoplankton and productivity studies.

The biogeochemical study under the land fast sea ice is a new initiative and the results have already made many scientists interested in working in this area. Same holds true for the iceberg study. The dissolved oxygen values under Fast ice reaching upto 600 µM is an interesting discovery and has developed interest among many researchers to work on Sea ice biogeochemistry. Also, the result of silicate depletion under sea ice would throw light on Global silicate depletion studies.

This study has also initiated Acidification studies and has provided with early signatures of acidification. Thus, ringing alarms about phytoplankton community shift.

This study suggests that influence of eddies on primary productivity is high in the Bay and could result in doubling the PP. The nutrients supplied to the surficial layer are high and thus results in increasing PP. However, it also pumps high CO_2 to surficial waters and this has major consequences towards climate change.

CHAPTER 6

Conclusions

The present study aimed at studying two major sinks for atmospheric CO_2, the Southern Ocean and the Bay of Bengal. A significant spatial variation in the sea surface pCO_2 was observed in the Indian Ocean sector of the SO and the processes that drawdown pCO_2 were modelled. Biological processes via primary production is the most dominant process regulating sea surface pCO_2, followed by thermal, mixing and air-sea flux. The Southern Ocean acted as a sink for atmospheric CO_2 in the late Austral Summer of March 2009, February 2010 and January 2012, except at a few stations around the Crozet Island, which were sources during March 2009. The organic carbon flux / inorganic carbon flux ratio was high during January 2012 as compared with March 2009, leading towards drawdown of surface pCO_2. A transition from pCO_2 saturated waters to pCO_2 undersaturated waters was observed from March 2009 to January 2012. The average sea surface pCO_2 was higher along 48°E, as compared to 57.30°E. The possible reason for this would be stronger physical forcing due to the bottom-topography and island mass effect along 48°E. The low pCO_2 concentrations during January 2012 are attributed to shallow MLD, high biological productivity (as seen from the PP, chlorophyll *a* and TOC concentrations and Diatom abundance), high Co/Ci ratio, light and nutrient availability, total ozone concentration and low upwelling intensity. This thesis is a major contribution of Indian Antarctic and Southern Ocean Expeditions to further our understanding of the Southern Ocean.

The Bay of Bengal acts as a weak sink for atmospheric CO_2 during winter monsoon, although at few stations the region acts as a source. Eddies increase the primary

productivity by pumping nutrients to surface waters, however despite the high primary productivity, eddies play an important role in elevating pCO_2 in the surface waters. Along the east coast of India, Bay of Bengal acts as a strong sink during spring intermonsoon, however Thamnapatnam is a site for coastal upwelling and elevated pCO_2 conditions.

Signatures of ocean acidification were observed on foraminifera, diatoms and sea urchins in the Southern Ocean. Foraminifera showed dissolution and shell thinning due to acidification. Diatom abundance was low in high pCO_2 low pH waters, and these waters were dominated by cyanobacteria *Nostoc sp.* and cyanobacterial dominance would rise in future with rise in temperature, decrease in salinity and decrease in pH. Sea urchin *Sterechinus neumayeri* is not affected at the current pH, but showed dissolution at the predicted pH for 2100. Southern Ocean with high CO_2 has major implications to global climate and provides a strong motivation to pursue long-term oceanic CO_2 observations to better characterize the global carbon budget, its evolution and its coupling with climate.

This thesis clearly highlights the need for carbon cycle and acidification studies in Indian Sector of Southern Ocean.

References

Anderson, R.F., Ali, S., Bradtmiller, L.I., 2009. Wind-Driven Upwelling in the Southern Ocean and the Deglacial Rise in Atmospheric CO_2. Science 323, 1443 –1448.

Anderson, L.A., 1995. The hydrogen and oxygen content of marine phytoplankton. Deep-Sea Research I 42, 1675-1680.

Anderson, L.A., Sarmiento, J.L., 1994. Redfield ratios of remineralization determined by nutrient data analysis. Global Biogeochemical Cycles 8, 65-80.

Anderson, L.G., Jones, E.P., 1991. The transport of CO_2 into the Arctic and Antarctic seas: similarities and differences in the driving processes. Journal of Marine Systems 2, 81–95.

Anilkumar, N., Dash, M.K., Luis, A.J., Ramesh Babu, V., Somayajulu, Y.K., Sudhakar, M., Pandey, P.C., 2005. Oceanic fronts along 45°E across Antarctic Circumpolar Current during austral summer 2004. Current Science 88, 1669-1773.

Anilkumar, N., Luis, A.J., Somayajulu, Y.K., Ramesh Babu, V., Dash, M.K., Pednekar, S.M., Babu, K.N., Sudhakar, M., Pandey, P.C., 2006. Fronts, water masses and heat content variability in the Western Indian sector of the Southern Ocean during austral summer 2004. Journal of Marine Systems 63, 20–34.

Anilkumar, N., Mohan, R., Shukla, S.K., Pednekar, S.M., Maruthadu, S., Ravindra, R., 2010. Signatures of coastal upwelling in Prydz Bay, East Antarctica during Austral summer 2006. Current Science 99, 1390-1394.

Archer, D., Meier-Reimer, E., 1994. Effect of deep-sea sedimentary calcite preservation on atmospheric CO_2 concentration. Nature 367,260-263.

Arrigo, K.R., Lubin, D., van Dijken, G.L., Holm-Hansen, O., Morrow, E., 2003. Impact of a deep ozone hole on Southern Ocean primary production. Journal of Geophysical Reearch 108(C5), doi: 10.1029/2001JC001226.

Arrigo, K. R., Thomas, D. N., 2004. Large scale importance of sea ice biology in the Southern Ocean. Antarctic Science 16, 471–486.

Arrigo, K.R., Worthen, D.L., Robinson, D.H., Dunbar, R.B., Ditullio, G.R., Vanwoert, M., Lizotte, M.P., 1999, Phytoplankton community structure and the drawdown of nutrients and CO_2 in the Southern Ocean. Science 283, 365–367.

Bakker, D.C.E., de Baar, H.J.W., Bathmann, U.V., 1997. Changes of carbon dioxide in surface waters during spring in the Southern Ocean. Deep Sea Research II 44, 91-127.

Bakker, D.C.E., Hoppema, M., Schroder, M., Geibert, W., de Baar, H.J.W., 2008. A rapid transition from ice covered CO_2–rich waters to a biologically mediated CO_2sink in the eastern Weddell Gyre. Biogeosciences 5, 1373–1386.

Bakker, D.C.E., Nielsdottira, M.C., Morris, P.J., Venables, H.J., Watson, A.J., 2007. The Island mass effect and biological carbon uptake for the subantarctic Crozet Archipelago. Deep-Sea Research II 54, 2174–2190.

Belkin, I.M., Gordon, A.L., 1996. Southern ocean fronts from the Greenwich Meridian to Tasmania. Journal of Geophysical Research 101, 3675–3696.

Behrenfeld, M.J., Falkowski, I., Paul. G., 1997. Photosynthetic rates derived from satellite-based chlorophyll concentration. Limnology Oceanography 42(l), I-20.

Berger, W.H., 1968. Planktonic foraminifera – selective dissolution and paleoclimatic interpretation. Deep-Sea Research I 15, 31-42.

Berger, W.H., Fisher, K., Lai, C., Wu, G., 1987. Ocean carbon flux: global maps of primary production and export production, in: Agegian, C. (Ed.),Biogeochemical Cycling and Fluxes between the Deep Euphotic Zone and Other Oceanic Realms, NOAA Symposium series for Under Sea Research Program, 3(2), Preprint in SIO ref. 87-30.

Bijma, J., Hönisch, B., Zeebe, R.E., 2002. Impact of the ocean carbonate chemistry on living foraminiferal shell weight: comment on “Carbonate ion concentration in glacial-age deep waters of the Caribbean Sea” by Broecker, W.S., Clark, E., Geochemica Geophysics Geosystems 3, 1064.

Blain, S., Sedwick, P., Gristh, B., Quéguiner, B., Bucciarelli, E., Fiala, M., Denis, M., Tréguer, P., 2000. Iron and nutrient limitation of phytoplankton growth in the Indian sector of the Southern Ocean: experimental results from the Antares campaign. Ocean Sciences Meeting, EOS, Transactions, American Geophysical Union 80 (49), 67.

Blain, S., Tréguer, P., Belviso, S., Bucciarelli, E., Denis, M., Desabre, S., Fiala, M., Jézéquel, V.M., Le Fèvre, J., Mayzaud, P., Marty, J.C., Razouls, S., 2001. A biogeochemical study of the island mass effect in the context of the iron hypothesis: Kerguelen Islands, Southern Ocean. Deep Sea Research I 48,163-187.

Boden, B.P., 1988. Observations of the island mass effect in the Prince Edward archipelago, Polar Biology 9, 161-168.

Broecker, W., Mix, A., Andree, M., 1984. Radiocarbon measurements on coexisting benthic and plankticforaminifera shells: potential for reconstructing ocean ventilation

times over the past 20,000 years. Nuclear Instruments and Methods in Physics Research Section B: Beam Interactions with Materials and Atoms 5, 331-339.

Broecker, W.S., Peng, T.H., 1989. The cause of the glacial to interglacial atmospheric CO_2 change: A polar alkalinity hypothesis. Global Bio geochemical Cycles 3, 215-239.

Byrne, R.H., Breland, J.A., 1989. High precision multiwavelength pH determinations in seawater using cresol red. Deep Sea Research I 36, 803-810.

Canadell, J.G., LeQuere, C., Raupach, M.R., Field, C.B., Buitehuis, E.T., Ciais, P., Conway, T.J., Gillett, N.P., Houghton, R.A., Maryland, G., 2007. Contributions to accelerating atmospheric CO_2 growth from economic activity, carbon intensity, and efficiency of natural sinks.Proceedings of the Natural Academy of Sciences 5, 18866–18870.

Cassar, N., DiFiore, P.J., Barnett, B.A., Bender, M.L., Bowie, A.R., Tilbrook, B., Petrou, K.,Westwood, K.J., Wright, S. W., Lefevre, D., 2011. The influence of iron and light on net community production in the Subantarctic and Polar Frontal Zones. Biogeosciences 8, 227–237.

Castle, J.W., Rodgers, J.H., 2011. Hypothesis for the role of toxin-producing algae in Phanerozoic mass extinctions based on evidence from the geologic record and modern environments. Environmental Geosciences 18, 58-60.

Comiso, J.C., McClain, C.R., Sullivan, C.W., Ryan, J.P., Leonard, C.L., 1993. Coastal zone colour scanner pigment concentrations in the southern ocean and relationships to geophysical surface features. Journal of Geophysical Research 98, 2419–2452.

Conway, M.A.,1994. Flashbulb memories. Hillsdale, NJ: Erlbaum.

Copin-Monte´gut, C., Avril, B., 1993. Vertical distribution and temporal variation of dissolved organic carbon in the north western Mediterranean Sea. Deep-Sea Research I 40, 1963–1972.

Corliss, B.H., Honjo, S., 1981. Dissolution of deep-sea benthonic foraminifera. Micropaleontology 27, 356–378.

Cooper, D.J., Watson, A.J., Ling, R.D., 2008. Variations of pCO_2 along a North Atlantic shipping route (UK to Jamaica): a year of automated observations. Marine Chemistry 60, 147–164.

DeGrandpre, M.D., Hammar, T.R., Wirick, C.D., 1998. Short-term pCO_2 and O_2 dynamics in California coastal waters. Deep-Sea Research II 45, 1557–1575.

DeGrandpre, M.D., Hammar, T.R.,Wallace, D.W.R., Wirick, C.D., 1997. Simultaneous mooring10 based measurements of seawater CO_2 and O_2 off Cape Hatteras, North Carolina. Limnology Oceanography 42, 21–28.

Dickson, A.G., Millero, F.J., 1987. A comparison of the equilibrium constantsfor the dissociation of carbonic acid in seawater media. Deep Sea Research I 34, 1733–1743.

Dieckmann, G.S., Nehrke, G., Papadimitriou, S., Göttlicher, J., Steininger, R., Kennedy, H., Wolf-Gladrow, D., Thomas, D.N., 2008.Calcium carbonate as ikaite crystals in Antarctic sea ice. Geophysical Research Letters 25, L08501-L033540.

DOE, 1994. Handbook of methods for the analysis of the various parameters of the carbon dioxide system in sea water: version 2, in: Dickson, A.G., Goyet, C., (Eds.), ORNL/CDIAC-74.

Dortch, Q., Whitledge, T.E., 1992. Does nitrogen or silicon limit phytoplankton production in the Mississippi River plume and nearby regions? Continental Shelf Research 12, 1293-1309.

Doty, M.S., Oguri, M., 1956.The island mass effect. ICESJournal of Marine Science 22, 33–37.

Dugdale, R.C., Goering, J.J., 1967. Uptake of new and regenerated primary productivity. Limnology and Oceanography 12,196-206.

Emery, W.J., Meincke, J., 1986. Global water masses: summary and review. Oceanologica Acta 9, 383–391.

Eynaud, F., Giraudeau, J., Pichon, J.J., Pudsey, C.J., 1999. Sea-surface distributions of coccolithophores, diatoms, silicoflagellates and dinoflagellates in the South Atlantic Ocean during the late austral summer 1995. Deep-Sea Research I 46, 451-482.

Fauchereau, N., Tagliabue, A., Monteiro, P., Bopp, L, 2011. The response of phytoplankton biomass to transient mixiing events in the Southern Ocean. Geophysical Research Letter 38, L17601.

Feely, R.A., Sabine, C., Lee, K., Berelson, W., Kleypas, J., Fabry, V.J., Millero, F.J., 2004. Impact of anthropogenic CO_2 on the $CaCO_3$ system in the oceans. Science 305, 362–366.

Fiala, M., Kopczynska, E.E., Jeandel, C., Oriol, L., Vetion, G., 1998a. Seasonal and interannual variability of size-fractionated phytoplankton biomass and community structure at station Kerfix, off the Kerguelen Islands, Antarctica. Journal of Plankton Research 20, 1341–1356

Fiala, M., Semeneh, M., Oriol, L., 1998. Size-fractionated phytoplankton biomass and species composition in the Indian sector of the Southern Ocean during austral summer. Journal of Marine System 17, 179–194.

Fielding, S., Seeyave, S., Read, J.F., Hughes, J.A., Smith, T., Castellani, C., 2007. Community structure and grazing impact of mesozooplankton during late spring/early summer 2004/2005 in the vicinity of the Crozet Islands (Southern Ocean). Deep-Sea Research II 54, 2106-2125.

Fischer, G., Ratmeyer, V., Wefer, G., 2000. Organic carbon fluxes in the Atlantic and the Southern Ocean: relationship to primary production compiled from satellite radiometer data. Deep-Sea Research II 47,1961-1997.

Frankignoulle, M., Canon, C., Gattuso, J.P., 1994. Marine calcification as a source of carbon dioxide: positive feedback of increasing atmospheric CO_2. Limnology and Oceanography 39, 458–462.

Fransson, A., Chierici, M., Anderson, L.G., David R., 2004b. Transformation of carbon and oxygen in the surface layer of the eastern Atlantic sector of the Southern Ocean, Deep Sea Research II, 51(22–24), 2757–2772.

Fu, F.X., Mulholland, M.R., Garcia, N.S., Beck, A., Bernhardt, P.W., Warner, M.E., Sanudo-Wilhelmy, S.A., Hutchins, D.A., 2008. Interactions between changing pCO_2, N_2 fixation, and Fe limitation in the marine unicellular cyanobacterium Crocosphaera. Limnology and Oceanography 53, 2472–2484.

Gandhi, N., Ramesh, R., Laskar, A.H., Sheshshayee, M.S., Shetye, S., Anilkumar, N., Patil, S.M., Mohan, R., 2012. Zonal variability in productivity and nitrogen uptake

rates in the southwestern Indian Ocean and Southern Ocean. Deep-Sea Research I 67, 32-43.

Gattuso, J.P., Frankignoulle, M., Bourge, I., 1998. Effect of calcium carbonate saturation of seawater on coral calcification. Global and Planetary Change 18, 37–46.

Geider, R.J., LaRoche, J., 1994. The role of iron in phytoplankton photosynthesis, and the potential for iron-limitation of primary productivity in the sea. Photosynthetic Research 39, 275–301.

Gieskes, J.M., 1969. Effect of temperature on the pH of seawater. Limnology and Oceanography 14, 679-685.

Glibert, P.M., Garside, C., 1992. Dial variability in nitrogenous nutrient uptake by phytoplankton in the Chesapeake Bay plume, Journal of Plankton Research 14, 271–288.

Gill, A.E, 1977. Coastally trapped waves in the atmosphere. Quarterly Journal of the Royal Meteorological Society 103, 430 - 440.

GLOBALVIEW-CO_2, Cooperative Atmospheric Data Integration Project—Carbon Dioxide. CD-ROM, NOAA. CMDL, Boulder, Colorado [Also available on Internet via anonymous FTP to ftp.cmdl.noaa.gov, Path: ccg/co2/GLOBALVIEW].

Gomes, H.R., Goes, J.I., Saino, T., 2000. Influence of physical processes and freshwater discharge on the seasonality of phytoplankton regime in the Bay of Bengal. Continental Shelf Research 20, 313–330.

Gordon, A.L., Chen, C.T.A., Metcalf, W.G., 1984. Winter mixed layer entrainment of Weddell Deep Water. Journal of Geophysical Research 89, 637–640.

Gosselin, M., Legendre, L., Therriault, J.C., Demers, S., 1990. Light and nutrient limitation of sea-ice microalgae (Hudson Bay, Canadian Arctic). Journal of Phycology, 26, 220-232.

Grasshoff, K., Ehrhardt, M., Kremling, K., (Eds.), 1983. Methods of Seawater Analysis. Verlag Chemie, Weinheim, 419.

Hales,B., Takahashi, T., Bandstra, L., 2005. Atmospheric CO_2 uptake by a coastal upwelling system. Global Biogeochemical Cycles 19, GB1009, doi:10.1029/2004GB002295.

Hasegawa, D., Yamazaki, H., Ishimaru, T., Nagashima, H., Koike, Y., 2008. Apparent phytoplankton bloom due to island mass effect. Journal of Marine System 69, 238-246.

Heinze, C., Maier-Reimer, E., Winn, K., 1991. Glacial pCO_2 reduction by the World Ocean: experiments with the Hamburg carbon cycle model. Paleoceanography6, 395–430.

Honda, M.C., Kusakabe, M., Nakabayashi, S., Manganini, S.J., Honjo, S., 1997. Change in pCO_2 through Biological Activity in the Marginal Seas of the Western North Pacific: The Efficiency of the Biological Pump Estimated by a Sediment Trap Experiment. Journal of Oceanography 53, 645- 662.

Hofmann, M., Schnellnhuber H.J., 2009. "Ocean acidification affects marine carbon pump and triggers extended marine oxygen holes." PNAS 106(9), 3017-3022.

Houghton, J.T., Ding, Y., Griggs, D.J., Noguer, M., van der Linden, P.J., Dai, X., Mashell, K., Johnson, C.A., 2001.in: Houghton, J.T. (Ed.), Climate Change 2001. The Scientific Basis. Cambridge University Press, ISBN 0521014956, pp. 185-237.

Hutchins, D.A., Bruland, K.W., 1998. Iron-limited growth and Si:N uptake ratios in a coastal upwelling regime. Nature 393, 561-564.

Ittekkot, V., Nair, R.R., Honjo, S., Ramaswamy, V., Bartsch, M., Manganini, S., Desai, B.N., 1991. Enhanced particle fluxes in the Bay of Bengal induced by injection of freshwater. Nature 351, 385–387, doi:10.1038/351385a.

Jabaud-Jan, A., Metzl, N., Brunet, C., Poisson, A., Schauer, B., 2004. Interannual variability of the carbon dioxide system in the southern Indian Ocean (20◦–60◦S): the impact of a warm anomaly in austral summer 1998. Global Biogeochemical Cycles 18, GB002017.

Joubert, W.R., Swart, S., Tagliabue, A., Thomalla, S.J., Monteiro. P.M.S., 2014. The sensitivity of primary productivity to intra-seasonal mixed layer variability in the sub-Antarctic Zone of the Atlantic Ocean. Biogeosciences Discussion 11, 4335–4358.

Jouandet, M.P., Blain, S., Metzl, N., Mathieu, M., 2011. Interannual variability of net community production and air-sea CO_2 flux in a naturally iron fertilized region of the Southern Ocean (Kerguelen plateau). Antarctic Science 1-8.

Jones, E.M., Bakker, D.C.E., Venables, H.J., Whitehouse, M.J., Korb, R.E., Watson, A.J., 2010. Rapid changes in surface water carbonate chemistry during Antarctic sea ice melt. Tellus 62B, 621–635.

Kaufman., D. E., Friedrichs M.A.M., Smith Jr, W. O., Queste, B.Y., Heywood, K.J., 2014. Biogeochemical variability in the southern Ross Sea as observed by a glider deployment. Deep Sea Research I 92, 93–106.

Keating, K.I., 1978. Blue-Green Algal Inhibition of Diatom Growth: Transition from Mesotrophic to Eutrophic Community Structure. Science 199, 971-973.

Keeling, C.D., 1968. Carbon dioxide in surface ocean waters: 4. Global distribution. Journal of Geophysical Research **73**, 4543-4553.

Kennett, J.P., Srinivasan, M.S., 1983. Neogene planktonic foraminefera, A Phylogenetic Atlas.Hutchinson Ross, Stroudsburg, 265.

Knox, G.A., 1994. The Biology of the Southern Ocean, Studies in Polar Research. Cambridge University Press, UK, p. 182.

Kuffner, I.B., Andersson, A.J., Jokiel, P.L., 2008. Decreased abundance of crustose coralline algae due to ocean acidification. Nature Geoscience 1, 114-117.

Kumar, M.D., Sarma, V.V.S.S., Ramaiah, N., Gauns, M. and De Sousa, S.N., 1998. Biogeochemical significance of transport exopolymer particles in the Indian Ocean. Geophysical Research Letters, 25, 81-84.

Kumar, S., Ramesh, R., Sardesai, S., Sheshshayee, M.S. 2004. High new production in the Bay of Bengal: Possible causes and Implications. Geophysical Research Letters, 31, L18304.

Lampitt, R.S., Antia, A.N., 1997. Particle flux in deep seas: regional characteristics and temporal variability. Deep-Sea Research 44, 1377-1403.

Lancelot, C., de Montetry, A.H.G., Becquevort, S., Schoemann, V., Pasquer, B., Vancoppenolle, M., 2009. Spatial distribution of the iron supply to phytoplankton in the Southern Ocean: a model study. Biogeosciences 6, 2861–2878.

Langdon, C., Broecker, W.S., Hammond, D.E., Glenn, E., Fitzsimmons, K., Nelson, S.G., Peng, T.H., Hajdas, I., Bonani, G., 2003. Effect of elevated CO_2 on the community metabolism of an experimental coral reef. Global Biogeochemical Cycles 17. 1011.

Langdon, C., Takahashi, T., Sweeney, C., Chipman, D., Goddard, J., Marubini, F., Aceves, H., Barnett, H., Atkinson, M.J., 2000.Effect of calcium carbonate saturation state on the calcification rate of an experimental coral reef. Global Biogeochemical Cycles 14, 639-654.

Larsen, S.H., 2005. Solar variability, dimethyl sulphide, clouds, and climate. Global Biogeochemical Cycles 19, GB002333.

Le Fe`vre, J., 2000. Mesoscale dynamics and phytoplankton biomass associated with a frontal system in the Southern Ocean: exploitation of SeaWIFS images received in near real time during cruise Antares 4, Southern Ocean JGOFS Symposium, Brest, France.

Legendre, L., 1992. Ecology of sea ice biota: 2. Global significance. Polar Biology 12, 429-444.

Lenton, A., Matear, R.J., 2007. The role of the Southern Annular Mode (SAM) in Southern Ocean CO_2 uptake. Global Biogeochemical Cycles, 5.DOI: 10.1029/2006GB002714

LeQuéré, C., Rodembeck, C., Buitenhuis, E., Conway, T., Langenfelds, R., Gomez, A., Labuschagne, C., Ramonet, M., Nakazawa, T., Metzl, N., Gillett, N., Heimann, M., 2007. Saturationof the Southern Ocean CO_2 sink due to recent climate change. Science 316, 1735–1738.

Levitus, S., Gelfeld, R., Boyer, T., Johnson, D., 1994. Results of the NODC Oceanographic Data Archaeology and Rescue Projects, Key to Oceanograhic Records Documentation No. 19, NODC, Washington, D.C., 73pp.

Lewis, E., Wallace, D.W.R., 1998. Program Developed for CO_2 System Calculations. ORNL/CDIAC-105. Oak Ridge National Laboratory, Oak Ridge.

Louanchi, F., Metzl, N., Poisson, A., 1996. A modeling the monthly sea surface fCO_2 fields in the Indian Ocean. Marine Chemistry 55, 265–280.

Louanchi, F., Ruiz-Pino, D., Jeandel, C., Brunet, C., Schauer, B., Masson, A., Fiala, M.I., Poisson, A., 2001. Dissolved inorganic carbon, alkalinity, nutrient and oxygen seasonal and interannual variations at the Antarctic Ocean. Deep-Sea Research I 481, 581-1603.

Lovenduski, N.S., Gruber, N., Doney, S.C., Lima, I.D., 2007. Enhanced CO_2 outgassing in the Southern Ocean from a positive phase of the Southern Annular Mode. Global Biogeochemical Cycles 21, GB2026.

Luis, A. J., Sudhakar, M., 2009. Upper-ocean hydrodynamics along meridional sections in the southwest Indian sector of the Southern Ocean during austral summer 2007. Polar Science 3, 13-30.

Madhu, N.V., Maheswaran, P.A., Jyothibabu, R., Sunil, V., Ravichandran, C., Balasubramanian, T., Gopalakrishnan, T.C. Nair, K.K.C., 2002. Enhanced biological production off Chennai triggered by October 1999 super cyclone (Orissa). Current Science, 82, 1472-1479.

Maldonado, M., Carmona, M.C., Uriz, M.J., Cruzado, A. 1999. Decline in Mesozoic reef-building sponges explained by silicon limitation. Nature 401, 785−788.

Marshall, G.J., 2003. Trends in the Southern Annular Mode from observations and reanalyses. Journal of Climate 16, 4134–4143.

Martin, J.H., 1990. Glacial-interglacial CO_2 change: the iron hypothesis. Paleoceanography 5, 1-13.

Martin, J.H., Fitzwater, S.T., Gordon, R.M., Hunter, C.N., Tanner, S.J., 1993. Iron, primary production and carbon-nitrogen flux studies during the JGOFS North Atlantic Bloom Experiment. Deep Sea Research I 40, 115–134.

Martin, J.H., Gordon, R.M., Fitzwater, S.E., 1990. Iron in Antarctic waters. Nature 345,156-158.

McGillis, W.R., Edson, J.B., Hare, J.E., Fairall, C.W., 2001. Direct covariance air-sea CO_2 fluxes. Journal of Geophysical Research 106, 16,729 - 16,745.

McNeil, B.I., Metzel, N., Key, R., Matear, M., Corbiere, R.J., 2007. An empirical estimate of the Southern Ocean air–sea CO_2 flux. Global Biogeochemical Cycles, 21, GB3011.

Mehrbach, C., Culberson, C.H., Hawley, J.E., Pytkowicz, R.M., 1973. Measurement of the apparent dissociation constants of carbonicacid in seawater at atmospheric pressure. Limnology and Oceanography 18,897–907.

Metzl, N., 2009. Decadal increase of oceanic carbon dioxide in Southern Indian Ocean surface waters (1991–2007). Deep-Sea Research. II 56, 607–619.

Metzl, N., 2014. Underway physical oceanography and carbon dioxide measurements during Marion Dufresne cruise OISO_03. Laboratoire d'Océanographie et du Climat: Expérimentation et Approches Numériques, Université Pierre-et-Marie-Curie, France, doi:10.1594/PANGAEA.813640.

Moore, C.M., Hickman, A.E., Poulton, A.J., Seeyave, S., Lucas, M.I., 2007. Iron-light interactions during the CROZet natural iron bloom and EXport experiment (CROZEX): II – Taxonomic responses and elemental stoichiometry. Deep-Sea Research II 54, 2066–2084.

Murata, A., Shimada, K., Nishino, S., Itoh, M., 2008. Distributions of surface water $CO_2$and air-sea flux of CO_2in coastal regions of the Canadian Beaufort Sea in late summer. Biogeosciences Discussion 5, 5093–5132.

Murata, A., Takizawa, T., 2003. Summertime CO_2 sinks in shelf and slope waters of the western Arctic Ocean. Continental Shelf Research 23, 753–776.

Narvekar, J., Prasanna Kumar, S., 2006. Seasonal variability of the mixed layer in the central Bay of Bengal and associated changes in nutrient and chlorophyll. Deep–Sea Res. Part I 53, 820–835.

Nooijer, L.J., Toyofuku, T., Kitazato, H., 2009. Foraminifera promote calcification by elevating their intracellular pH. Proceedings of the Natural Academy of Sciences 106, 15374–15378.

Nuncio, M., 2007. Role of eddies in the Bay of Bengal circulation and hydrography and in the distribution of nutrients and chlorophyll, Ph.D thesis, Goa University, 118pp.

Orsi, A.H., Whitworth III, T., Nowlin, Jr. W. D., 1995. On the meridional extent and fronts of the Antarctic Circumpolar Current. Deep-Sea Research I 42, 641–673.

O'Reilly, J.E., Maritorena, S., O'Brien, M.C., Siegel, D.A., Toole, D., Menzies, D., Smith, R.C., Mueller, J.L., Mitchell, B.G., Kahru, M., Chavez, F.P., Strutton, P., Cota, G.F., Hooker, S.B., McClain, C.R., Carder, K.L., Müller-Karger, F., Harding, L., Magnuson, A., Phinney, D., Moore, G.F., Aiken, J., Arrigo, K.R., Letelier, R., Culver, M., 2000. Sea-WiFS Post launch Calibration and Validation Analyses, Part 3, in: Hooker, S.B., Firestone, E. R., (Eds.), NASA Technical Memorandum, vol. 11, p.49.

Pace, M.L., Knauer, G.A., Karl, D.M., Martin, J.H., 1987. Primary production and vertical flux in the eastern Pacific Ocean. Nature 325, 803–804.

Park, Y.H., Charriaud, E., Fieux, M., 1998. Thermohaline structure of Antarctic surface water/winter water in the Indian sector of the Southern Ocean. Journal of Marine Systems 17, 5–23.

Patil, S.M., Mohan, R., Shetye, S.S., Gazi, S., 2009. Diatom abundance and community structure at the Antarctic Polar Frontal Region during austral summer of 2009. Chinese Journal of Oceanology and Limnology 31, 21-30.

Pavithran, S., Anilkumar, N., Krishnan, K.P., Noronha, S.B., George, J.V., Nanajkar, M., Chacko, R., Dessai, D.R.G., Achuthankutty, C.T., 2011. Contrasting pattern in chlorophyll ‘a’ distribution within the Polar Front of the Indian sector of Southern Ocean during austral summer 2010. Current Science 102(6), 899-903.

Pespeni M. H., Sanford E., Gaylord B., 2013. Evolutionary change during experimental ocean acidification. PNAS 1220673, 1-6.

Pilson, M.E.Q., 1998. An introduction to the chemistry of the sea. Prentice-Hall, Inc.

Pipko, I.I., Semiletov, I.P., Tishchenko, P.Y., Pugach, S.P., Christensen, J.P., 2002. Carbonate chemistry dynamics in Bering Strait and the Chukchi Sea. Progress in Oceanography 55, 77–94.

Poisson, A., 2014. Underway physical oceanography and carbon dioxide measurements during MINERVA cruise MIN08. Institut de Modélisation et d'Analyse en Géo-Environnement et Santé, Université de Perpignan Via Domitia, France, doi:10.1594/PANGAEA.813678.

Poisson, A., Chen, C.T.A., 1987. Why is there little anthropogenic CO_2 in the Antarctic Bottom Water? Deep-Sea Research I 34, 1255–1275.

Prasanna Kumar, S., Nuncio, M., Narvekar, J., Kumar, A., Sardesai, S., de Souza, S.N., Gauns, M., Ramiah, N., Madhupratap, M., 2004. Are eddies nature's trigger to enhance biological productivity in the Bay of Bengal? Geophysical Research Letters 31, L07309.

Prasanna Kumar, S., Muraleedharan, P.M, Prasad, T.G., Gauns, M., Ramaiah, N., de Souza, S.N., Sardesai, S., Madhupratap, M., 2002. Why is the Bay of Bengal less productive during summer monsoon compared to the Arabian Sea? Geophysical Research Letters 29, 223.

Prasanna Kumar, S., Nuncio, M., Ramaiah, N., Sardesai, S., Narvekar, J., Fernandes, V., Jane, T.P., 2007. Eddy-mediated biological productivity in the Bay of Bengal during fall and spring intermonsoons. Deep-Sea Research I 54, 1619-1640.

Prasanna Kumar, S., Narvekar, J., Nuncio, M., Kumar, A., Ramaiah, N., Sardesai, S., Gauns, M., Fernandes, V., Paul, J., 2010b. Is the biological productivity in the Bay of Bengal light limited?, Current Science, 98, 1331–1339.

Raiswell, R., 2011. Iceberg-hosted nanoparticulate Fe in the Southern Ocean: mineralogy, origin, dissolution kinetics and source of bioavailable Fe. Deep-Sea Research II 58, 1364–1375.

Raiswell, R., Canfield, D.E., 2012. The iron biogeochemical cycle past and present. Geochemical Perspectives 1, 1–214.

Raven, J., Caldeira, K., Elderfield, H., Hoegh-Guldberg, O., Liss, P., Riebesell, U., Shepherd, J., Turley, C., Watson, A., 2005. Ocean Acidification due to Increasing Atmospheric Carbon Dioxide. The Royal Society, London, UK.

Redfield, A.C., Ketchum, B.H.,Richards, F.A., 1963. The influence of organisms on the composition of sea water, in:Hill,M.N.,(Ed.), The Sea, vol.2. Interscience, New York.26-77.

Richards, F.A., 1958. Dissolved silicate and related properties of some western North Atlantic and Carribean waters. Journal of Marine Research 17, 449-465.

Ricketts, E.R., Kennett, J.P., Hill, T.M., Barry, J.P., 2009. Effects of carbon dioxide sequestration on California margin deep-sea foraminiferal assemblages. Marine Micropaleontology 72, 165-175.

Riebesell, U., Schulz, K.G., Bellerby, R.G.J., Botros, M., Fritsche, P., Meyerhöfer, M., Neill, C., Nondal, G., Oschlies, A., Wohlers, J., Zöllner, E., 2007. Enhanced biological carbon consumption in a high CO_2 ocean. Nature 450, 545–548.

Riebesell, U., Zondervan, I., Rost, B., Tortell, P.D., Zeebe, E., Morel, F.M.M., 2000. Reduced calcification in marine plankton in response to increased atmospheric CO_2. Nature 407, 634–637.

Rost, B., Richter, K., Riebesell, U., Hansen, P.J., 2006. Inorganic carbon acquisition in red tide dinoflagellates. Plant Cell and Environment 29, 810-822.

Sabine, C.L., Feely, R.A., Gruber, N., Key, R.M., Lee, K., Bullister, J.L., Wanninkhof, R., Wong, C.S., Wallace, D.W.R., Tilbrook, B., Peng, T.H., Kozyr, A., Ono, T., Rios, A.F., 2004.The oceanic sink for anthropogenic CO_2. Science 305, 367–371.

Sakshaug, E.L, Holm-Hansen, O., 1986. Photoadaptation in Antarctic phytoplankton: variations in growth rate, chemical composition and P vs. I curves. Journal of Plankton Research 8, 459–473.

Sardessai, S., Maya, M.V., Shetye, S.S., Kumar, P., Fernandes, V., Paul, J., Ramaiah, N., 2010. Environmental controls on the seasonal carbon dioxide fluxes in the northeastern Indian Ocean. Indian Journal of Marine Sciences 39, 192-200.

Sarmiento, J.L., Hughes, T.M.C., Stouger, R.J., Manabe, S., 1998.Ocean carbon cycle response to future greenhouse warming. Nature 393, 245-249.

Sarmiento, J.L., Murnane, R., LeQuéré, C., 1995. Air-sea CO_2transfer and the carbon budget of the North Atlantic. Philosophical Transactions of the Royal Society of London 348, 211-219.

Schmitz, Jr., W.J., 1996a. On the World Ocean Circulation: Volume I, Some Global Features/North Atlantic Circulation. Woods Hole Oceanographic Institution Technical Report WHOI-96-03, 141 pp.

Semiletov, I. P., 1995. Carbon cycle and global changes in past and present, in: Bordovsky, O.K., Rozanov, A.G., (Ed.), Chemistry of the Seas and Oceans, Nauka Press, Moscow, 130–154.

Sen Gupta, A., England, M.H., 2006. Coupled ocean–atmosphere–ice response to variations in the Southern Annular Mode. Journal of Climate 19, 4457–4486.

Shetye, S.S., Marathadu, S., Ramesh, R., Mohan, R., Patil, S., Laskar, A., 2012. Sea surface pCO_2 in the Indian Sector of the Southern Ocean during Austral summer of 2009. Advances in Geosciences 28, 79-92.

Shetye, S.R., Gouveia, A.D., Shenoi, S.S.C., Sundar, D., Michael, G.S., Nampoothiri, G., 1993. The western boundary current of the seasonal subtropical gyre in the Bay of Bengal. Journal of Geophysical Research 98, 945-954.

Siegenthaler, U., Wenk, T., 1984. Rapid accumulation of atmospheric CO_2 variations and ocean circulation. Nature 308, 624-626.

Siegenthaler, U., Stocker, T.F., Monnin, E., Luthi, D., Schwander, J., Stauffer, B., Raynaud, D., Barnola, J.M., Fischer, H., Masson-Delmotte, V., Jouzel, J., 2005. "Stable carbon cycle-climate relationship during the late Pleistocene." Science 310(5752), 1313-1317.

Singh, A., Gandhi, N., Ramesh, R., Prakash, S., 2015. Role of Cyclonic Eddy in enhancing Primary and New production in the Bay of Bengal. Journal of Sea Research 97, 5-13.

Smetacek, V., Klaasb, C., Menden-Deuerc, S., Rynearsonc, T.A. 2002. Mesoscale distribution of dominant diatom species relative to the hydrographical field along the Antarctic Polar Front. Deep-Sea Research II 49(3), 835-3 848.

Smetacek, V., 2002. The ocean's veil. Nature 419, 565.

Spero, H.J., Bijma, J., Lee, D.W., Bemis, B.E., 1997. Effect of seawater carbonate concentration on foraminiferal carbon and oxygen isotopes. Nature 390, 497–500.

Spero, H.J., Bijma, J., Lea, D.W., Bemis, B.E., 1997. Effect of seawater carbonate concentration on foraminiferal carbon and oxygen isotopes. Nature 390, 497–500.

Stephens, B.B., Keeling, R.F., 2000. The influence of Antarctic sea ice on glacial-interglacial CO_2 variations. Nature 404, 171–174.

Stoll, M.H.C., de Baar, H.J.W., Hoppema, M., Fahrbach, E., 1999. New early winter fCO_2 data reveal continuous uptake of CO_2 by the Weddell Sea. Tellus 51B, 679–687.

Stoll, M.H.C., Thomas, H., de Baar, H.J.W., Zondervan, I., de Jong, E., Bathmann, U.V., Fahrbach, E., 2002. Biological versus physical processes as drivers of large

oscillations of the air–sea CO_2 flux in the Antarctic marginal ice zone during summer. Deep-Sea Research I 49, 1651–1667.

Stramma, L., Johnson, G.C., Sprintall, J., Mohrholz, V., 2008. "Expanding oxygen-minimum zones in the tropical oceans." Science 320(5876), 655-658.

Subramanian, V., 1993. Sediment load of Indian Rivers. Current Science 64, 928-930.

Suess, E., 1980. Particle organic carbon flux in the Ocean's surface productivity and oxygen utilization. Nature 288, 260–263.

Sverdrup, H. U., 1953. On conditions for the vernal blooming of phytoplankton. J. Cons. Cons. Int. Explor. Mer. 18, 287–295.

Takahashi, T., Chipman, D.W., 2012. CO_2 transport in deep waters off Wilkes Land. Oceanography 25(3):24–25.

Takahashi, T., Sutherland, S.C., Feely, R.A., Wanninkhof, R., 2006. Decadal change of the surface water pCO_2 in the North Pacific: a synthesis of 35 years of observations. Journal of Geophysical Research 111, C07S05.

Takahashi, T., Sutherland, S.C., Wanninkhof, R., Sweeney, C., Feely, R.A., Chipman, D.W., Hales, B., Friederich, G., Chavez, F., Sabine, C., Watson, A., Bakker, D.C.E., Schuster, U., Metzl, N., Yoshikawa, I.H., Ishii, M., Midorikawa, T., Nojiri, Y., Ko¨rtzingerm, A., Steinhoffm, T., Hoppema, M., Olafsson, J., Amarson, T.S., Tilbrook, B., Johannessen, T., Olsen, A., Bellerby, R., Wong, C.S., Delille, B., Bates, N.R., debar, H.J.W., 2009. Climatological mean and decadal change in surface ocean pCO_2, and net sea–air CO_2 flux over the global oceans. Deep-Sea Research II 56, 607–619.

Takahashi, T., Olafsson, J. Goddard, J.G. Chipman, D.W., Sutherland, S.C. 1993. "Seasonal-Variation of CO_2 and Nutrients in the High-Latitude Surface Oceans - a Comparative- Study." Global Biogeochemical Cycles 7(4), 843-878.

Takeda, S., 1998. Influence of iron availability on nutrient consumption ratio of diatoms in oceanic waters. Nature 393, 774-777.

Taylor, J. R., Lovera, C., Whaling, P. J., 2013. Physiological compensation for environmental acidification is limited in the deep-sea urchin *Strongylocentrotus fragilis.* Biogeosciences Discussion 10, 8313–8341.

Thomas, D. N., Dieckmann, G. S., 2010. Sea Ice,Second Edition, Wiley-Blackwell, Oxford, UK, pp. 621.

Thompson, D.W.J., Solomon, S., 2002. Interpretation of recent Southern Hemisphere climate change. Science 296, 895–899.

Timmermans, K.R., Davey, M.S., van der Wagt, B., Snoek, J., Geider, R.J., Veldhuis, M.J.W., Gerringa, L.J.A., de Baar, H.J.W., 2001. Colimitation by iron and light of Chaetoceros brevis, C. dichaeta and C. calcitrans (Bacillariophyceae). Marine Ecology Progress Series 217, 287–297.

Tortell, P.D., DiTullino, G.R., Sigman, D.M., Morel, F.M.M., 2002. CO_2 effects on taxonomic composition and nutrient utilization in an Equatorial Pacific phytoplankton assemblage. Marine Ecology Progress Series 236, 37–43.

Tortell, P.D., Gue´guen, C., Long, M.C., Payne, C.D., Lee, P., DiTullio, G.R., 2011. Spatial variability and temporal dynamics of surface water pCO_2, DO_2/Ar and dimethyl sulphide in the Ross Sea, Antarctica. Deep-Sea Research I 58, 241–2

Tréguer, P., Jacques, G., 1992. Dynamics of nutrients and phytoplankton, and fluxes of carbon, nitrogen and silicon in the Antarctic Ocean. Polar Biology 12, 149-162.

Trull, T.W., Rintoul, S.R., Hadfield, M., Abraham, E.R., 2001. Circulation and seasonal evolution of Polar waters south of Australia: Implications for iron fertilization of the Southern Ocean. Deep-Sea Research II 48, 2439-2466.

Turner, D.R., Owens, N.J.P., 1995. A biogeochemical study in the Bellingshausen Sea: Overview of the STERNA 1992 expedition. Deep-Sea Research II 42, 907–932.

Tyrrell, T., Merico, A., Waniek, J.J., Wong, C.S., Metzl, N., Whitney, F., 2005. The effect of seafloor depth and phytoplankton blooms in high nitrate, low chlorophyll (HNLC) regions. Journal of Geophysical Research 110(G2), G02007.

Uthermöhl, H., 1958 Mitteilungen-Internationale Vereinigung für. Limnlogie 9, 1-38.

Vernet, M., Sines, K., Chakos, D., Cefarelli, A.O., Ekern, L., 2011. Impacts on phytoplankton dynamics by free-drifting icebergs in the NW Weddell Sea. Deep-Sea Research II 58, 1422–1435.

Vidya, P.J., Prasanna Kumar, S., 2013. Role of mesoscale eddies on the variability of biogenic flux in the northern and central Bay of Bengal. Journal of Geophysical Research Oceans 118(10), 5760-5771.

Vinayachandran, P.N., Murty, V.S.N., Ramesh Babu, V., 2002a. Observations of barrier layer formation in the Bay of Bengal during summer monsoon. Journal of Geophysical Research,107(C12), 8018.

Volk, T., Hoffert, M.I., 1985. Ocean carbon pumps: analysis of relative strengths andefficiencies in ocean-driven atmospheric CO_2 changes. The Carbon Cycle and

AtmosphericCO2: Natural Variations Archean to Present. E. T. Sunquist and W. S. Broecker. Washington, DC. Geophysical Monographical Series 32, 99-111.

Wallace, D.W.R., 2001. Storage and Transport of excess CO_2 in the Oceans: TheJGOFS/WOCE Global CO_2 Survey. in: Ocean Circulation and Climate, 489-521.

Wanninkhof, R. 1992. Relationship between wind speed and gas exchange over the ocean. Journal of Geophysical Research 97, 7373–7382.

Weeks, S.J., Shillington, F.A., 1996. Phytoplankton pigment distribution and frontal structure in the subtropical convergence region south of Africa. Deep-Sea Research Part I 43,739–76.

Weiss, R.F., 1974. Carbon dioxide in water and seawater: the solubility of a non- ideal gas. Marine Chemistry 2, 203–212.

Weiss, R.F., VanWoy, F.A., Salameh, P.K., 1992. Surface water and atmospheric carbon dioxide and nitrous oxide observations by shipboard automated gas chromatography: Results from expeditions between 1977 and 1990, Scripps Institute of Oceanography, Ref. 92-11, ORNL/CDIAC-59, NDP-044, Carbon Dioxide Information Analysis Center. pp. 144.

Wolf-Gladrow, D.A., Riebesell, U., Burkhardt, S., Bijma, J., 1999. Direct effects of CO_2 concentration on growth and isotopic composition of marine plankton. Tellus Series B51, 461–476.

Yelland, M., Taylor, P.K., 1996. Wind stress measurements from the open ocean. Journal of Physical Oceanography 26(4), 541–558.

Zeebe, R.E., Wolf-Gladrow, D., 2001. CO_2 in Seawater: Equilibrium, kinetics, isotopes. Elsevier Science.